THE QUARTERLY JOURNAL OF

MECHANICS AND APPLIED MATHEMATICS

VOLUME IX PART 4

DECEMBER 1956

OXFORD

AT THE CLARENDON PRESS

1956

Price 18*s. net*

PRINTED IN GREAT BRITAIN BY CHARLES BATEY AT THE UNIVERSITY PRESS, OXFORD

THE QUARTERLY JOURNAL OF MECHANICS AND APPLIED MATHEMATICS

THE QUARTERLY JOURNAL OF MECHANICS AND APPLIED MATHEMATICS is published at 18*s.* net for a single number with an annual subscription (for four numbers) of 60*s.* post free.

NOTICE TO CONTRIBUTORS

1. *Communication.* Papers should be communicated to one or other of the Executive Editors, by name, at King's College, Strand, London, W.C. 2.

2. *Presentation.* Manuscripts should preferably be typewritten, and each paper should be preceded by a summary not exceeding 300 words in length. References to literature should be given in standard order, *author, title of journal, volume number, date, page.* These should be placed at the end of the paper and arranged according to the order of reference in the paper.

3. *Diagrams.* The number of diagrams should be kept to the minimum consistent with clarity. The lines of the figures should be drawn in ink either on draughtsman's paper or on good quality white paper. Each individual line in the figure should bear reducing to one-half of the size of the original, and great care should be exercised to see that the lines are regular in thickness, especially where they meet. Lettering of the figure should be in pencil and should be sufficient to define clearly the lines and curves in it. The writing of formulae or of explanations on the diagram itself should be avoided. All explanations of symbols, etc., should be given in underline. Contributors should indicate on their manuscripts where figures should be inserted.

4. *Tables.* Tables should preferably be arranged so that they can be printed with the columns parallel to the longer edge of the page.

5. *Notation.* All single letters used to denote vectors in the manuscript should be marked by underlining with a wavy line. Scalar and vector products should be denoted by $\underset{\sim}{a} . \underset{\sim}{b}$ and $\underset{\sim}{a} \wedge \underset{\sim}{b}$ respectively. Real and imaginary parts of complex quantities should be denoted by re and im respectively.

6. *Offprints.* Authors of papers will be entitled to 25 free offprints. This number is available for sharing between authors of joint papers.

7. All correspondence other than that dealing with contributions should be addressed to the publishers:

OXFORD UNIVERSITY PRESS
AMEN HOUSE, LONDON, E.C. 4

NOTICE

Beginning in 1957, it is intended that the Journal shall be published in the months of February, May, August and November, instead of March, June, September and December. The change is being made at the request of the Printer.

SOURCES AND SINKS AT THE AXIS OF A ROTATING LIQUID†

By ROBERT R. LONG

(*The Johns Hopkins University, Baltimore, Maryland*)

[Received 16 June 1955; revise received 27 March 1956]

SUMMARY

A solution is obtained for the flow of a rotating, frictionless, incompressible fluid due to a strong source or sink at the axis of rotation. The type of motion is controlled by the value of the Rossby number, *Ro*, a ratio of inertial and Coriolis forces. The solution resembles potential flow if *Ro* is very large. As *Ro* decreases the sink draws more and more from the axis of rotation until, at $Ro = 0{\cdot}261$, the fluid approaches the sink in a jet centred at the axis and with a radius about half that of the cylinder. No solution is obtained for smaller values of *Ro*. If a jet is postulated for small values of *Ro*, it is shown that its radius decreases as the cube root of the flux. Several experimental photographs are shown. They contain some of the features of the theory. The jet type of motion becomes very pronounced for weak sinks.

1. Theory

In a previous paper the author (**1**) has shown that a solution of the differential equation

$$\frac{\partial^2\psi}{\partial x^2}+\frac{\partial^2\psi}{\partial\rho^2}-\frac{1}{\rho}\frac{\partial\psi}{\partial\rho}+\sigma^2\psi=-\tfrac{1}{2}\sigma^2 u_0\rho^2 \qquad (1)$$

represents steady-state, axially symmetric flow of a rotating, frictionless, incompressible fluid; ψ is the Stokes's stream-function. The coordinate system is shown in Fig. 1. In the derivation of equation (1) it was assumed that at $x=-\infty$ the fluid has a constant absolute angular velocity Ω about the x-axis and a constant linear velocity u_0 parallel to the axis of rotation. The parameter σ is $2\Omega/u_0$.

The purpose of this note is to apply (1) to the problem of sources and sinks located on the axis of rotation. We suppose first that there is a sink at the point $x=0$, $\rho=0$ in an infinitely long cylinder of radius b containing rotating liquid. We require the streamline pattern to be symmetric about the plane $x=0$ and assume that at $|x|=\infty$ the absolute velocity field is a constant angular velocity Ω and constant velocity u_0 toward the sink. In view of the symmetry, the problem is equivalent to flow from the negative x-axis toward a hole at $x=0$, $\rho=0$ in a wall coincident with the plane $x=0$. An appropriate solution of (1) is

$$\psi=-\frac{u_0\rho^2}{2}+\rho\sum_\alpha A_\alpha e^{(\alpha^2-\sigma^2)^{\frac{1}{2}}x}J_1(\alpha\rho). \qquad (2)$$

† This research was sponsored by the Office of Naval Research under Contract N–onr–248(31).

Unless $\alpha = \sigma$ the solution (2) yields uniform flow, u_0, as $x \to -\infty$. It was also shown by the author (**2**) that w, the component of the absolute velocity tangent to a circle centred at the axis of rotation, is related to ψ by the equation

$$w\rho = -\sigma\psi. \tag{3}$$

Equations (2) and (3) show that $w \to \Omega\rho$ as $x \to -\infty$, or solid rotation.

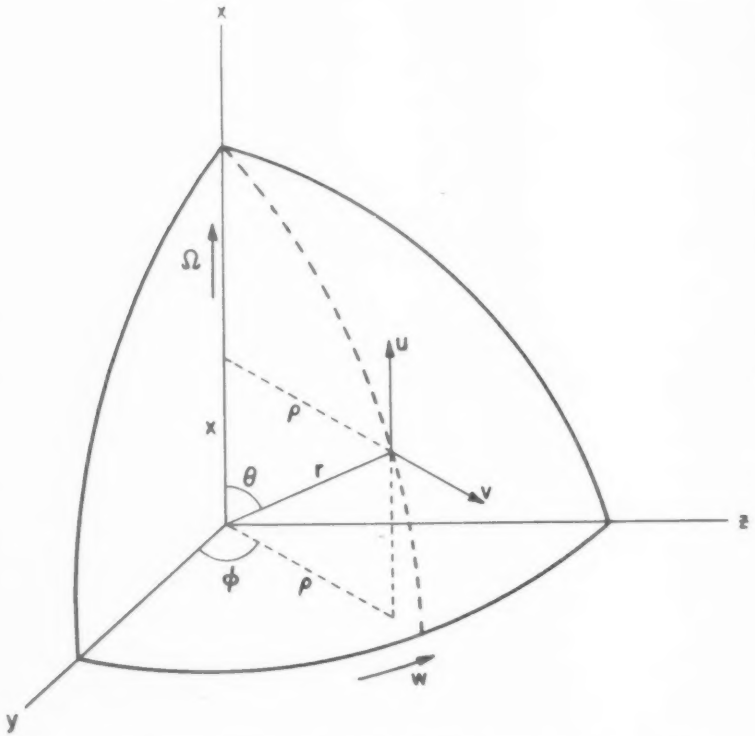

FIG. 1. Coordinate system. The x-axis is taken along the axis of rotation.

At the wall of the cylinder, the uniform flux through a plane perpendicular to the axis is $-2\pi\psi$. Hence at $\rho = b$, $\psi = -u_0 b^2/2$. Therefore, $\alpha b = z_n$, where z_n are the zeros of the Bessel function $J_1(z)$, the first two being $z_1 = 3{\cdot}8317$, $z_2 = 7{\cdot}0156$. The solution (2) becomes

$$\psi = -\frac{u_0 \rho^2}{2} + \rho \sum_{n=n_1}^{\infty} A_n e^{(z_n^2 - Ro^{-2})^{\frac{1}{2}}(x/b)} J_1\left(z_n \frac{\rho}{b}\right). \tag{4}$$

We have substituted for $(\sigma b)^{-1}$ the symbol $Ro = u_0/2\Omega b$. This is called

the Rossby number in meteorological literature (**1**). It is a measure of the importance of the rotational or Coriolis forces in rotating systems. The summation in (4) begins at n_1, where n_1 is the first integer for which $Ro > 1/z_n$. For smaller integers we would have oscillating functions of x in (4) and disturbed motion at infinity.

We notice that $\psi = 0$ on the axis $\rho = 0$. We obtain a sink at $x = 0$, $\rho = 0$ by requiring that ψ has the same value at the plane $x = 0$ (except at the point $x = 0$, $\rho = 0$) as it has on the cylinder wall, namely $-u_0 b^2/2$. The resulting jump discontinuity of ψ yields the infinite velocity at $(0, 0)$ required in a sink. Hence for $x = 0$, $0 < \rho/b \leqslant 1$,

$$\frac{u_0 b^2}{2}\left(\frac{\rho^2}{b^2} - 1\right) = \rho \sum_{n=n_1}^{\infty} A_n J_1\left(z_n \frac{\rho}{b}\right). \tag{5}$$

Multiplying both sides of (5) by $J_1(z_m \rho/b)$ and integrating with respect to ρ/b from 0 to 1, we find

$$A_m = -\frac{u_0 b}{z_m J_0^2(z_m)}. \tag{6}$$

The solution becomes

$$\psi = -\frac{u_0 \rho^2}{2} - u_0 b \rho \sum_{n=1}^{\infty} \frac{\exp[(z_n^2 - Ro^{-2})^{\frac{1}{2}} x/b]}{z_n J_0^2(z_n)} J_1(z_n \rho/b). \tag{7}$$

Since the summation begins at $n = 1$, *the solution exists only if Ro exceeds* $1/z_1$, *or* $Ro \geqslant 0{\cdot}261$. This corresponds to low or moderate values of the angular velocity of the system or to strong sinks. Obviously we may change the sign of u_0 and (7) will still satisfy the differential equation (1). With the proper choice of pressure, the resulting motion will then satisfy the primitive equations of motion and continuity for the steady symmetric flow of a frictionless, incompressible, rotating fluid. The pressure may be found from the equation

$$\frac{p}{q} + \frac{u^2 + v^2 + w^2}{2} = \frac{p_\infty(\rho_0)}{q} + \frac{u_0^2}{2} + \frac{\Omega^2 \rho_0^2}{2}, \tag{8}$$

where q is the constant density, p_∞ is the pressure at $x = -\infty$, and ρ_0 is the Lagrangian distance of a streamline from the axis. Equation (7), with a negative value of u_0, yields flow due to the emission of fluid from the point $(0, 0)$. The emitted fluid possesses vorticity so that this system may be regarded as a source combined with a vortex of a special type. The case of a source emitting irrotational fluid has been considered by Barua (**3**). In the latter problem the irrotational fluid moves along the axis in the form of a cylindrical jet.

The flow patterns given by (7) are shown for several values of *Ro* in Fig. 2. We note that as *Ro* decreases from ∞ the sink draws more and more from

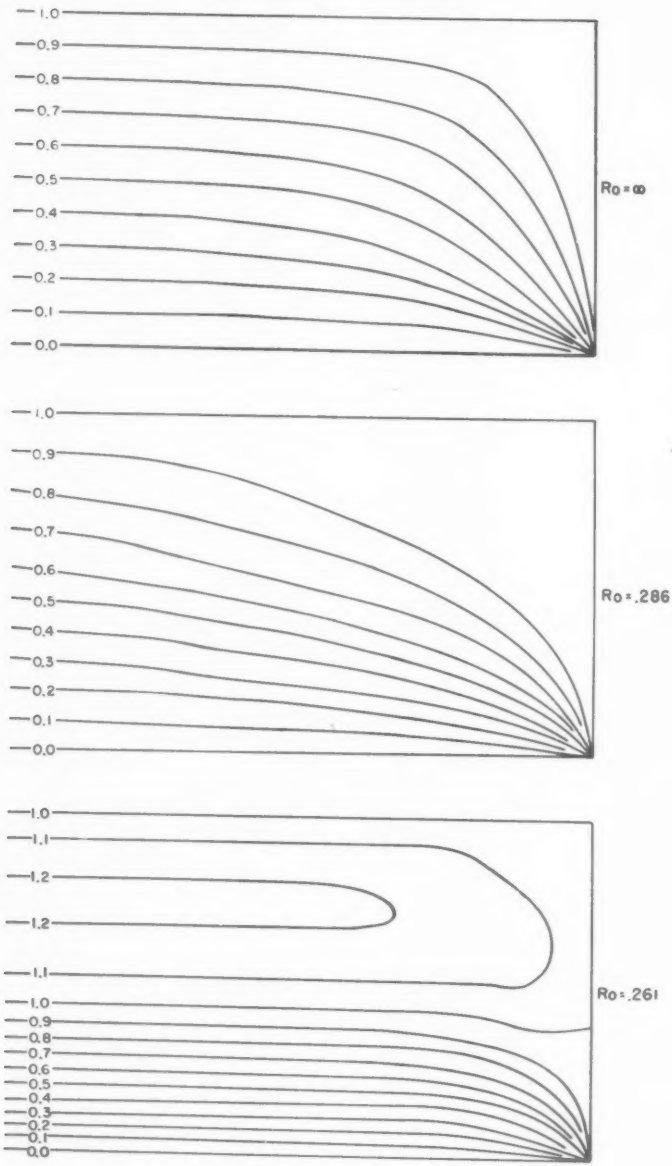

FIG. 2. Flow patterns computed from equation (7). The curves are isolines of $\rho_0/b = (-2\psi/u_0\, b^2)^{\frac{1}{2}}$ (see Long, 1953).

the axis of rotation. This tendency is a maximum for the critical value of $Ro = 0{\cdot}261$, in which case the fluid approaches the sink in a 'jet'. As $x \to -\infty$ the velocity tends to

$$u = u_0\left[1+\frac{J_0(z_1\,\rho/b)}{J_0^2(z_1)}\right]. \tag{9}$$

This is a maximum in the vicinity of the axis, becoming negative near the cylinder wall. Although the condition that $u \to u_0$ at $x = -\infty$ is violated, the difficulty is avoided by choosing Ro slightly larger than $0{\cdot}261$.

If we solve equation (1) for free stationary waves in an infinite cylinder we find, typically,

$$\psi = -\frac{u_0\,\rho^2}{2}+\rho B_n\, e^{ik_n x} J_1\!\left(z_n\,\frac{\rho}{b}\right), \tag{10}$$

where

$$k_n = \left(\sigma^2-\frac{z_n^2}{b^2}\right)^{\frac{1}{2}}. \tag{11}$$

For a given value of n we may interpret (10) and (11) as a wave moving along the axis of a cylinder at a speed $c = u_0$ relative to the liquid. Then

$$c^2 = \frac{4\Omega^2 b^2}{z_n^2+4\pi^2 b^2/\lambda_n^2}, \tag{12}$$

where λ_n is the wavelength. The speed decreases with n and increases with wavelength. The maximum speed of any possible wave of this type is a wave of infinite length with no internal nodal surfaces, i.e. $z_n = z_1$. Applying these results to the problem of the sink, if $\sigma b < z_1$, the fluid approaches the sink at great distances with a speed greater than that of any wave. Hence no free wave can advance against this current. If σb exceeds z_1 slightly, a long wave can move upstream against the current. The steady-state solution at $\sigma b = z_1$ shows that this has happened and the wave has altered the upstream velocity distribution to that of equation (9). This reasoning supports the assumption that the flow at $x = -\infty$ is uniform for strong sinks.

Although a steady-state solution exists for all values of Ro greater than $0{\cdot}261$, we find that closed circulations begin to form in some parts of the system when Ro is close to the critical value. These circulations remain weak (Fig. 2) even at $Ro = 0{\cdot}286$. Very near $Ro = 0{\cdot}261$ the closed circulation strengthens, spreads upstream, and develops finally into the pattern of $Ro = 0{\cdot}261$ shown in Fig. 2. The significance of the appearance of negative values of u follows from the equation

$$u = -\frac{1}{\rho}\frac{\partial\psi}{\partial\rho} = \frac{1}{\sigma\rho}\frac{\partial}{\partial\rho}(w\rho). \tag{13}$$

When u is negative the absolute angular momentum *decreases outward*

locally, and we would expect this to be unstable. This suggests the possibility that weak sinks may lead to flows that are essentially turbulent and unsteady, and that no physically meaningful steady-state solution may exist. Since we may write

$$Ro = \frac{F}{2\Omega\pi b^3}, \tag{14}$$

where F is the volume flux through the sink, we are led to the further possibility that no steady-state flow exists for a sink of any finite strength in a completely unbounded rotating fluid ($b = \infty$). In this case, however, we may postulate the existence of a quasi-steady jet of radius b_0 moving toward the sink. If so, the only pertinent quantities, F, Ω, b_0, lead to only one non-dimensional number, say

$$Ro' = \frac{F}{2\pi\Omega b_0^3}, \tag{15}$$

which must therefore be an absolute constant. The magnitude of the constant may be inferred from a consideration of the jet existing theoretically at $Ro = 0{\cdot}261$. Taking the boundary of the jet at the value of ρ where $|du/d\rho|$ is a maximum, $b_0/b \cong 0{\cdot}48$ and

$$Ro' = Ro\frac{b^3}{b_0^3} \cong 2{\cdot}3. \tag{16}$$

This is probably a crude estimate since the theoretical jet has a radius that is not small compared to that of the cylinder and therefore does not resemble a jet in an unlimited fluid.†

2. Experimental results

An experimental study was made of the effect of a sink at the axis of rotation of a tall cylinder. A cylinder of water of radius $b = 5{\cdot}7$ cm. and height 125 cm. is positioned on a rotating turntable and brought up to solid rotation. Water is then extracted at the bottom at the axis of rotation through a hole of radius 0·66 cm. The flux and rotation rate may be varied to obtain different values of $Ro = F/2\Omega\pi b^3$. The flow pattern is recorded by streak photography, using a camera rotating with the turntable, with line of sight perpendicular to a plane of light passed through the axis of rotation. Aluminium particles are used as tracers.

The experimental photographs are shown in Figs. 3–7 in order of decreasing Rossby number. Figs. 3 and 4, with Ro values of ∞ and 0·281 respectively, show the effect of a moderate amount of rotation. The sink draws more strongly from regions near the axis of rotation in Fig. 4, and there is

† Sir Geoffrey Taylor, in a private communication to the author, remarked that Barua obtained $Ro' = 0{\cdot}31$ for a jet due to a source at the axis of a rotating fluid.

a definite indication of the eddies near the walls, predicted by the theory and shown in the 0·286 drawing of Fig. 2. No abrupt change of flow pattern occurs in the experiments at the critical value of the Rossby number.

FIG. 3. Flow toward a sink. No rotation, $Ro = \infty$.

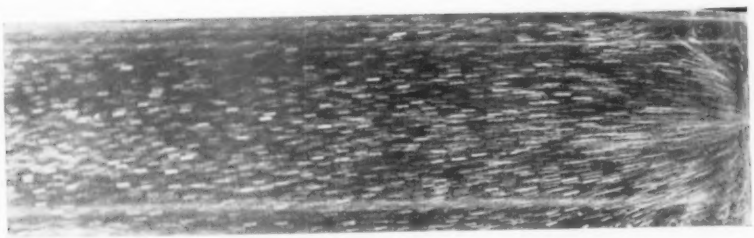

FIG. 4. Flow toward a sink. $Ro = 0{\cdot}281$.

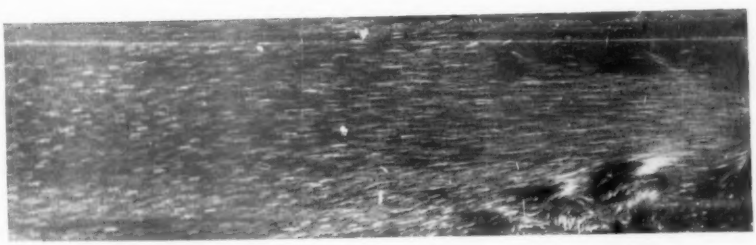

FIG. 5. Flow toward a sink. $Ro = 0{\cdot}203$.

Instead, the tendency for a jet formation seems to increase in a continuous manner. This is not surprising in view of the fact that the experiment is only quasi-steady. This point is illustrated in Fig. 5. The Rossby number,

0·203, is well below the critical value. A well-defined jet is being formed in the vicinity of the sink, apparently by upstream propagation of the waves seen in the photograph. These waves have progressed a short distance

FIG. 6. Flow toward a sink. $Ro = 0{\cdot}100$.

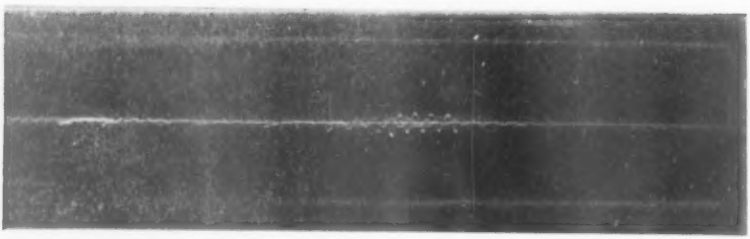

FIG. 7. Flow toward a sink. $Ro = 0{\cdot}006$.

ahead of the sink and the approaching flow is only affected in this vicinity. For smaller Rossby numbers the formation of the jet is more rapid. In Fig. 6 it exists far ahead of the sink.

Fig. 7 illustrates the flow at an extremely low value of $Ro = 0{\cdot}0061$. The jet is concentrated very near the axis of rotation and is spinning very rapidly. A single tracer particle has performed five revolutions about the axis in the $\frac{1}{5}$ sec. time exposure of the photograph, yielding an angular velocity about 60 times the basic rotation (27 r.p.m.).

An effort may be made to recompute the constant in equation (16) from experimental observation. Thus in Fig. 6, if we take the diameter of the jet as, perhaps, $\frac{1}{3}$ the diameter of the vessel, equation (16) yields $Ro' \cong 1{\cdot}6$. Similar calculations for experiments with lower Rossby numbers also lead to values around 1·0. In all cases, however, the diameter of the jet is difficult to estimate in the photographs and Ro' is very sensitive to variations in this estimate.

REFERENCES

1. R. R. Long, 'The flow of a liquid past a barrier in a rotating spherical shell', *J. Meteor.* **9** (1952), 187.
2. —— 'Steady motion around a symmetrical obstacle moving along the axis of a rotating liquid', ibid. **10** (1953), 197.
3. S. N. Barua, 'A source in a rotating fluid', *Quart. J. Mech. App. Math.* **8** (1955), 22.

THE SHAPE OF THE NAPPE OF A THIN WATERFALL

By G. N. LANCE *and* E. C. DELAND

(*Department of Mathematics, The University, Southampton, and Department of Engineering, University of California, Los Angeles*)

[Received 27 October 1955]

SUMMARY

The shape of the nappe of a thin waterfall is obtained by solving the non-linear differential equation which describes the shape, on a mechanical differential analyser. All forces acting on the waterfall, namely, gravity, surface tension, and air-pressure, are incorporated in the analysis. Previous writers have considered only the force of gravity. It is shown that the shape is extremely sensitive to air-pressure. Throughout, a comparison is made with the water-bell phenomenon which has been discussed previously and which is the three-dimensional analogue of the present work.

1. Introduction

Equations have been derived giving the shape of the nappe of a waterfall by several authors. R. V. Southwell and G. Vaisey (**1**) obtained the shape of a thick fall by relaxation methods. F. W. Blaisdell (**2**) and A. Fathy and M. S. Amin (**3**) assumed the fall to be thin, an assumption that is also made here; however, all these authors assumed that the surface tension and air-pressure forces were negligible. Nevertheless, it has been shown in connexion with the water-bell problem by G. N. Lance and R. L. Perry (**4**) and by G. N. Lance and E. C. Deland (**5**) that air-pressure plays an important role in determining the shape of the nappe.

The present paper gives the derivation of the differential equation whose solution gives the shape of the nappe of a waterfall. The depth of water flowing over is assumed to be small so that the velocity of all particles is the same. The direction of projection need not be horizontal. The differential equation, which is non-linear, contains three parameters, one involves T the surface tension and one involves the air-pressure difference $\Pi - p$, where Π is the air-pressure on the upper nappe and p that on the lower nappe. Such a pressure difference could be produced either by air trapped below the nappe or by a wind blowing across the face of the fall.

A first integral of the second order differential equation can readily be obtained but a complete solution involves incomplete elliptic integrals of the third kind. It was decided, therefore, to solve the equation on the differential analyser at the University of California, Los Angeles. This enables us to obtain curves for a wide variety of parameters.

2. Derivation of the differential equation of the nappe

In Fig. 1 the origin of coordinates is the point from which the water is projected, the x-axis is horizontal, x being positive in the direction of flow, the y coordinate is measured positive downwards.

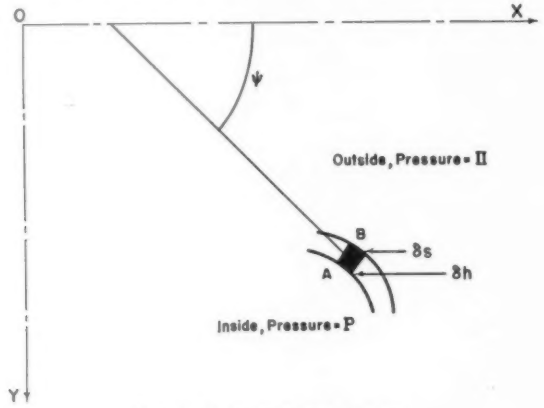

FIG. 1. The coordinate system.

Let Q be the mass of water flowing per unit length of fall per unit time; then if ρ is the density of water, v is the velocity of the water, and h is the thickness of the fall at a general point of its path, the equation of continuity may be written

$$Q = \rho h v. \tag{1}$$

The tangential equation of motion is

$$h\,\delta s\,\rho g \sin\psi = h\,\delta s\,\rho v\,dv/ds, \tag{2}$$

where ds is the arc length, ψ is the slope of the curve, and g is the acceleration due to gravity. The normal equation of motion may be written

$$(\Pi - p + 2T/R) + \rho h g \cos\psi = v^2 \rho h / R, \tag{3}$$

where T is the surface tension of water, R is the radius of curvature, and Π and p are the air-pressures on upper and lower nappes respectively.

Now (2) can be integrated and gives the energy equation

$$v^2 = v_0^2 + 2gy, \tag{4}$$

where v_0 is the velocity of projection. Also, using (1) to eliminate $h\rho$ from (3), we get

$$\frac{2T}{Q}\frac{d\psi}{ds} + \frac{(\Pi - p)}{Q} + \frac{g\cos\psi}{v} = v\frac{d\psi}{ds}, \tag{5}$$

and v may be eliminated from (5). We introduce the following three parameters

$$\alpha = (\Pi - p)/Qv_0, \qquad \beta = 2T/Qv_0, \quad \text{and} \quad \gamma = g/v_0^2.$$

The equation which results, namely

$$y''[(1+2\gamma y)^{\frac{1}{2}}-\beta] = \alpha(1+y'^2)^{\frac{3}{2}}+\gamma(1+y'^2)(1+2\gamma y)^{-\frac{1}{2}}, \tag{6}$$

is the differential equation of the nappe, the prime denotes differentiation with respect to x. Since the thickness h is small the solution of (6) gives the shape of either nappe.

A first integral of this equation can be obtained since x does not appear explicitly in the equation; we find

$$(1+y'^2)^{-\frac{1}{2}}[(1+2\gamma y)^{\frac{1}{2}}-\beta] = \text{const}-\alpha(1+2\gamma y)/2\gamma.$$

The constant is chosen so that $y' = \tan\psi_0$ when $y = 0$.

In the special case of horizontal projection we let $\psi_0 = 0$. Hence

$$(1+y'^2)^{-\frac{1}{2}}[(1+2\gamma y)^{\frac{1}{2}}-\beta] = (1-\beta)\cos\psi_0-\alpha y. \tag{7}$$

The expression for x may be written down

$$x = \int_0^y \left[\left(\frac{(1+2\gamma t)^{\frac{1}{2}}-\beta}{(1-\beta)\cos\psi_0-\alpha t}\right)^2 - 1\right]^{-\frac{1}{2}} dt. \tag{8}$$

However, it can be shown that the integral on the right-hand side of (8) involves elliptic integrals of the third kind. For this reason we do not pursue this line of attack further.

3. Discussion of the first integral

Several interesting results may be obtained directly from (7). The curve has maxima or minima when $y' = 0$. The values of y at which $y' = 0$ are given by

$$(1+2\gamma y)^{\frac{1}{2}} = \pm\{(1-\beta)\cos\psi_0+\beta-\alpha y\}. \tag{9}$$

Since $v = v_0(1+2\gamma y)^{\frac{1}{2}}$ is necessarily positive, it is required to find the roots of (9) which make the right-hand side positive. In the special case of horizontal projection ($\psi_0 = 0$) these are

$$y = 0 \quad \text{and} \quad [\alpha+\gamma-2\alpha\beta+(\alpha^2+\gamma^2+2\alpha\gamma-4\alpha\beta\gamma)^{\frac{1}{2}}]/\alpha^2. \tag{10}$$

The water will be falling (or rising) vertically when y' is infinite, this occurs when $\alpha y = (1-\beta)\cos\psi_0$ in the general case and when

$$\alpha y = 1-\beta \tag{11}$$

in the case of horizontal projection.

The integral curve will contain a singular point when y' is indeterminate, which occurs when (10) and (11) are satisfied simultaneously. The value of α for such a curve is given by

$$(1-\beta)/\alpha = [\alpha+\gamma-2\alpha\beta+(\alpha^2+\gamma^2+2\alpha\gamma-4\alpha\beta\gamma)^{\frac{1}{2}}]/\alpha^2 \tag{12}$$

or

$$\alpha = -2\gamma/(1+\beta). \tag{13}$$

The y-coordinate of the singular point is $-(1-\beta^2)/2\gamma$. It can easily be shown that near this point the shape of the curve is approximated to by

the vertex of a semi-cubical parabola whose tangent is vertical. Since $\beta \ll 1$ and $\gamma > 0$ the cusp always occurs above the horizontal; also for a given β and γ there is just one value of α, namely, that given by (13), which gives a curve with a cusp.

Thus the present case is easier to solve than the three-dimensional one (**4** and **5**) because in the latter case no first integral can be found and hence the value of α which gives the singular curve is unknown.

4. Differential analyser solution of equations

Since a complete solution cannot be obtained in terms of elementary functions it was decided to use the differential analyser for this purpose. The values of β and γ are obtained from reasonable assumptions about the magnitude of Q and v_0. Then solutions were obtained for varying values of α. The curves of particular interest are those for which α takes the particular values

(i) $\alpha = 0$: natural waterfall;

(ii) $\alpha = -2\gamma/(1+\beta)$: cuspidal curve.

Some typical curves are shown as Figs. 2, 3, and 4. The curves of Fig. 2 are obtained using $Q = 13{\cdot}26$ g./sec./unit length and $v_0 = 90$ cm./sec., with the result that $\beta = \gamma = 0{\cdot}12$. The values of α chosen lie between $+0{\cdot}2$ and $-0{\cdot}4$, with the critical value corresponding to (ii) above, i.e. $\alpha = -0{\cdot}216$, giving the cuspidal solution.

The curves of Fig. 3 differ from those of Fig. 2 in that the velocity of projection is $v_0 = 30$ cm./sec., so that $\beta = 0{\cdot}362$ and $\gamma = 1{\cdot}09$. In the present case $-2{\cdot}0 \leqslant \alpha \leqslant +0{\cdot}4$ and the cusp occurs for $\alpha = -1{\cdot}60$. It can easily be verified that the maxima and minima of the curves occur at the levels given by (10); in particular they all touch the line $y = 0$. It should be noted that the integral curves are oscillatory in the x-direction and that the period depends on the value of α. When $\alpha < 0$ the period decreases as $|\alpha|$ increases. This periodicity could also have been foreseen from (8) since the elliptic functions are periodic.

Fig. 4, in which the parameters have the same values as in Fig. 2, shows the effects of projection at $\pm 15°$.

5. Conclusions

One important difference between the water-bells (**5**) and the present problem is the fact that in the former the 'loops' occurred *below* the axis, whereas in the latter all the looped curves are above and bounded by the axis. Hence it would be surprising if the unstable cusp-shaped curves actually appear on a waterfall, even if the pressure difference could be made great enough.

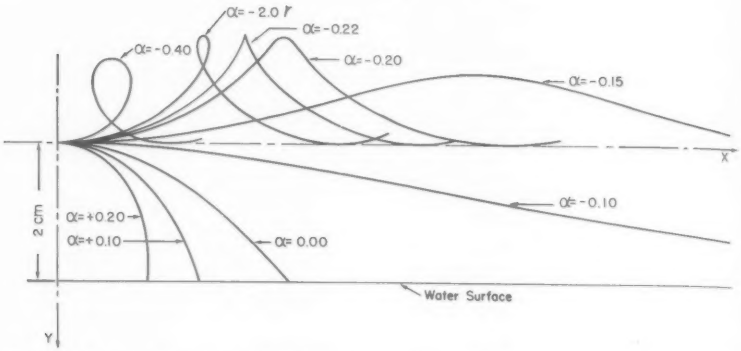

FIG. 2. Shape of nappe for horizontal projection. Parameters β and $\gamma = 0{\cdot}12$, α as shown

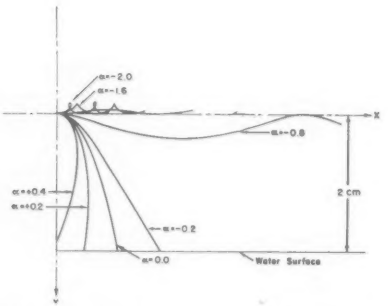

FIG. 3. Shape of nappe for horizontal projection. Parameters $\beta = 0{\cdot}362$ and $\gamma = 1{\cdot}09$; α as shown.

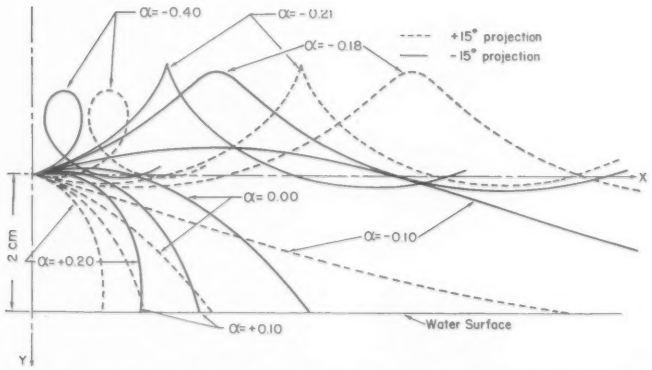

FIG. 4. Effect of projection at $\pm 15°$. Parameters have the values β and $\gamma = 0{\cdot}12$, α as shown.

Previously, it was impossible to derive theoretically the value of α required to give the 'singular' curve; it is clear, however, that such a curve would intersect the water surface. In the falls case the singular curve does not intersect the water surface.

Acknowledgements

This work was performed when one author (G. N. L.) was a National Academy of Sciences Research Fellow, and acknowledgement is made of a maintenance grant from the Foreign Operations Administration Scientific Research Project TA 01–101–3006 (OEEC 151). In addition, the work was assisted by a University of California Research Grant.

REFERENCES

1. R. V. Southwell and G. Vaisey, *Phil. Trans. Roy. Soc.* A, **240** (1946), 117.
2. F. W. Blaisdell, *Proc. Amer. Soc. Civil Engnrs.* **80**, separate No. 482, Aug. 1954.
3. A. Fathy and M. S. Amin, ibid. separate No. 564, Dec. 1954.
4. G. N. Lance and R. L. Perry, *Proc. Phys. Soc.* B, **66** (1953), 1067.
5. —— and E. C. Deland, ibid. **68** (1955), 54.

THE MOVING AEROFOIL IN THE NEIGHBOURHOOD OF A PLANE BOUNDARY

By D. E. EDMUNDS (*University College, Cardiff*)

[Received 22 August 1955]

SUMMARY

This paper deals with a two-dimensional aerofoil moving in an inviscid, incompressible fluid bounded by a plane wall. The solution is obtained by extending the method of Green (**1**) developed for a stationary aerofoil in a uniform stream near a plane boundary, in which the results are given in series form. The results given apply to a fairly general type of aerofoil, but special attention is paid to those of the flat plate, symmetrical, and circular arc types in order to assess the effects of thickness and camber.

1. Introduction

THE problem of finding the lift and moment forces acting on a stationary two-dimensional aerofoil in a uniform stream of inviscid incompressible fluid bounded by a plane wall has been treated quite extensively by several authors (Green (**1**, **2**), Tomotika and co-authors (**3**), Havelock (**4**), and Fujikawa (**5**)), but the case of an aerofoil moving in a general manner in such a bounded region has not been discussed. The most suitable method of solution was found to be an extension of that developed by Green (**1**) for the stationary aerofoil in a uniform stream, in which results are given in series form.

A fairly general type of aerofoil is considered, and the complex potential function appropriate for this is determined, allowance being made for a circulation around the aerofoil. The pressure distribution throughout the fluid and on the aerofoil boundary may be determined by using a modification of the usual pressure equation, and this enables the forces and couple acting to be calculated by using the ordinary contour integrals containing the pressure. The results thus obtained may be expressed in series form, and this is done for three different types of aerofoil.

2. The conditions governing the complex potential Ω

Consider the two-dimensional motion due to a cylinder of aerofoil cross-section moving in a general manner in the neighbourhood of a plane boundary extending to infinity, the fluid being assumed at rest at infinity where the presence of the aerofoil is unnoticed. Since the motion is purely two-dimensional, we may simply consider the flow in a plane defined by a normal cross-section of the cylinder.

To specify the motion, we define two sets of moving rectangular Cartesian axes, the (x, y)-axes fixed in the aerofoil and moving with it in all respects, and the (x', y')-axes whose origin is also fixed inside the aerofoil section but which do not rotate with the aerofoil and so remain at all times parallel to a set of axes fixed in space. The orientation of these (x', y')-axes is so chosen that their real axis and the boundary wall are parallel. This enables us to write the boundary wall as $y' = -b$ at any time (b being a function of the time τ), and the force components perpendicular to and parallel to the wall as Y' and X' respectively.

The (x, y)- and (x', y')-axes are chosen to have a common origin, and this is taken to be inside the boundary curve C of the aerofoil. Thus, defining $z = x+iy$, $z' = x'+iy'$, the relation $z' = ze^{i\theta}$ holds at all times, θ being the angle between the (x, y)- and (x', y')-axes at any time.

The problem to be solved is essentially one in which two prescribed boundary conditions have to be satisfied, one on the fixed wall and the other on the boundary of the moving aerofoil. Also the stream function ψ must reduce to zero at infinity, where the fluid is at rest. Clearly we require that ψ be constant on the plane boundary. Further, if the aerofoil possesses velocity components u', v' along the x'- and y'-axes respectively, and has an angular velocity ω about the origin of coordinates, then it is well known that the boundary condition on the aerofoil to be satisfied by ψ is

$$\psi = -u'y' + v'x' + \tfrac{1}{2}\omega(x'^2 + y'^2).$$

The boundary conditions are thus known, and must be satisfied simultaneously by ψ. Defining the complex potential Ω by $\Omega = \phi + i\psi$, it is therefore clear that Ω must also satisfy two boundary conditions, and in addition must reduce to zero at infinity. Bearing all these conditions in mind, we follow Green (**1**) in choosing Ω so that conditions both on the rigid wall and at infinity are automatically satisfied. The condition holding on the aerofoil boundary is then used to determine the various arbitrary coefficients occurring in the expression assumed for Ω.

3. The formulation of Ω

To define the aerofoil considered here, we adopt the transformation

$$z = t^{-1} \sum_{n=0}^{\infty} a_n t^n \tag{3.1}$$

which maps the boundary of the unit circle $|t| = 1$ in the t-plane on to the boundary of the aerofoil in the z-plane. The region outside the aerofoil C transforms conformally to the region inside the unit circle γ in the t-plane, while description of C in a positive sense corresponds to description of γ in a negative sense.

Assuming circulation $K = 2\pi A_0$ around the aerofoil, a suitable complex potential function is

$$\Omega = iA_0\{\log z' - \log(z'+2ib)\} + \sum_{n=1}^{\infty}\left\{\frac{A_n}{(z')^n} + \frac{\bar{A}_n}{(z'+2ib)^n}\right\} \tag{3.2}$$

which automatically makes the boundary wall $y' = -b$ a streamline, and vanishes at infinity. (Throughout this paper a bar placed over a quantity will be used to denote the complex conjugate of that quantity.) The method of solution is now similar to that given by Green, and we rewrite (3.2) in the form

$$\Omega = iA_0 \log z' + \sum_{n=1}^{\infty}\left\{\frac{A_n}{(z')^n} + B_n(z')^n\right\}, \tag{3.3}$$

omitting terms independent of z', which do not contribute to the forces acting. Here

$$B_n = {}^n\alpha_0 A_0 b^{-n} + \sum_{r=1}^{\infty} {}^n\alpha_r \bar{A}_r b^{-(n+r)} \tag{3.4}$$

and

$${}^n\alpha_0 = \frac{i^{n+1}}{n.2^n}, \qquad {}^n\alpha_r = \binom{n+r-1}{n}\frac{i^{n-r}}{2^{n+r}} \quad (n, r \geqslant 1). \tag{3.5}$$

To satisfy the boundary condition on the aerofoil we need to express Ω as a function of t. Using (3.1) and omitting terms independent of t we have the results

$$(z')^{-r} = \sum_{n=r}^{\infty} {}^r\beta_n t^n, \quad \log z' = -\log t + \sum_{n=0}^{\infty} {}^0\beta_n t^n, \quad (z')^r = \sum_{n=-r}^{\infty} {}^r\gamma_n t^n, \tag{3.6}$$

where the coefficients ${}^0\beta_n$, ${}^r\beta_n$, ${}^r\gamma_n$ are easily expressed in terms of a_n. Thus in terms of t, Ω becomes

$$\Omega = -iA_0 \log t + \sum_{n=1}^{\infty}(C_n t^n + D_n t^{-n}), \tag{3.7}$$

where

$$C_n = i\,{}^0\beta_n A_0 + \sum_{r=1}^{n} {}^r\beta_n A_r + \sum_{r=1}^{\infty} {}^r\gamma_n B_r, \qquad D_n = \sum_{r=n}^{\infty} {}^r\gamma_{-n} B_r. \tag{3.8}$$

The boundary condition on the aerofoil is equivalent to

$$\operatorname{im}\{\Omega + \bar{w}'z'(t) - \tfrac{1}{2}i\omega z'(t)\bar{z}'(\bar{t})\} = \text{constant} \tag{3.9}$$

on the aerofoil $t\bar{t} = 1$, where $w' = u' + iv'$ is the complex velocity of the origin of coordinates, referred to the z'-axes.

Now on the aerofoil

$$\left.\begin{aligned} z'(t)\bar{z}'(\bar{t}) &= \sum_{n=0}^{\infty} b_n t^n + \sum_{n=1}^{\infty} \bar{b}_n t^{-n} \\ \text{where} \qquad b_r &= \sum_{n=r}^{\infty} \bar{a}_{n-r} a_n \end{aligned}\right\}. \tag{3.10}$$

Hence, equating coefficients of t^n to the conjugates of coefficients of $\bar{t}^n$, (3.9) gives the relations

$$\left.\begin{aligned} C_n+\bar{w}'a_{n+1}e^{i\theta} &= \bar{D}_n+i\omega b_n \quad (n>1) \\ C_1+\bar{w}'a_2 e^{i\theta} &= \bar{D}_1+i\omega b_1+w'e^{-i\theta}\bar{a}_0 \end{aligned}\right\}. \tag{3.11}$$

We now need to find the coefficients A_n, and following Green we assume that

$$A_n = \sum_{k=0}^{\infty} {}^nA_k b^{-k} \quad (n \geqslant 0). \tag{3.12}$$

Thus from (3.4) and (3.8) we obtain the expansions

$$B_n = \sum_{k=0}^{\infty} \left\{ {}^n\alpha_0 {}^0A_k + \sum_{r=1}^{\infty} {}^n\alpha_r {}^r\bar{A}_k b^{-r} \right\} b^{-(n+k)}, \tag{3.13}$$

$$\left.\begin{aligned} C_n = \sum_{k=0}^{\infty} \left\{ i\,{}^0\beta_n {}^0A_k + \sum_{r=1}^{n} {}^r\beta_n {}^rA_k \right\} b^{-k} + \sum_{k=1}^{\infty} \sum_{m=1}^{k} {}^m\gamma_n {}^m\alpha_0 {}^0A_{k-m} b^{-k} + \\ + \sum_{k=2}^{\infty} \sum_{r=1}^{k-1} \sum_{m=1}^{r} {}^m\gamma_n {}^m\alpha_{k-r} {}^{k-r}\bar{A}_{r-m} b^{-k} \\ D_n = \sum_{k=n}^{\infty} \sum_{m=n}^{k} {}^m\gamma_{-n} {}^m\alpha_0 {}^0A_{k-m} b^{-k} + \\ + \sum_{k=n+1}^{\infty} \sum_{r=n}^{k-1} \sum_{m=n}^{r} {}^m\gamma_{-n} {}^m\alpha_{k-r} {}^{k-r}\bar{A}_{r-m} b^{-k} \end{aligned}\right\}. \tag{3.14}$$

The boundary conditions (3.11) must be true for every value of b, so that using (3.14) and equating coefficients of corresponding powers of b^{-1}, we obtain the relations

$$\left.\begin{aligned} i\,{}^0\beta_1 {}^0A_0 + {}^1\beta_1 {}^1A_0 + \bar{w}'e^{i\theta}a_2 &= i\omega b_1 + w'e^{-i\theta}\bar{a}_0 \\ i\,{}^0\beta_n {}^0A_0 + \sum_{r=1}^{n} {}^r\beta_n {}^rA_0 + \bar{w}'e^{i\theta}a_{n+1} &= i\omega b_n \quad (n \geqslant 2) \end{aligned}\right\}, \tag{3.15}$$

$$i\,{}^0\beta_n {}^0A_1 + \sum_{r=1}^{n} {}^r\beta_n {}^rA_1 + {}^1\gamma_n {}^1\alpha_0 {}^0A_0 = \begin{cases} {}^1\bar{\gamma}_{-1} {}^1\bar{\alpha}_0 {}^0A_0 & (n=1) \\ 0 & (n>1) \end{cases}, \tag{3.16}$$

$$\left.\begin{aligned} & i\,{}^0\beta_n {}^0A_k + \sum_{r=1}^{n} {}^r\beta_n {}^rA_k + \sum_{m=1}^{k} {}^m\gamma_n {}^m\alpha_0 {}^0A_{k-m} + \sum_{r=1}^{k-1} \sum_{m=1}^{r} {}^m\gamma_n {}^m\alpha_{k-r} {}^{k-r}\bar{A}_{r-m} \\ & = \begin{cases} \displaystyle\sum_{m=n}^{k} {}^m\bar{\gamma}_{-n} {}^m\bar{\alpha}_0 {}^0A_{k-m} + \sum_{r=n}^{k-1} \sum_{m=n}^{r} {}^m\bar{\gamma}_{-n} {}^m\bar{\alpha}_{k-r} {}^{k-r}A_{r-m} & (k \geqslant 2,\ k>n) \\ {}^k\bar{\gamma}_{-k} {}^k\bar{\alpha}_0 {}^0A_0 \quad (n=k\geqslant 2) \\ 0 \quad (n>k\geqslant 2) \end{cases} \end{aligned}\right\}. \tag{3.17}$$

By means of these equations the coefficients ${}^nA_k$ for $n \geqslant 1$ can be expressed successively in terms of the circulation coefficients ${}^0A_k$, and then the potential function Ω is completely defined in terms of these coefficients.

4. The forces and couple on the aerofoil in terms of Ω

The force components Y', X' and the moment of the couple Γ about the origin are given by the integrals

$$Y'+iX' = \int_C p\, d\bar{z}', \qquad \Gamma = \mathrm{re} \int_C pz'\, d\bar{z}' \tag{4.1}$$

taken round the boundary curve C of the aerofoil, p being the pressure at any point of the surface. Here the dashes denote that the particular quantities in question are referred to the (x', y')-axes. The pressure distribution throughout the fluid of density ρ is given by

$$p = \text{constant} - \tfrac{1}{2}\rho(u^2+v^2) + \tfrac{1}{2}\rho\left(\frac{\partial\Omega}{\partial\tau}+\frac{\partial\overline{\Omega}}{\partial\tau}\right),$$

where u, v are the components of the velocity of the fluid referred to a set of axes fixed in space. But the axes (x, y) to which Ω may be referred are moving axes, and if we make our fixed axes coincide instantaneously with the position of these moving axes, then

$$\frac{\partial\Omega}{\partial z} = -u+iv, \quad \text{i.e.} \quad u^2+v^2 = \frac{\partial\Omega}{\partial z}\frac{\partial\overline{\Omega}}{\partial\bar{z}},$$

and since $z' = ze^{i\theta}$, $\bar{z}' = \bar{z}e^{-i\theta}$, we also have

$$u^2+v^2 = \frac{\partial\Omega}{\partial z'}\frac{\partial\overline{\Omega}}{\partial\bar{z}'}.$$

Again, by employing well-known methods (cf. (**6**)), we find that

$$\frac{\partial\Omega}{\partial\tau} = -(w'e^{-i\theta}+i\omega z)\frac{\partial\Omega}{\partial z}+\omega\frac{\partial\Omega}{\partial\theta}+v'\frac{\partial\Omega}{\partial b}+\dot{w}'\frac{\partial\Omega}{\partial w'}+\dot{\bar{w}}'\frac{\partial\Omega}{\partial\bar{w}'}+\dot{\omega}\frac{\partial\Omega}{\partial\omega},$$

where the first two terms take account of the moving axes, and the remaining terms allow for the fact that Ω is a function of θ, b, w', $\bar{w}'$, and ω, which may all vary with time. Allowance has been made for a variable circulation K by assuming it can be expressed as

$$K = K(w', \bar{w}', \theta, \omega, b).$$

Thus the pressure equation may be written in terms of t as

$$\frac{2p}{\rho} = \text{constant} - \frac{\partial\Omega}{\partial t}\frac{\partial\overline{\Omega}}{\partial\bar{t}}\left(\frac{dz'}{dt}\frac{d\bar{z}'}{d\bar{t}}\right)^{-1} - (w'e^{-i\theta}+i\omega z)\frac{\partial\Omega}{\partial t}\left(\frac{dz}{dt}\right)^{-1} -$$

$$-(\bar{w}'e^{i\theta}-i\omega\bar{z})\frac{\partial\overline{\Omega}}{\partial\bar{t}}\left(\frac{d\bar{z}}{d\bar{t}}\right)^{-1}+\left(\omega\frac{\partial}{\partial\theta}+v'\frac{\partial}{\partial b}+\dot{w}'\frac{\partial}{\partial w'}+\dot{\bar{w}}'\frac{\partial}{\partial\bar{w}'}+\dot{\omega}\frac{\partial}{\partial\omega}\right)(\Omega+\overline{\Omega}),$$

and then the forces are given by

$$Y'+iX' = \int_C p\, d\bar{z}' = -\int_\gamma p\frac{d\bar{z}'}{d\bar{t}}\, d\bar{t}$$

and the couple by

$$\Gamma = -\mathrm{re}\int_\gamma pz'\frac{d\bar{z}'}{d\bar{t}}\, d\bar{t}.$$

By using expression (3.7) for Ω it is now possible to calculate the forces and couple. In the first place we need several expansions about $t = 0$. These are:

$$\left.\begin{aligned} \left(\frac{dz}{dt}\right)^{-1} &= -t^2 \sum_{n=0}^{\infty} c_n t^n \\ \text{where} \quad c_0 = \frac{1}{a_0}, \quad c_1 = 0, \quad c_2 = \frac{a_2}{a_0^2}, \quad c_3 = \frac{2a_3}{a_0^2}, \quad c_4 &= \frac{3a_0a_4+a_2^2}{a_0^3} \\ c_5 = \frac{4(a_0a_5+a_2a_3)}{a_0^3}, \quad c_6 &= \frac{5a_0^2a_6+4a_0a_3^2+6a_0a_2a_4+a_2^3}{a_0^4}, \text{ etc.} \end{aligned}\right\}; \quad (4.2)$$

$$\left.\begin{aligned} z\left(\frac{dz}{dt}\right)^{-1} &= -t \sum_{n=0}^{\infty} g_n t^n \\ \text{where} \quad g_n &= \sum_{r=0}^{n} a_r c_{n-r} \end{aligned}\right\}. \quad (4.3)$$

Now on γ, $\dfrac{d\bar{z}}{d\bar{t}} = t^2 \sum_{n=0}^{\infty} (n-1)\bar{a}_n t^{-n}$, and so we obtain the expansions about $t = 0$:

$$\left.\begin{aligned} \left(\frac{dz}{dt}\right)^{-1} \frac{d\bar{z}}{d\bar{t}} &= -t^4\Big(\sum_{n=0}^{\infty} d_n t^n + \sum_{n=1}^{\infty} d'_n t^{-n}\Big) \\ \text{where} \quad d_n = \sum_{r=0}^{\infty} (r-1)c_{n+r}\bar{a}_r, \quad d'_n &= \sum_{r=0}^{\infty} (n+r-1)\bar{a}_{n+r}c_r \end{aligned}\right\} \quad (4.4)$$

$$\left.\begin{aligned} \text{and} \quad z\left(\frac{dz}{dt}\right)^{-1} \frac{d\bar{z}}{d\bar{t}} &= -t^3\Big(\sum_{n=0}^{\infty} h_n t^n + \sum_{n=1}^{\infty} h'_n t^{-n}\Big) \\ \text{where} \quad h_n = \sum_{r=0}^{\infty} (r-1)g_{n+r}\bar{a}_r, \quad h'_n &= \sum_{r=0}^{\infty} (n+r-1)g_r\bar{a}_{n+r} \end{aligned}\right\}. \quad (4.5)$$

$$\left.\begin{aligned} \text{Also} \quad z^2\left(\frac{dz}{dt}\right)^{-1} \frac{d\bar{z}}{d\bar{t}} &= -t^2\Big(\sum_{n=0}^{\infty} l_n t^n + \sum_{n=1}^{\infty} l'_n t^{-n}\Big) \\ \text{where} \quad l'_n = \sum_{r=0}^{\infty} h'_{n+r}a_r, \quad l_n &= \sum_{r=0}^{n} h_{n-r}a_r + \sum_{r=1}^{\infty} a_{n+r}h'_r \end{aligned}\right\}. \quad (4.6)$$

Using these results we may proceed with the evaluation of the integrals occurring in the expressions for the forces and couple. The integration is quite straightforward, and the integrals have poles at $t = 0$. When the integrand has a factor $(dz/dt)^{-1}$, we note that $(dz/dt)^{-1}$ is regular within and on γ provided that all the singular points of the transformation $z = z(t)$ lie within the original aerofoil contour C. In the usual case where the aerofoil has a sharp trailing edge, the transformation ceases to be conformal at this point, so that any integral involving $(dz/dt)^{-1}$ must include a partial residue at the trailing edge. This is avoided in the ordinary way by choosing the

circulation so that $\partial\Omega/\partial t = 0$ at the trailing edge. This is, of course, the usual Joukowski condition.

By employing these methods we find expressions for the forces and couple in the form:

$$\left.\begin{aligned}\frac{Y'+iX'}{\rho\pi i e^{-i\theta}} = &-iA_0\sum_{n=1}^{\infty} nc_{n-1}(\bar{C}_n+D_n)+\\ &+\sum_{n=1}^{\infty}c_{n-1}\Big\{\sum_{r=1}^{\infty}r(n+r)(C_r\bar{C}_{n+r}+\bar{D}_r D_{n+r})\Big\}-\\ &-\sum_{n=2}^{\infty}c_{n-1}\Big\{\sum_{r=1}^{n-1}r(n-r)\bar{C}_r D_{n-r}\Big\}-i\bar{w}'e^{i\theta}A_0+\\ &+w'e^{-i\theta}\Big(-iA_0 d_2'+\sum_{n=1}^{\infty}nd_{n+2}'C_n-\\ &\qquad-\sum_{n=2}^{\infty}nd_{n-2}D_n-D_1d_1'\Big)+\\ &+i\omega\Big(iA_0(\bar{a}_1-h_1')+\sum_{n=1}^{\infty}n(C_nh_{n+1}'-D_nh_{n-1}-\\ &\qquad-\bar{a}_{n+1}\bar{D}_n)+\bar{C}_1\bar{a}_0\Big)+\\ &+\Big(\omega\frac{\partial}{\partial\theta}+v'\frac{\partial}{\partial b}+\dot{w}'\frac{\partial}{\partial w'}+\dot{\bar{w}}'\frac{\partial}{\partial\bar{w}'}+\dot{\omega}\frac{\partial}{\partial\omega}\Big)\times\\ &\times\Big\{2iA_0\Big(\bar{a}_0+\sum_{n=2}^{\infty}\bar{a}_n\Big)-\bar{a}_0(\bar{C}_1+D_1)+\\ &\qquad+\sum_{n=1}^{\infty}n\bar{a}_{n+1}(C_n+\bar{D}_n)\Big\}\end{aligned}\right\},\tag{4.7}$$

and

$$\left.\begin{aligned}\frac{\Gamma}{\pi\rho} = \mathrm{im}\Big[&\sum_{n=2}^{\infty}g_n\Big\{\sum_{r=1}^{n-1}r(n-r)\bar{C}_rD_{n-r}\Big\}-\\ &-w'e^{-i\theta}\Big\{-iA_0h_1'+\sum_{n=1}^{\infty}n(C_nh_{n+1}'-D_nh_{n-1})\Big\}-\\ &-\sum_{n=1}^{\infty}g_n\Big\{-iA_0n(\bar{C}_n+D_n)+\sum_{r=1}^{\infty}r(n+r)(C_r\bar{C}_{n+r}+\bar{D}_rD_{n+r})\Big\}+\\ &+\bar{w}'e^{i\theta}\Big\{iA_0a_1-\bar{D}_1a_0+\sum_{n=1}^{\infty}n\bar{C}_na_{n+1}\Big\}-\\ &-i\omega\Big\{iA_0(b_0-l_0)+\sum_{n=1}^{\infty}n(C_nl_n'-D_nl_n+\bar{C}_nb_n-\bar{D}_n\bar{b}_n)\Big\}-\\ &-\Big(\omega\frac{\partial}{\partial\theta}+v'\frac{\partial}{\partial b}+\dot{w}'\frac{\partial}{\partial w'}+\dot{\bar{w}}'\frac{\partial}{\partial\bar{w}'}+\dot{\omega}\frac{\partial}{\partial\omega}\Big)\times\\ &\times\Big\{2iA_0\sum_{n=1}^{\infty}\bar{b}_n+\sum_{n=1}^{\infty}(\bar{C}_n+D_n)\Big(\sum_{r=0}^{\infty}(r-1)a_{n+r}\bar{a}_r\Big)+\\ &\qquad+\sum_{n=1}^{\infty}(C_n+\bar{D}_n)\Big(\sum_{r=0}^{\infty}(n+r-1)\bar{a}_{n+r}a_r\Big)\Big\}\Big].\end{aligned}\right\}\tag{4.8}$$

By using equations (3.11) and (3.14) in conjunction with (4.8) and (4.7) it is possible to express the forces and couple as power series in b^{-1}, i.e. we can write

$$Y'+iX' = \sum_{k=0}^{\infty} (Y'_k+iX'_k)b^{-k}, \qquad \Gamma = \sum_{k=0}^{\infty} \Gamma_k b^{-k}. \tag{4.9}$$

This process will not be carried out for the general aerofoil defined by (3.1) as the expressions become so long and complicated that little of relevance can be deduced from them. Accordingly we shall consider later the expression of the forces and couple as power series, when three specific types of aerofoil will be considered in order to assess the effects of thickness and camber.

5. The Joukowski condition

To discuss fully the forces acting on the aerofoil, it is desirable to obtain a value for the circulation. The usual procedure is adopted of choosing the circulation so that the fluid leaves the trailing edge smoothly, and since the transformation (3.1) can always be chosen so that the trailing edge corresponds to $t = -1$, we have the condition $\partial\Omega/\partial t = 0$ at $t = -1$. From (3.7) this gives

$$A_0 - iw'e^{-i\theta}\bar{a}_0 + i\sum_{n=1}^{\infty}(-1)^n n(\bar{D}_n - D_n + i\omega b_n - \bar{w}'e^{i\theta}a_{n+1}) = 0,$$

using the boundary condition (3.11). Thus we have:

$${}^0A_0 = i(w'e^{-i\theta}\bar{a}_0 - \bar{w}'e^{i\theta}a_0) + \omega\sum_{n=1}^{\infty}(-1)^n n b_n,$$

$${}^0A_1 = -\tfrac{1}{2}i(\bar{a}_0 e^{-i\theta} - a_0 e^{i\theta})\,{}^0A_0,$$

$${}^0A_k = i\sum_{n=1}^{k}\sum_{m=n}^{k}(-1)^{n+1}n({}^m\bar{\gamma}_{-n}\,{}^m\bar{\alpha}_0\,{}^0A_{k-m} - {}^m\gamma_{-n}\,{}^m\alpha_0\,{}^0A_{k-m}) +$$

$$+ i\sum_{n=1}^{k-1}\sum_{r=n}^{k-1}\sum_{m=n}^{r}(-1)^{n+1}n({}^m\bar{\gamma}_{-n}\,{}^m\bar{\alpha}_{k-r}\,{}^{k-r}A_{r-m} - {}^m\gamma_{-n}\,{}^m\alpha_{k-r}\,{}^{k-r}\bar{A}_{r-m}) \qquad (k \geqslant 2)$$

equating to zero the coefficient of each power of b^{-1}.

The complex potential function Ω, and hence the forces and couple, are now uniquely determined.

6. The flat plate aerofoil

Here the transformation (3.1) assumes a particularly simple form, and if the plate is instantaneously inclined to the plane boundary at an angle θ,

then our transformations are

$$z = \frac{l}{4}(t^{-1}+t), \qquad z' = ze^{i\theta}, \tag{6.1}$$

l being the length of the plate. Expanding the forces and couple in the form (4.9) we find that:

$$\left.\begin{aligned}
\frac{Y_0'}{\pi\rho} &= lu'(u'\sin\theta - v'\cos\theta) - \frac{l^2}{8}\cos\theta\{2(\dot{u}'\sin\theta - \dot{v}'\cos\theta) + l\dot{\omega}\} \\
\frac{Y_1'}{\pi\rho} &= -\frac{l^2}{4}(u'\sin\theta - v'\cos\theta)\left\{(2u'\sin\theta - v'\cos\theta) + \omega\frac{l}{4}(1+\sin^2\theta)\right\} + \\
&\quad + \left(\frac{l}{4}\right)^3\left\{2(\dot{u}'\sin\theta - \dot{v}'\cos\theta) + \dot{\omega}\frac{l}{2}\right\}\sin 2\theta \\
\frac{Y_2'}{\pi\rho} &= \frac{l^3}{16}(u'\sin\theta - v'\cos\theta)\{u'(1+3\sin^2\theta) - 2v'\sin 2\theta\} + \\
&\quad + 4\omega^2\left(\frac{l}{4}\right)^5(4-3\sin^2\theta)\sin\theta - \\
&\quad - \frac{\omega l^4}{64}\{u'(1-9\sin^2\theta+4\sin^4\theta) + \tfrac{1}{2}v'\sin 2\theta(9-4\sin^2\theta)\} - \\
&\quad - 4\dot{\omega}\left(\frac{l}{4}\right)^5\cos^3\theta - 2\left(\frac{l}{4}\right)^4(\dot{u}'\sin\theta - \dot{v}'\cos\theta)(3-2\sin^2\theta)\cos\theta
\end{aligned}\right\}, \tag{6.2}$$

$$\left.\begin{aligned}
\frac{X_0'}{\pi\rho} &= -lv'(u'\sin\theta - v'\cos\theta) + \frac{l^2}{8}\sin\theta\{2(\dot{u}'\sin\theta - \dot{v}'\cos\theta) + l\dot{\omega}\} \\
\frac{X_1'}{\pi\rho} &= \frac{l^2}{4}(u'\sin\theta - v'\cos\theta)\left(v' - \omega\frac{l}{4}\cos\theta\right)\sin\theta - \\
&\quad - \left(\frac{l}{4}\right)^3\sin^2\theta\{4(\dot{u}'\sin\theta - \dot{v}'\cos\theta) + l\dot{\omega}\} \\
\frac{X_2'}{\pi\rho} &= -\frac{l^3}{16}v'(u'\sin\theta - v'\cos\theta)\cos^2\theta - 6\omega^2\left(\frac{l}{4}\right)^5\sin\theta\sin 2\theta + \\
&\quad + 4\omega\left(\frac{l}{4}\right)^4\{u'\sin\theta\cos\theta(1-4\sin^2\theta) + v'(5-4\sin^2\theta)\sin^2\theta\} + \\
&\quad + 2\left(\frac{l}{4}\right)^4(\dot{u}'\sin\theta - \dot{v}'\cos\theta)(3-2\sin^2\theta)\sin\theta + 2\dot{\omega}\left(\frac{l}{4}\right)^5\cos\theta\sin 2\theta
\end{aligned}\right\}, \tag{6.3}$$

and

$$\left.\begin{aligned}
\frac{\Gamma_0}{\pi\rho} &= \frac{l^2}{4}(u'\cos\theta+v'\sin\theta)\left\{(u'\sin\theta-v'\cos\theta)-\omega\frac{l}{4}\right\}- \\
&\qquad -\frac{l^3}{16}(\dot{u}'\sin\theta-\dot{v}'\cos\theta)-6\dot{\omega}\left(\frac{l}{4}\right)^4 \\
\frac{\Gamma_1}{\pi\rho} &= -\frac{l^3}{16}(u'\sin\theta-v'\cos\theta)(u'\sin 2\theta-v'\cos 2\theta)+ \\
&\quad +4\omega^2\left(\frac{l}{4}\right)^5\cos\theta+4\dot{\omega}\left(\frac{l}{4}\right)^5\sin\theta+4\left(\frac{l}{4}\right)^4(\dot{u}'\sin\theta-\dot{v}'\cos\theta)\sin\theta \\
\frac{\Gamma_2}{\pi\rho} &= 2\left(\frac{l}{4}\right)^4(u'\sin\theta-v'\cos\theta)\times \\
&\qquad \times\{u'\cos\theta(1+10\sin^2\theta)-v'\sin\theta(9-10\sin^2\theta)\}- \\
&\quad -\omega\left(\frac{l}{4}\right)^5\{u'\cos\theta(5-34\sin^2\theta)+v'\sin\theta(37-34\sin^2\theta)\}+ \\
&\quad +6\omega^2\left(\frac{l}{4}\right)^6\sin 2\theta-\left(\frac{l}{4}\right)^5(\dot{u}'\sin\theta-\dot{v}'\cos\theta)(5-2\sin^2\theta)- \\
&\quad -\dot{\omega}\left(\frac{l}{4}\right)^6(3-2\sin^2\theta)
\end{aligned}\right\}. \qquad (6.4)$$

7. The symmetrical aerofoil of small thickness

Consideration of this aerofoil enables us to assess the effect of thickness on the results. The appropriate coefficients a_n have been given by Fujikawa (5) in the form

$$\left.\begin{aligned}
a_0 &= \frac{l}{4}(1+\epsilon-\epsilon^2), \qquad a_1 = \frac{l}{4}\epsilon, \qquad a_2 = \frac{l}{4}(1-\epsilon) \\
a_3 &= -\frac{l}{4}\epsilon(1-2\epsilon), \qquad a_4 = \frac{l}{4}\epsilon^2, \qquad a_n = 0 \quad (n>4)
\end{aligned}\right\}, \qquad (7.1)$$

where ϵ is small and real, and l is the aerofoil chord. It may easily be shown that the thickness ratio of the aerofoil, defined as usual by the ratio of maximum thickness to chord length, is given by $\frac{3\sqrt{3}}{4}\epsilon(1-\epsilon)$. For most purposes it is sufficiently accurate to neglect the square of ϵ, but we shall retain it for purposes of comparison with Fujikawa.

The power series expansions for the forces thus become:

$$\left.\begin{aligned}
\frac{Y_0'}{\pi\rho} &= l(1+\epsilon-\epsilon^2)u'(u'\sin\theta-v'\cos\theta)- \\
&\quad -\epsilon^2\omega\left(\frac{l}{4}\right)^2\{u'(15-8\sin^2\theta)+4v'\sin 2\theta\}- \\
&\quad -2\omega^2\left(\frac{l}{4}\right)^3\epsilon(2-3\epsilon)\sin\theta- \\
&\quad -\left(\frac{l}{4}\right)^2[4(1+\epsilon)(\dot{u}'\sin\theta-\dot{v}'\cos\theta)\cos\theta+2\epsilon^2\dot{u}'\sin 2\theta+ \\
&\qquad +\epsilon^2\dot{v}'(3+4\sin^2\theta)+2\dot{\omega}l\cos\theta(1+\tfrac{1}{2}\epsilon-\tfrac{5}{4}\epsilon^2)] \\
\frac{Y_1'}{\pi\rho} &= -\frac{l^2}{4}(1+2\epsilon-\epsilon^2)(u'\sin\theta-v'\cos\theta)(2u'\sin\theta-v'\cos\theta)+ \\
&\quad +8\epsilon^2\omega^2\left(\frac{l}{4}\right)^4(2-\sin^2\theta)- \\
&\quad -\omega\frac{l^3}{16}\{(1+2\epsilon)(1+\sin^2\theta)(u'\sin\theta-v'\cos\theta)- \\
&\qquad -\epsilon^2 u'\sin\theta(11-3\sin^2\theta)+\epsilon^2 v'\cos\theta(7-3\sin^2\theta)\}+ \\
&\quad +2(1+2\epsilon+\epsilon^2)\left(\frac{l}{4}\right)^3\left\{(\dot{u}'\sin\theta-\dot{v}'\cos\theta)+\dot{\omega}\frac{l}{4}\right\}\sin 2\theta \\
\frac{Y_2'}{\pi\rho} &= \frac{l^3}{16}(u'\sin\theta-v'\cos\theta)\{u'(1+3\sin^2\theta)-2v'\sin 2\theta+ \\
&\quad +\tfrac{1}{2}\epsilon u'(7+18\sin^2\theta)-5\epsilon v'\sin 2\theta+\tfrac{1}{4}\epsilon^2 u'(3+4\sin^2\theta)\}- \\
&\quad -2\omega\left(\frac{l}{4}\right)^4[2u'(1-9\sin^2\theta+4\sin^4\theta)+v'\sin 2\theta(9-4\sin^2\theta)+ \\
&\qquad +\epsilon\{u'(1-32\sin^2\theta+4\sin^4\theta)+v'\sin 2\theta(17-2\sin^2\theta)\}+ \\
&\qquad +\epsilon^2\{u'(59-8\sin^2\theta)\sin^2\theta-v'\sin 2\theta(53-40\sin^2\theta)\}]+ \\
&\quad +\omega^2\left(\frac{l}{4}\right)^5\sin\theta[4(4-3\sin^2\theta)+\epsilon(21-8\sin^2\theta)- \\
&\qquad -\epsilon^2(99-80\sin^2\theta)]- \\
&\quad -\dot{\omega}\left(\frac{l}{4}\right)^5\cos\theta\{4\cos^2\theta+8\epsilon-\epsilon^2(15-32\sin^2\theta)\}- \\
&\quad -\left(\frac{l}{4}\right)^4[(\dot{u}'\sin\theta-\dot{v}'\cos\theta)\cos\theta\{2(3-2\sin^2\theta)+11\epsilon\}+ \\
&\quad +\epsilon^2\{-\tfrac{3}{2}\dot{u}'\sin 2\theta(1-8\sin^2\theta)+\dot{v}'(5-27\sin^2\theta+24\sin^4\theta)\}]
\end{aligned}\right\}, \qquad (7.2)$$

and

$$\left.\begin{aligned}
\frac{X_0'}{\pi\rho} &= -l(1+\epsilon-\epsilon^2)v'(u'\sin\theta-v'\cos\theta)+\\
&\quad+\epsilon^2\omega\left(\frac{l}{4}\right)^2\{4u'\sin 2\theta+v'(7+8\sin^2\theta)\}-\\
&\quad-2\epsilon\left(\frac{l}{4}\right)^3\omega^2(2-3\epsilon)\cos\theta+\\
&\quad+\left(\frac{l}{4}\right)^2[4(1+\epsilon)(\dot u'\sin\theta-\dot v'\cos\theta)\sin\theta-\epsilon^2(7-4\sin^2\theta)\dot u'-\\
&\quad-2\epsilon^2\dot v'\sin 2\theta+2\dot\omega l\sin\theta(1+\tfrac12\epsilon-\tfrac54\epsilon^2)]\\
\frac{X_1'}{\pi\rho} &= \frac{l^2}{4}(1+2\epsilon-\epsilon^2)(u'\sin\theta-v'\cos\theta)v'\sin\theta-4\epsilon^2\omega^2\left(\frac{l}{4}\right)^4\sin 2\theta-\\
&\quad-\frac{\omega l^3}{32}[(u'\sin\theta-v'\cos\theta)\sin 2\theta-\\
&\qquad-2\epsilon\{u'\cos\theta\cos 2\theta+v'\sin\theta(3-2\sin^2\theta)\}-\\
&\qquad\quad-\epsilon^2\{3u'\cos\theta\cos 2\theta+v'\sin\theta(1-6\sin^2\theta)\}]-\\
&\quad-\frac{l^3}{16}(\dot u'\sin\theta-\dot v'\cos\theta)\left\{\sin^2\theta-\epsilon\cos 2\theta+\frac{\epsilon^2}{2}(3-2\sin^2\theta)\right\}-\\
&\quad-4\dot\omega\left(\frac{l}{4}\right)^4\left\{\sin^2\theta-\epsilon\cos 2\theta-\frac{\epsilon^2}{2}(3+2\sin^2\theta)\right\}\\
\frac{X_2'}{\pi\rho} &= -\frac{l^3}{16}v'(u'\sin\theta-v'\cos\theta)\left\{\cos^2\theta+\frac{\epsilon}{2}(7-2\sin^2\theta)+\right.\\
&\qquad\qquad\left.+\frac{\epsilon^2}{4}(3+4\sin^2\theta)\right\}+\\
&\quad+2\omega\left(\frac{l}{4}\right)^4\left[u'\sin 2\theta(1-4\sin^2\theta)+2v'\sin^2\theta(5-4\sin^2\theta)+\right.\\
&\qquad+\epsilon\left\{-\frac{u'}{2}\sin 2\theta(5+4\sin^2\theta)+v'\cos^2\theta(3+4\sin^2\theta)\right\}+\\
&\qquad\quad\left.+\epsilon^2\{-5u'\sin 4\theta+2v'(6-27\sin^2\theta+20\sin^4\theta)\}\right]-\\
&\quad-\omega^2\left(\frac{l}{4}\right)^5\cos\theta\{12\sin^2\theta+\epsilon(5+8\sin^2\theta)+\epsilon^2(17-80\sin^2\theta)\}+\\
&\quad+\dot\omega\left(\frac{l}{4}\right)^5\sin\theta\{4\cos^2\theta+2\epsilon-\epsilon^2(31-32\sin^2\theta)\}+\\
&\quad+\left(\frac{l}{4}\right)^4[(\dot u'\sin\theta-\dot v'\cos\theta)\sin\theta\{2(3-2\sin^2\theta)+5\epsilon\}-\\
&\quad-\epsilon^2\dot u'(2+19\sin^2\theta-24\sin^4\theta)+\tfrac12\dot v'\epsilon^2\sin 2\theta(19-24\sin^2\theta)]
\end{aligned}\right\}. \quad (7.3)$$

(7.2)

8. The circular arc aerofoil of small camber

Green (**1**) has obtained the coefficients a_n for a circular arc aerofoil of chord l inclined to the boundary wall at an angle θ, and subtending an angle 4α at its centre. The camber σ of this aerofoil is, of course, given by $\sigma = \frac{1}{2}\tan\alpha$. Applying our restriction that the camber is small, we may write $\epsilon_1 = \tan\alpha$ and neglect third and higher powers of ϵ_1. Thus the coefficients a_n become:

$$\left.\begin{aligned} a_0 &= \frac{l}{4}(1+i\epsilon_1), \qquad a_1 = -i\epsilon_1\frac{l}{4}, \qquad a_2 = \frac{l}{4}(1-i\epsilon_1-\epsilon_1^2),\\ a_3 &= -\frac{l}{4}\epsilon_1(i+2\epsilon_1), \qquad a_4 = -\frac{l}{4}\epsilon_1^2, \qquad a_n = 0 \quad (n>4) \end{aligned}\right\}. \tag{8.1}$$

After suitable reduction the expansions for the forces Y' and X' become:

$$\left.\begin{aligned} \frac{Y'_0}{\pi\rho} &= lu'\{(u'\sin\theta - v'\cos\theta)+\epsilon_1(u'\cos\theta+v'\sin\theta)\}+2\omega^2\left(\frac{l}{4}\right)^3\epsilon_1\cos\theta\\ &\quad+\omega\frac{l^2}{4}\epsilon_1[u'\sin 2\theta - v'(3-2\sin^2\theta)+2\epsilon_1\{u'(3-2\sin^2\theta)+v'\sin 2\theta\}]\\ &\quad-\frac{l^2}{4}\Big[(\dot u'\sin\theta-\dot v'\cos\theta)\cos\theta+\dot\omega\frac{l}{2}\cos\theta+\\ &\qquad+\epsilon_1\Big(\tfrac{1}{2}\dot v'\sin 2\theta+\dot u'(2-\sin^2\theta)+\dot\omega\frac{l}{4}\sin^2\theta\Big)-\\ &\qquad-\tfrac{1}{2}\epsilon_1^2\{3\dot u'\sin 2\theta-3\dot v'(3-2\sin^2\theta)+\dot\omega l\cos\theta\}\Big],\\ \frac{Y'_1}{\pi\rho} &= -\frac{l^2}{4}\Big[(u'\sin\theta-v'\cos\theta)(2u'\sin\theta-v'\cos\theta)+\\ &\qquad+\epsilon_1(2u'^2\sin 2\theta-3u'v'\cos 2\theta-v'^2\sin 2\theta)+\\ &\qquad+\frac{\epsilon_1^2}{2}(4u'^2\cos^2\theta-3u'v'\sin 2\theta+2v'^2\sin^2\theta)\Big]-\\ &\quad-\omega\frac{l^3}{16}[(u'\sin\theta-v'\cos\theta)(1+\sin^2\theta+2\epsilon_1\sin 2\theta)+\\ &\qquad+\epsilon_1^2\{u'\sin\theta(15-10\sin^2\theta)-v'\cos\theta(9-10\sin^2\theta)\}]-\\ &\quad-4\omega^2\left(\frac{l}{4}\right)^4\epsilon_1\{\sin 2\theta+2\epsilon_1(3-2\sin^2\theta)\}+\\ &\quad+2\left(\frac{l}{4}\right)^3\Big[\Big(\dot u'\sin\theta-\dot v'\cos\theta+\dot\omega\frac{l}{4}\Big)\sin 2\theta+\\ &\qquad+2\epsilon_1\Big\{\dot u'(3-2\sin^2\theta)\sin\theta-2\dot v'\cos^3\theta+\dot\omega\frac{l}{4}(2-\sin^2\theta)\Big\}+\\ &\qquad+2\epsilon_1^2\Big\{2\dot u'\cos\theta\cos 2\theta+\dot v'(5-4\sin^2\theta)\sin\theta-\dot\omega\frac{l}{4}\sin 2\theta\Big\}\Big] \end{aligned}\right\}. \tag{8.2}$$

$$\frac{Y_2'}{\pi\rho}=\frac{l^3}{16}[(u'\sin\theta-v'\cos\theta)\{u'(1+3\sin^2\theta)-2v'\sin 2\theta\}+$$
$$+\tfrac{1}{2}\epsilon_1\{u'^2\cos\theta(1+10\sin^2\theta)-u'v'\sin\theta(17-26\sin^2\theta)+$$
$$+2v'^2\cos\theta(3-8\sin^2\theta)\}+$$
$$+\tfrac{1}{4}\epsilon_1^2\{u'^2\sin\theta(13-8\sin^2\theta)-u'v'\cos\theta(17-40\sin^2\theta)-$$
$$-4v'^2\sin\theta(7-8\sin^2\theta)\}]-$$
$$-2\omega\left(\frac{l}{4}\right)^4[2u'(1-9\sin^2\theta+4\sin^4\theta)+v'(9-4\sin^2\theta)\sin 2\theta+$$
$$+\epsilon_1\{-u'\sin 2\theta(11-6\sin^2\theta)+\tfrac{1}{2}v'(31-60\sin^2\theta+24\sin^4\theta)\}-$$
$$-\epsilon_1^2\{u'(20-21\sin^2\theta+12\sin^4\theta)+\tfrac{1}{2}v'\sin 2\theta(23-12\sin^2\theta)\}]+$$
$$+4\omega^2\left(\frac{l}{4}\right)^5[(4-3\sin^2\theta)\sin\theta+\tfrac{1}{4}\epsilon_1(13-4\sin^2\theta)\cos\theta+2\epsilon_1^2\sin\theta]-$$
$$-\left(\frac{l}{4}\right)^4[2(\dot u'\sin\theta-\dot v'\cos\theta)(3-2\sin^2\theta)\cos\theta+l\dot\omega\cos^3\theta+$$
$$+\epsilon_1\{\dot u'(4-9\sin^2\theta+8\sin^4\theta)+\tfrac{1}{2}\dot v'\sin 2\theta(5-8\sin^2\theta)-$$
$$-\tfrac{1}{4}\dot\omega l(3-4\sin^2\theta)\sin\theta\}+$$
$$+\epsilon_1^2\{-\tfrac{1}{2}\dot u'\sin 2\theta(23-8\sin^2\theta)+\dot v'(20-27\sin^2\theta+8\sin^4\theta)-$$
$$-\tfrac{3}{2}\dot\omega l\cos\theta\}]$$

and

$$\frac{X_0'}{\pi\rho}=-lv'\{(u'\sin\theta-v'\cos\theta)+\epsilon_1(u'\cos\theta+v'\sin\theta)\}-2\epsilon_1\omega^2\left(\frac{l}{4}\right)^3\sin\theta$$
$$-\epsilon\omega\frac{l^2}{4}[u'(1+2\sin^2\theta)-v'\sin 2\theta+2\epsilon_1\{u'\sin 2\theta+v'(1+2\sin^2\theta)\}]$$
$$+\frac{l^2}{8}\Big[2\Big(\dot u'\sin\theta-\dot v'\cos\theta+\dot\omega\frac{l}{2}\Big)\sin\theta+$$
$$+\epsilon_1\Big\{\dot u'\sin 2\theta+2\dot v'(1+\sin^2\theta)-\dot\omega\frac{l}{2}\cos\theta\Big\}-$$
$$-\epsilon_1^2\{3\dot u'(1+2\sin^2\theta)-3\dot v'\sin 2\theta+l\dot\omega\sin\theta\}\Big],$$
$$\frac{X_1'}{\pi\rho}=\frac{l^2}{4}v'[(u'\sin\theta-v'\cos\theta)\sin\theta+\epsilon_1(u'\sin 2\theta-v'\cos 2\theta)+$$
$$+\epsilon_1^2\cos\theta(u'\cos\theta+v'\sin\theta)]-$$
$$-\omega\frac{l^3}{16}\Big[(u'\sin\theta-v'\cos\theta)(\cos\theta-4\epsilon_1\sin\theta)\sin\theta+$$
$$+\frac{\epsilon_1^2}{2}\{-5u'(1+4\sin^2\theta)\cos\theta+v'\sin\theta(3-20\sin^2\theta)\}\Big]+$$

$$
\begin{aligned}
&+4\epsilon_1\omega^2\left(\frac{l}{4}\right)^4\{(1+2\sin^2\theta)+2\epsilon_1\sin 2\theta\}- \\
&-\frac{l^3}{16}\Big[\Big(\dot{u}'\sin\theta-\dot{v}'\cos\theta+\dot{\omega}\frac{l}{4}\Big)\sin^2\theta+ \\
&\quad+\epsilon_1\sin\theta\Big(\dot{u}'\sin 2\theta-\dot{v}'\cos 2\theta+\dot{\omega}\frac{l}{4}\cos\theta\Big)+ \\
&\quad+\frac{\epsilon_1^2}{2}\Big\{-\dot{u}'(1+8\sin^2\theta)\sin\theta+\dot{v}'\cos\theta(3+8\sin^2\theta)- \\
&\qquad-\dot{\omega}\frac{l}{4}(3+4\sin^2\theta)\Big\}\Big]
\end{aligned}
\Bigg\} \quad (8.3)
$$

$$
\begin{aligned}
\frac{X_2'}{\pi\rho} = &-\frac{l^3}{16}v'\Big[(u'\sin\theta-v'\cos\theta)\cos^2\theta+\frac{\epsilon_1}{2}\{u'(1-6\sin^2\theta)\cos\theta+ \\
&\quad+v'(5-6\sin^2\theta)\sin\theta\}- \\
&\quad-\frac{\epsilon_1^2}{4}\{3u'(1-8\sin^2\theta)\sin\theta+v'(5+24\sin^2\theta)\cos\theta\}\Big]+ \\
&+2\omega\left(\frac{l}{4}\right)^4\Big[u'(1-4\sin^2\theta)\sin 2\theta+2v'(5-4\sin^2\theta)\sin^2\theta+ \\
&\quad+\frac{\epsilon_1}{4}\{-u'(10+38\sin^2\theta-48\sin^4\theta)+2v'\sin 2\theta(5-12\sin^2\theta)\}- \\
&\quad-\epsilon_1^2\{2u'(2-3\sin^2\theta)\sin 2\theta+v'(5+22\sin^2\theta-12\sin^4\theta)\}\Big]- \\
&-\omega^2\left(\frac{l}{4}\right)^5[6\sin\theta\sin 2\theta+\epsilon_1(1-4\sin^2\theta)\sin\theta-2\epsilon_1^2\cos\theta]+ \\
&+2\left(\frac{l}{4}\right)^4[(\dot{u}'\sin\theta-\dot{v}'\cos\theta)(3-2\sin^2\theta)\sin\theta+\tfrac{1}{4}\dot{\omega}l\cos\theta\sin 2\theta+ \\
&+\tfrac{1}{4}\epsilon_1\{-\dot{u}'\sin 2\theta(1+8\sin^2\theta)+2\dot{v}'(5+8\sin^2\theta)\cos^2\theta- \\
&\qquad-\tfrac{1}{2}\dot{\omega}l(3+4\sin^2\theta)\cos\theta\}+ \\
&+\tfrac{1}{2}\epsilon_1^2\{-\dot{u}'(3+19\sin^2\theta-8\sin^4\theta)+ \\
&\qquad+\tfrac{1}{2}\dot{v}'(15-8\sin^2\theta)\sin 2\theta-\dot{\omega}l\sin\theta\}]
\end{aligned}
$$

9. Discussion of the results for the three aerofoils

We may now discuss some of the more interesting cases of motion, making the stipulation that the velocity component of the origin in a direction perpendicular to the aerofoil chord shall be small compared with the component along the aerofoil chord. This is in order that the aerofoil will not become a bluff obstacle, as it is known that the Joukowski condition

gives results in good agreement with experimental results only when such a stipulation is made. We therefore require that $(u' \sin\theta - v' \cos\theta)$ be small compared with $(u' \cos\theta + v' \sin\theta)$. Again, the expansions for forces and couple are actually written in powers of l/b, and hence are more likely to be convergent for $l/b < 1$, so that we shall consider only values of b greater than the chord length. Further, any conclusions we may draw from the results must be treated with some caution as only three terms of the series are given.

(8.3) Bearing all these conditions in mind, we consider the following cases:

Case 1. u' *constant*, $v' = 0$, $\omega = 0$

This is equivalent to the simple stationary aerofoil problem which has been discussed by various authors. It is easily seen that the expressions for this case obtained here agree in all respects with those obtained by Tomotika, Green, Havelock, and Fujikawa, so that there is no point in reproducing their discussions of this case.

It is believed that the following cases include some new results.

Case 2. v' *constant*, $u' = 0$, $\omega = 0$

If the aerofoil moves directly towards the wall, we write $\theta = -(\frac{1}{2}\pi - \alpha)$, α being small to conform with our stipulation regarding the velocity component perpendicular to the aerofoil chord. For the flat plate we then have:

$$\left.\begin{aligned} \frac{Y'}{\pi\rho} &= -\frac{l}{4}\left(\frac{l}{b}\right)v'^2 \sin^2\alpha\left(1+\frac{l}{b}\cos\alpha\right)+O(b^{-3}) \\ \frac{X'}{X'_0} &= 1+\frac{1}{4}\left(\frac{l}{b}\right)\cos\alpha+\frac{1}{16}\left(\frac{l}{b}\right)^2\sin^2\alpha+O(b^{-3}), \qquad X'_0 = \pi\rho l v'^2 \sin\alpha \\ \frac{\Gamma}{\Gamma_0} &= 1+\frac{1}{4}\left(\frac{l}{b}\right)\frac{\cos 2\alpha}{\cos\alpha}+\frac{1}{32}\left(\frac{l}{b}\right)^2(1-10\sin^2\alpha)+O(b^{-3}), \qquad \Gamma_0 = \pi\rho\frac{l^2}{8}v'^2\sin 2\alpha \end{aligned}\right\}. \tag{9.1}$$

It follows that one of the effects of the wall is to induce a small force Y' acting on the plate and directed towards the wall. The sign of the force is independent of the sign of α, and Y' increases in magnitude as the plate approaches nearer the wall. Further, X'/X'_0, $\Gamma/\Gamma_0 > 1$ for all small positive or negative α, and both expressions increase as b decreases.

For the symmetrical aerofoil we find

$$\left.\begin{aligned} \frac{Y'}{\pi\rho} &= -\frac{l}{4}\left(\frac{l}{b}\right)v'^2\sin^2\alpha\left((1+2\epsilon-\epsilon^2)+\frac{l}{b}(1+\tfrac{5}{2}\epsilon)\cos\alpha\right)+O(b^{-3}) \\ \frac{X'}{X'_0} &= 1+\frac{1}{4}\left(\frac{l}{b}\right)(1+\epsilon-\epsilon^2)\cos\alpha+\frac{1}{16}\left(\frac{l}{b}\right)^2(\sin^2\alpha+\tfrac{5}{2}\epsilon-\tfrac{3}{4}\epsilon^2)+O(b^{-3}) \end{aligned}\right\}, \tag{9.2}$$

so that the effect of thickness is to increase both Y' and X'/X'_0 in magnitude.

The expressions for the circular arc become:

$$\left.\begin{aligned}\frac{Y'}{\pi\rho} &= -\frac{l}{4}\left(\frac{l}{b}\right)v'^2\left[(\sin\alpha+\epsilon_1\cos\alpha)^2+\frac{l}{b}\left\{\sin^2\alpha\cos\alpha+\right.\right.\\ &\qquad\left.\left.+\frac{\epsilon_1}{4}\sin\alpha(5-8\sin^2\alpha)+\frac{\epsilon_1^2}{4}(1-8\sin^2\alpha)\cos\alpha\right\}\right]+O(b^{-3})\\ \frac{X'}{X_0'} &= 1+\tfrac{1}{4}(\cos\alpha-\epsilon_1\sin\alpha)\frac{l}{b}+\frac{1}{16}\left(\frac{l}{b}\right)^2\left[\sin^2\alpha-\right.\\ &\qquad\left.-\left\{\frac{2\epsilon_1(1-4\sin^2\alpha)\cos\alpha-\epsilon_1^2\sin\alpha(29-24\sin^2\alpha)}{(\sin\alpha+\epsilon_1\cos\alpha)}\right\}\right]+O(b^{-3})\end{aligned}\right\}. \quad (9.3)$$

Thus for small positive values of α, the force Y' induced by the wall is considerably increased in magnitude by the camber. Considering X'/X_0' we see that X_1'/X_0' is affected very little by ϵ_1, while, since $\sin\alpha$ and $\epsilon_1\cos\alpha$ are of the same order of magnitude for small α, X_2'/X_0' is considerably diminished by the camber terms, and may even be changed in sign. Hence camber tends to diminish X'/X_0' below the values it assumes for the flat plate.

These conclusions are best illustrated by considering a numerical case. Thus for $\alpha = 5°$, for the flat plate we have

$$\frac{Y'}{\pi\rho l v'^2} = -\frac{l}{b}\left(0{\cdot}001901+0{\cdot}001894\frac{l}{b}\right)+\ldots,$$

$$\frac{X'}{X_0'} = 1+0{\cdot}2491\left(\frac{l}{b}\right)+0{\cdot}0005\left(\frac{l}{b}\right)^2+\ldots,$$

$$\frac{\Gamma}{\Gamma_0} = 1+0{\cdot}2472\left(\frac{l}{b}\right)+0{\cdot}0289\left(\frac{l}{b}\right)^2+\ldots,$$

while for the symmetrical aerofoil with $\epsilon = 0{\cdot}1$, i.e. thickness ratio 0·117

$$\frac{Y'}{\pi\rho l v'^2} = -\frac{l}{b}\left(0{\cdot}002266+0{\cdot}002368\frac{l}{b}\right)+\ldots,$$

$$\frac{X'}{X_0'} = 1+0{\cdot}2715\left(\frac{l}{b}\right)+0{\cdot}0156\left(\frac{l}{b}\right)^2+\ldots,$$

and for the circular arc with $\epsilon_1 = 0{\cdot}1$, i.e. camber equal to 0·05,

$$\frac{Y'}{\pi\rho l v'^2} = -\frac{l}{b}\left(0{\cdot}008725+0{\cdot}005166\frac{l}{b}\right)+\ldots,$$

$$\frac{X'}{X_0'} = 1+0{\cdot}2469\left(\frac{l}{b}\right)-0{\cdot}0558\left(\frac{l}{b}\right)^2+\ldots.$$

Case 3. *u' constant, v' constant, $\omega = 0$*

For the flat plate the results are:

$$\left.\begin{aligned}
&\frac{Y'}{Y'_0} = 1-\frac{1}{4}\left(2\sin\theta-\frac{v'}{u'}\cos\theta\right)\frac{l}{b}+\\
&\qquad\qquad+\frac{1}{16}\left\{(1+3\sin^2\theta)-\frac{2v'}{u'}\sin 2\theta\right\}\left(\frac{l}{b}\right)^2+\dots\\
&Y'_0 = \pi\rho l u'(u'\sin\theta-v'\cos\theta)\\
&\frac{X'}{X'_0} = 1-\frac{1}{4}\left(\frac{l}{b}\right)\sin\theta+\frac{1}{16}\left(\frac{l}{b}\right)^2\cos^2\theta+\dots\\
&X'_0 = -\pi\rho l v'(u'\sin\theta-v'\cos\theta)\\
&\frac{\Gamma}{\Gamma_0} = 1-\frac{1}{4}\left(\frac{l}{b}\right)\frac{u'\sin 2\theta-v'\cos 2\theta}{u'\cos\theta+v'\sin\theta}+\\
&\qquad+\frac{1}{32}\left(\frac{l}{b}\right)^2\left[\frac{u'\cos\theta(1+10\sin^2\theta)-v'\sin\theta(9-10\sin^2\theta)}{u'\cos\theta+v'\sin\theta}\right]+\dots\\
&\Gamma_0 = \pi\rho\frac{l^2}{4}(u'\sin\theta-v'\cos\theta)(u'\cos\theta+v'\sin\theta)
\end{aligned}\right\}. \qquad (9.4)$$

If there is no velocity component perpendicular to the plate, i.e. if $(u'\sin\theta-v'\cos\theta) = 0$, then both the forces and couple vanish (at least to our order of approximation).

Consider the case where θ is small, $(u'\sin\theta-v'\cos\theta)$ small compared with $(u'\cos\theta+v'\sin\theta)$, and θ, v', u', $(u'\sin\theta-v'\cos\theta)$ all positive. Then as b decreases from infinity, X'/X'_0 first decreases and then tends to increase, possibly to a value above unity. With Y'/Y'_0 we may compare the corresponding case with $v' = 0$, and we see that there will be less initial decrease of Y'/Y'_0, and a greater final increase, as b decreases from infinity.

Since $(u'\sin 2\theta-v'\cos 2\theta) = 2(u'\sin\theta-v'\cos\theta)\cos\theta+v' > 0$, Γ/Γ_0 also exhibits an initial decrease and final increase as the plate approaches nearer the wall.

Since $v' > 0$ (by assumption) the aerofoil is actually moving away from the wall, and so it is perhaps better to state our conclusions in terms of increasing b. If then we assume that we commence with some minimum value of b ($> l$), we may say that Y'/Y'_0, X'/X'_0, and Γ/Γ_0 all decrease from values which may be greater than unity to values less than unity, and finally increase again to assume the value unity as the distance of the plate from the wall increases to infinity.

The forces on the symmetrical aerofoil are:

$$\left.\begin{aligned}
\frac{Y'}{Y'_0} &= 1-\frac{1}{4}(1+\epsilon-\epsilon^2)\left(2\sin\theta-\frac{v'}{u'}\cos\theta\right)\frac{l}{b}+\frac{1}{16}\left(\frac{l}{b}\right)^2\left\{(1+3\sin^2\theta)+\right.\\
&\quad\left.+\frac{\epsilon}{2}(5+12\sin^2\theta)-\frac{\epsilon^2}{4}(3+8\sin^2\theta)-2\frac{v'}{u'}\left(1+\tfrac{3}{2}\epsilon-\frac{\epsilon^2}{2}\right)\sin 2\theta\right\}+\dots\\
\frac{X'}{X'_0} &= 1-\tfrac{1}{4}(1+\epsilon-\epsilon^2)\frac{l}{b}\sin\theta+\frac{1}{16}\left(\frac{l}{b}\right)^2(\cos^2\theta+\tfrac{5}{2}\epsilon-\tfrac{3}{4}\epsilon^2)+\dots\\
Y'_0 &= \pi\rho l u'(u'\sin\theta-v'\cos\theta)(1+\epsilon-\epsilon^2)\\
X'_0 &= -\pi\rho l(1+\epsilon-\epsilon^2)v'(u'\sin\theta-v'\cos\theta)
\end{aligned}\right\}. \tag{9.5}$$

Under the same assumptions as for the plate case, the aerofoil thickness will emphasize the tendency for X'/X'_0 to decrease and then increase as l/b increases. Writing Y'/Y'_0 in the form

$$\frac{Y'}{Y'_0}=1+\frac{1}{16}\left(\frac{l}{b}\right)\left[-8(1+\epsilon-\epsilon^2)\sin\theta+\frac{l}{b}\left\{(1+3\sin^2\theta)+\frac{\epsilon}{2}(5+12\sin^2\theta)-\right.\right.$$
$$\left.\left.-\frac{\epsilon^2}{4}(3+8\sin^2\theta)\right\}\right]+\frac{v'}{4u'}\left\{(1+\epsilon-\epsilon^2)-\frac{l}{b}\left(1+\tfrac{3}{2}\epsilon-\frac{\epsilon^2}{2}\right)\sin\theta\right\}\frac{l}{b}\cos\theta+O(b^{-3})$$

we see that, for all l/b, the term involving v' is numerically increased by the small thickness parameter ϵ, and this will tend to compensate for the decrease produced by ϵ in the terms independent of v', for small l/b. Hence it seems likely that Y'/Y'_0 will behave much as it does for the flat plate.

Neglecting ϵ_1^2 for a first approximation, the expressions for the circular arc become:

$$\left.\begin{aligned}
\frac{Y'}{Y'_0} &= 1-\frac{1}{4}\left(\frac{l}{b}\right)\left\{2\sin\theta-\frac{v'}{u'}\cos\theta+\epsilon_1\left(2\cos\theta+\frac{v'}{u'}\sin\theta\right)\right\}+\\
&\quad+\frac{1}{16}\left(\frac{l}{b}\right)^2\left[(1+3\sin^2\theta)-\frac{2v'}{u'}\sin 2\theta-\right.\\
&\quad\left.-\frac{\epsilon_1\{u'^2\cos\theta(1-4\sin^2\theta)+\\ +u'v'(11-12\sin^2\theta)\sin\theta-2v'^2(3-4\sin^2\theta)\cos\theta\}}{2u'\{(u'\sin\theta-v'\cos\theta)+\epsilon_1(u'\cos\theta+v'\sin\theta)\}}\right]+\\
&\quad+O(b^{-3})\\
Y'_0 &= \pi\rho l u'\{(u'\sin\theta-v'\cos\theta)+\epsilon_1(u'\cos\theta+v'\sin\theta)\}\\
\frac{X'}{X'_0} &= 1-\tfrac{1}{4}(\sin\theta+\epsilon_1\cos\theta)\frac{l}{b}+\\
&\quad+\frac{1}{16}\left(\frac{l}{b}\right)^2\left[\cos^2\theta-\frac{2\epsilon_1\{u'\cos\theta(1+4\sin^2\theta)-v'\sin\theta(3-4\sin^2\theta)\}}{(u'\sin\theta-v'\cos\theta)+\epsilon_1(u'\cos\theta+v'\sin\theta)}\right]\\
&\quad+O(b^{-3})\\
X'_0 &= -\pi\rho l v'\{(u'\sin\theta-v'\cos\theta)+\epsilon_1(u'\cos\theta+v'\sin\theta)\}
\end{aligned}\right\}. \tag{9.6}$$

Under the usual assumptions we find that the camber tends to keep both Y'/Y'_0 and X'/X'_0 below 1 for a considerably greater range of values of l/b than for a flat plate aerofoil.

Taking $u'/v' = 20$, $\theta = 10°$, the expressions for the flat plate become

$$\frac{Y'}{Y'_0} = 1 - 0{\cdot}07475\left(\frac{l}{b}\right) + 0{\cdot}06602\left(\frac{l}{b}\right)^2 + \ldots,$$

$$\frac{X'}{X'_0} = 1 - 0{\cdot}04353\left(\frac{l}{b}\right) + 0{\cdot}06063\left(\frac{l}{b}\right)^2 + \ldots,$$

$$\frac{\Gamma}{\Gamma_0} = 1 - 0{\cdot}07450\left(\frac{l}{b}\right) + 0{\cdot}03800\left(\frac{l}{b}\right)^2 + \ldots.$$

For the symmetrical aerofoil $\epsilon = 0{\cdot}1$ we then have

$$\frac{Y'}{Y'_0} = 1 - 0{\cdot}08148\left(\frac{l}{b}\right) + 0{\cdot}08194\left(\frac{l}{b}\right)^2 + \ldots,$$

$$\frac{X'}{X'_0} = 1 - 0{\cdot}04745\left(\frac{l}{b}\right) + 0{\cdot}07576\left(\frac{l}{b}\right)^2 + \ldots,$$

and the forces on the circular arc $\epsilon_1 = 0{\cdot}1$ are

$$\frac{Y'}{Y'_0} = 1 - 0{\cdot}1242\left(\frac{l}{b}\right) + 0{\cdot}0531\left(\frac{l}{b}\right)^2 + \ldots,$$

$$\frac{X'}{X'_0} = 1 - 0{\cdot}06814\left(\frac{l}{b}\right) + 0{\cdot}00045\left(\frac{l}{b}\right)^2 + \ldots.$$

Case 4. *u', v', and ω all constant and non-zero*

This may be used for comparison with the case of an aircraft taking off from the ground, as usual, after a certain minimum value of b. We require θ and ω small, and v' small in comparison with u', all these quantities being positive. Also $(u'\sin\theta - v'\cos\theta)$ must be small compared with $(u'\cos\theta + v'\sin\theta)$ and positive (for a positive vertical force Y'). The behaviour of the vertical force is of primary importance here, and for the flat plate

$$\left.\begin{aligned}\frac{Y'}{\pi\rho} = {} & lu'(u'\sin\theta - v'\cos\theta)\left[1 + \frac{1}{16}\left(\frac{l}{b}\right)\left\{-8\sin\theta + \frac{l}{b}(1+3\sin^2\theta)\right\} + \right.\\ & \left. + \frac{v'}{4u'}\left(1 - \frac{l}{b}\sin\theta\right)\frac{l}{b}\cos\theta\right] - \\ & - \frac{\omega l^2}{64}\left(\frac{l}{b}\right)\left[4(u'\sin\theta - v'\cos\theta)(1+\sin^2\theta) + \right.\\ & \left. + \frac{l}{b}\left\{u'(1 - 9\sin^2\theta + 4\sin^4\theta) + \frac{v'}{2}(9 - 4\sin^2\theta)\sin 2\theta\right\}\right] + \\ & + \frac{\omega^2 l^3}{256}\left(\frac{l}{b}\right)^2(4 - 3\sin^2\theta)\sin\theta + O(b^{-3})\end{aligned}\right\}. \quad (9.7)$$

Under the above assumptions the terms involving ω will be negative in sign, and will decrease in magnitude as b increases. It follows that the effect of introducing the rotation ω is to lessen the magnitude of Y'. By comparison with Case 3 it is possible to determine the variation of Y' with b, and we see that as the distance of the plate from the ground increases, Y' will diminish to values less than Y'_0 and then exhibit the usual increase to attain the value Y'_0. Thus for $u'/v' = 20$, $\theta = 10°$,

$$\frac{Y'}{Y'_0} = 1 - 0{\cdot}0748\left(\frac{l}{b}\right) + 0{\cdot}0660\left(\frac{l}{b}\right)^2 -$$

$$- \frac{\omega l}{u'}\left(\frac{l}{b}\right)\left(0{\cdot}0644 + 0{\cdot}1015\frac{l}{b}\right) + 0{\cdot}0213\left(\frac{\omega l}{u'}\right)^2\left(\frac{l}{b}\right)^2 + \ldots.$$

For the symmetrical and circular arc aerofoils, the effect of a small rotation ω may be found by restricting ω to be so small that the products $\epsilon\omega$, $\epsilon_1\omega$, etc., may be neglected. The forces will then be modified by ω in exactly the same manner as in the flat plate case.

Case 5. *u' constant, v' variable, $\omega = 0$*

For the flat plate the force X' takes the form

$$\frac{X'}{\pi\rho} = -lv'(u'\sin\theta - v'\cos\theta)\left\{1 - \frac{1}{4}\left(\frac{l}{b}\right)\sin\theta + \frac{1}{16}\left(\frac{l}{b}\right)^2\cos^2\theta\right\} -$$

$$- \frac{l^2}{8}\dot{v}'\sin 2\theta\left\{1 - \frac{1}{4}\left(\frac{l}{b}\right)\sin\theta + \frac{1}{32}\left(\frac{l}{b}\right)^2(3 - 2\sin^2\theta)\right\} + O(b^{-3}). \quad (9.8)$$

An interesting case is one in which the plate describes translational oscillations in the direction of the y'-axis, and this may be obtained by writing $v' = v_0\sin n\tau$, v_0 and n being constant. Since

$$\frac{db}{d\tau} = v' = v_0\sin n\tau,$$

we have $$b = b_0\left(1 - \frac{v_0}{nb_0}\cos n\tau\right), \quad b_0 \text{ constant}.$$

Clearly b_0 is the mean distance of the plate centre from the wall. Since $v_0/nb_0 < 1$ we may obtain the expansions

$$\frac{1}{b} = \frac{1}{b_0}\left(1 + \frac{v_0}{nb_0}\cos n\tau\right) + O(b_0^{-3}), \qquad \frac{1}{b^2} = \frac{1}{b_0^2} + O(b^{-3}).$$

Thus X' may be written as

$$\frac{X'}{\pi\rho l} = \tfrac{1}{2}v_0^2\cos\theta\left\{1-\frac{1}{4}\left(\frac{l}{b_0}\right)\sin\theta+\frac{1}{16}\left(\frac{l}{b_0}\right)^2\right\}-$$

$$-u'v_0\sin\theta\left\{1-\frac{1}{4}\left(\frac{l}{b_0}\right)\sin\theta+\frac{1}{16}\left(\frac{l}{b_0}\right)^2\cos^2\theta\right\}\sin n\tau-$$

$$-\frac{l}{8}nv_0\sin 2\theta\left\{1-\frac{1}{4}\left(\frac{l}{b_0}\right)\sin\theta+\frac{1}{32}\left(\frac{l}{b_0}\right)^2(3-2\sin^2\theta)+\frac{v_0^2}{4n^2b_0^2}\right\}\cos n\tau+$$

$$+\frac{v_0^2u'l}{8nb_0^2}\sin^2\theta\sin 2n\tau-\tfrac{1}{2}v_0^2\cos\theta\left\{1-\frac{1}{4}\left(\frac{l}{b_0}\right)\sin\theta+\frac{1}{16}\left(\frac{l}{b_0}\right)^2\cos 2\theta\right\}\cos 2n\tau+$$

$$+\frac{lv_0^3}{32nb_0^2}\sin 2\theta\cos 3n\tau+O(b_0^{-3}).$$

We notice the presence in the variable part of X' of terms which have a frequency twice that of the main motion; also there is a term (involving b_0^{-2}) with a frequency three times that of the main motion. Further, it is evident that from X' a thrust can be obtained on the plate. The mean value of X' over an interval of time $2\pi/n$ (the period of oscillation of the plate) follows immediately, and we have

$$\frac{{}_mX'}{\pi\rho} = \frac{l}{2}v_0^2\cos\theta\left\{1-\frac{1}{4}\left(\frac{l}{b_0}\right)\sin\theta+\frac{1}{16}\left(\frac{l}{b_0}\right)^2\right\}+O(b_0^{-3}),$$

where ${}_mX'$ denotes the mean value of X' over the specified interval of time. Writing ${}_mX'_0$ for the mean value of X'_0, then

$$\frac{{}_mX'}{{}_mX'_0} = 1-\frac{1}{4}\left(\frac{l}{b_0}\right)\sin\theta+\frac{1}{16}\left(\frac{l}{b_0}\right)^2+\dots, \qquad {}_mX'_0 = \tfrac{1}{2}l\pi\rho v_0^2\cos\theta. \quad (9.9)$$

Now ${}_mX'$ is positive, i.e. the plate experiences not a resistance but a propelling force, assuming u' positive. This type of motion resembles a simple form of flapping flight, and from (9.9) the wall effect on this force X' may be found. For $\theta > 0$ and small, as b_0 decreases from infinity, ${}_mX'$ first decreases and then tends to rise above the isolated value ${}_mX'_0$. Clearly the energy of the propulsion is derived from the work done in producing the periodic transverse oscillations of the plate. Of course, in actual practice this mean force will be considerably modified by the influence of a system of free vortices accompanying the plate.

For the symmetrical aerofoil, the corresponding case yields

$$\frac{{}_mX'}{{}_mX'_0} = 1-\tfrac{1}{4}(1+\epsilon-\epsilon^2)\frac{l}{b_0}\sin\theta+$$

$$+\frac{1}{16}\left(\frac{l}{b_0}\right)^2\left\{1+\frac{\epsilon}{2}(3+2\sin^2\theta)-\frac{\epsilon^2}{4}(5-4\sin^2\theta)\right\}+O(b_0^{-3}). \quad (9.10)$$

The effect of thickness is to diminish ${}_mX'/{}_mX'_0$ for small l/b_0, but as b_0 decreases the ratio may eventually be increased by the thickness.

Similarly for the circular arc we find

$$\frac{{}_mX'}{{}_mX'_0} = 1 - \tfrac{1}{4}(\sin\theta + \epsilon_1\cos\theta)\frac{l}{b_0} + \\ + \frac{1}{16}\left(\frac{l}{b_0}\right)^2\left[1 - \left\{\frac{2\epsilon_1\sin\theta\cos 2\theta + \epsilon_1^2(1-8\sin^2\theta)\cos\theta}{4(\sin\theta+\epsilon_1\cos\theta)}\right\}\right] + O(b_0^{-3}). \quad (9.11)$$

Clearly the effect of the camber is to decrease the ratio ${}_mX'/{}_mX'_0$ found for the flat plate.

By way of illustration, we find that for $\theta = 5°$, the flat plate case gives

$$\frac{{}_mX'}{{}_mX'_0} = 1 - 0{\cdot}02179\left(\frac{l}{b_0}\right) + 0{\cdot}06250\left(\frac{l}{b_0}\right)^2 + \ldots,$$

while for the symmetrical aerofoil $\epsilon = 0{\cdot}1$,

$$\frac{{}_mX'}{{}_mX'_0} = 1 - 0{\cdot}02375\left(\frac{l}{b_0}\right) + 0{\cdot}07114\left(\frac{l}{b_0}\right)^2 + \ldots,$$

and for the circular arc $\epsilon_1 = 0{\cdot}1$,

$$\frac{{}_mX'}{{}_mX'_0} = 1 - 0{\cdot}04670\left(\frac{l}{b_0}\right) + 0{\cdot}06028\left(\frac{l}{b_0}\right)^2 + \ldots.$$

The lift force Y' and couple Γ may be treated in the same way as X', and for the flat plate we find

$$\frac{Y'}{\pi\rho l} = u'^2\sin\theta\left\{1 - \frac{1}{2}\left(\frac{l}{b_0}\right)\sin\theta + \frac{1}{16}\left(\frac{l}{b_0}\right)^2(1+3\sin^2\theta)\right\} - \\ - \tfrac{1}{8}v_0^2\left(\frac{l}{b_0}\right)\cos^2\theta\left(1 - \frac{3l}{4b_0}\sin\theta\right) - \\ - u'v_0\cos\theta\sin n\tau\left\{1 - \frac{3}{4}\left(\frac{l}{b_0}\right)\sin\theta + \frac{1}{16}\left(\frac{l}{b_0}\right)^2(1+7\sin^2\theta)\right\} + \\ + \frac{l}{4}v_0 n\cos n\tau\left[\cos^2\theta\left\{1 - \frac{1}{4}\left(\frac{l}{b_0}\right)\sin\theta + \right.\right. \\ \left.\left. + \frac{1}{32}\left(\frac{l}{b_0}\right)^2(3-2\sin^2\theta) - \left(\frac{v_0}{2nb_0}\right)^2\right\} - \frac{2u'^2}{n^2b_0^2}\sin^2\theta\right] + \\ + \tfrac{1}{8}v_0^2\left(\frac{l}{b_0}\right)\cos\theta\left[\frac{3u'}{nb_0}\sin\theta\sin 2n\tau + \right. \\ \left. + \left(1 - \frac{5l}{4b_0}\sin\theta\right)\cos\theta\cos 2n\tau + \frac{v_0}{2nb_0}\cos\theta\cos 3n\tau\right] + O(b_0^{-3})$$

and

$$\frac{\Gamma}{\pi\rho l^2} = \tfrac{1}{8}u'^2\sin 2\theta\left(1-\frac{1}{2}\left(\frac{l}{b_0}\right)\sin\theta+\frac{1}{32}\left(\frac{l}{b_0}\right)^2(1+10\sin^2\theta)\right)-$$
$$-\tfrac{1}{8}v_0^2\cos\theta\left(\sin\theta+\frac{1}{4}\left(\frac{l}{b_0}\right)\cos 2\theta-\frac{1}{32}\left(\frac{l}{b_0}\right)^2(7-10\sin^2\theta)\sin\theta\right)+$$
$$+\tfrac{1}{4}u'v_0\sin n\tau\left[\sin\theta\left(\sin\theta+\frac{1}{4}\left(\frac{l}{b_0}\right)\cos 2\theta-\frac{1}{32}\left(\frac{l}{b_0}\right)^2(9-10\sin^2\theta)\sin\theta\right)-\right.$$
$$\left.-\cos^2\theta\left(1-\frac{1}{2}\left(\frac{l}{b_0}\right)\sin\theta+\frac{1}{32}\left(\frac{l}{b_0}\right)^2(1+10\sin^2\theta)\right)\right]+$$
$$+\frac{l}{16}nv_0\cos\theta\cos n\tau\left(1-\frac{1}{4}\left(\frac{l}{b_0}\right)\sin\theta+\right.$$
$$\left.+\frac{1}{64}\left(\frac{l}{b_0}\right)^2(5-2\sin^2\theta)-\frac{2}{n^2b_0^2}(u'^2\sin^2\theta+\tfrac{1}{8}v_0^2\cos 2\theta)\right)+$$
$$+\tfrac{1}{8}v_0^2\cos\theta\cos 2n\tau\left(\sin\theta+\frac{1}{4}\left(\frac{l}{b_0}\right)\cos 2\theta-\frac{1}{32}\left(\frac{l}{b_0}\right)^2(11-10\sin^2\theta)\sin\theta\right)+$$
$$+\frac{lv_0^2}{32nb_0^2}(u'\sin 3\theta\sin 2n\tau+\tfrac{1}{2}v_0\cos\theta\cos 2\theta\cos 3n\tau)+O(b_0^{-3}).$$

Once again we note the presence of terms of twice and three times the frequency of the main motion. Averaging as before,

$$\frac{m Y'}{\pi\rho l} = u'^2\sin\theta\left(1-\frac{1}{2}\left(\frac{l}{b_0}\right)\sin\theta+\frac{1}{16}\left(\frac{l}{b_0}\right)^2(1+3\sin^2\theta)\right)-$$
$$-\tfrac{1}{8}v_0^2\left(\frac{l}{b_0}\right)\left(1-\frac{3l}{4b_0}\sin\theta\right)\cos^2\theta+O(b_0^{-3}),$$

$$\frac{m\Gamma}{\pi\rho l^2} = \tfrac{1}{8}u'^2\sin 2\theta\left(1-\frac{1}{2}\left(\frac{l}{b_0}\right)\sin\theta+\frac{1}{32}\left(\frac{l}{b_0}\right)^2(1+10\sin^2\theta)\right)-$$
$$-\tfrac{1}{8}v_0^2\cos\theta\left(\sin\theta+\frac{1}{4}\left(\frac{l}{b_0}\right)\cos 2\theta-\frac{1}{32}\left(\frac{l}{b_0}\right)^2(7-10\sin^2\theta)\sin\theta\right)+O(b_0^{-3}).$$

For the sake of completeness we give the average values for Y' for the symmetrical and circular arc aerofoils. For the symmetrical aerofoil,

$$\frac{m Y'}{\pi\rho l} = u'^2(1+\epsilon-\epsilon^2)\sin\theta\left[1-\frac{1}{2}\left(\frac{l}{b_0}\right)(1+\epsilon-\epsilon^2)\sin\theta+\right.$$
$$\left.+\frac{1}{16}\left(\frac{l}{b_0}\right)^2\left\{(1+3\sin^2\theta)+\frac{\epsilon}{2}(5+12\sin^2\theta)-\frac{\epsilon^2}{4}(3+8\sin^2\theta)\right\}\right]-$$
$$-\tfrac{1}{8}v_0^2\left(\frac{l}{b_0}\right)(1+2\epsilon-\epsilon^2)\left\{1-\frac{1}{4}\left(\frac{l}{b_0}\right)(3+2\epsilon-2\epsilon^2)\sin\theta\right\}\cos^2\theta+O(b_0^{-3})$$

and for the circular arc aerofoil,

$$\frac{mY'}{\pi\rho l} = u'^2(\sin\theta+\epsilon_1\cos\theta)\Big[1-\frac{1}{2}\Big(\frac{l}{b_0}\Big)(\sin\theta+\epsilon_1\cos\theta)+$$

$$+\frac{1}{16}\Big(\frac{l}{b_0}\Big)^2\Big\{(1+3\sin^2\theta)-\frac{\epsilon_1}{4}\frac{2(1-4\sin^2\theta)\cos\theta-\epsilon_1(13-8\sin^2\theta)\sin\theta}{(\sin\theta+\epsilon_1\cos\theta)}\Big\}\Big]-$$

$$-\tfrac{1}{8}v_0^2\Big(\frac{l}{b_0}\Big)\Big[(\cos\theta-\epsilon_1\sin\theta)^2-$$

$$-\frac{1}{8}\Big(\frac{l}{b_0}\Big)\{3\cos\theta\sin 2\theta+2\epsilon_1\cos\theta(1-6\sin^2\theta)-4\epsilon_1^2\sin\theta\cos 2\theta\}\Big]+O(b_0^{-3}).$$

The general force and moment expressions (6.2)–(6.4), (7.2), (7.3), (8.2), and (8.3) enable other cases of oscillatory or accelerated motion to be discussed if desired.

10. Conclusion

The calculations of this paper have all been based on the simple Joukowski trailing edge condition, and no system of free vortices has been considered. It is realized that for the majority of cases of motion considered above, the circulation around the cylinder will continually vary (e.g. with the distance b of the origin of coordinates from the wall), and hence some sort of assessment of the effects of a vortex wake would be desirable. However, the results already obtained with no vortex system are complicated, and introduction of the further complication of a vortex wake would tend to make the results almost incapable of profitable discussion.

In spite of the approximation just mentioned, it is hoped that the results obtained will at least give some idea of the wall effects for various types of motion.

It is felt that to deal adequately with the problem of the effect of a vortex wake, a separate paper is required.

In conclusion, I should like to thank Dr. R. M. Morris for suggesting the problem, and for her helpful advice throughout the work.

REFERENCES

1. A. E. Green, *Quart. J. Math.* (Oxford), **18** (1947), 167.
2. —— *Proc. Lond. Math. Soc.* (2), **46** (1940), 19.
3. S. Tomotika, T. Nagamiya, and Y. Takenouti, *Rep. Aero. Res. Inst. Tokio*, **8** (1933), 1.
4. T. H. Havelock, *Proc. Roy. Soc.* A, **166** (1938), 178.
5. H. Fujikawa, *J. Phys. Soc. Japan*, **9** (1954), 233.
6. R. M. Morris, *Proc. Roy. Soc.* A, **161** (1937), 406.

THE EFFECT OF DIHEDRAL ON THE AERODYNAMIC DERIVATIVES WITH RESPECT TO SIDESLIP FOR AIRFOILS IN SUPERSONIC FLOW

By J. B. L. POWELL

(*Department of Mathematics, The University, Bristol*)

[Received 1 December 1955]

SUMMARY

A thin dihedral wing in supersonic flow is given a small velocity in sideslip. By a linearized theory the surface pressure distribution is investigated for wings whose planform is symmetrical about the line of undisturbed flow through the vertex. This involves dividing the problem into two parts, depending on whether the wing leading edges lie outside or inside the Mach cone from their vertex. For each case the force derivatives are determined and graphs are exhibited which give the value of these derivatives for wings of delta planform. For other wing shapes graphs are shown which give the contribution from the interference pressure alone.

For a delta wing it is found that to a good approximation the rolling derivative varies with the sine of the angle of dihedral and the yawing and sideslip derivatives vary with the square of the sine of this angle. As the values of the derivatives at small dihedral are known explicitly, this provides a useful method for obtaining the values at more general dihedral angles.

1. Introduction

In a previous paper (**1**) (hereafter referred to as Part I), the effect of dihedral upon the lift and drag coefficients in supersonic flow was investigated for thin airfoils symmetrical about their centre chord. The present paper is intended to complete the determination of the force coefficients by the calculation of the aerodynamic derivatives with respect to sideslip. The derivative of the pitching moment is obtained in Appendix I and is given in terms of the results of Part I. As in Part I, the equations of motion are linearized on the basis of small perturbations imposed on an otherwise uniform main stream. Wings having swept-back leading edges are included in the analysis and two cases arise depending on whether the leading edges lie inside or outside the Mach cone originating from their vertex. These two cases are considered separately.

Previous work upon the derivatives in sideslip has been devoted to the case when the angle of dihedral is small. A first order theory was first obtained by Robinson and Hunter-Tod (**2**) using a uniform distribution of sources. The problem was later treated by Multhopp (**3**) who used both the cone-field theory and conformal mapping to advantage. Since then, an attempt has been made by Nocilla (**4**) to develop a theory giving values

of the pressure distribution on the wing at larger values of dihedral by an expansion in powers of this angle. He does this for the case of a wing lying entirely within its vertex Mach cone, and in a later paper (**5**) he succeeds in obtaining values for the force derivatives on a delta wing which at a Mach number of 1·5 has a 60° sweepback. These values, which are for dihedral angles less than 30°, are in good agreement with the results given here.

2. Notation and basic equations

The angles of dihedral and sweepback are denoted by α and λ respectively. Cylindrical polar coordinates (r, θ, z) are defined with the origin at the vertex of the wing leading edges such that the z-axis is in the direction of undisturbed flow and the wing leading edges are given by $z = r\tan\lambda$, $\theta = \alpha,\ \pi-\alpha$. The wing is assumed to be symmetrical about the plane $\theta = \frac{1}{2}\pi$.

We will consider small deviations of the wing from the above neutral position and investigate the forces acting upon it. The only deviation that can produce such forces is a combination of the following displacements. Firstly, a displacement of the line of symmetry of the wing through a small angle in the plane $\theta = \frac{1}{2}\pi$ (an angle of incidence). This has been considered in Part I. Secondly, a displacement of the line of symmetry through a small angle in the plane $\theta = 0$ (an angle of yaw). This will be considered in the present paper. It has been sufficient to investigate each of these displacements independently, for on a linear theory they may be superimposed. Another consequence of this is that the case of yaw need only be examined for a wing which consists of two plane surfaces intersecting on the line of symmetry. If the angle of yaw is denoted by ϵ, this line of symmetry is given by $r = \epsilon z$, $\theta = 0$.

For the remainder of this section we refer briefly to the theory of Part I since the initial steps of the two boundary value problems are essentially the same.

Let the velocity, pressure, density, and Mach number of the incident flow be U, p_0, ρ_0, and M respectively and write $\beta^2 = M^2-1$. A velocity potential ϕ is introduced such that the perturbation velocity has components

$$V_r = U\frac{\partial\phi}{\partial r}, \qquad V_\theta = \frac{1}{r}U\frac{\partial\phi}{\partial\theta}, \qquad V_z = U\frac{\partial\phi}{\partial z}. \tag{1}$$

On a linear theory, the potential function ϕ satisfies the equation

$$\phi_{rr}+r^{-1}\phi_r+r^{-2}\phi_{\theta\theta} = \beta^2\phi_{zz},$$

and as the pressure p is a linear function of ϕ_z it follows that p also satisfies this equation. Furthermore, as the problem is of the cone-field flow type

(i.e. the boundary conditions involve no fundamental length) it is possible to make the following transformation into the polar coordinates ρ, θ,

$$\frac{\beta r}{z} = R = \frac{2\rho}{1+\rho^2}. \tag{2}$$

The Mach cone with vertex at the origin (henceforth called simply the Mach cone) becomes the unit circle in the (ρ, θ)-plane, and inside this circle the wave equation transforms into Laplace's equation with ρ, θ as polar coordinates.

3. The leading edges outside the Mach cone

The perturbation of the flow by the wing will be confined to the region enclosed by the envelope of the Mach cones which emanate from each point of the wing leading edges. Upstream of this region the wing will have no influence upon the flow and the pressure will be the free stream pressure p_0. When the wing lies totally inside the Mach cone from the vertex, the region of perturbation will consist solely of the interior of this cone. When the wing leading edges lie outside the Mach cone the region will consist of the interior of this cone together with two wedge-shaped regions, each formed by two plane surfaces which are tangential to the cone and intersect along a leading edge. It was shown in Part I that due to the hyperbolic nature of the flow outside the Mach cone, the pressure is discontinuous across such plane surfaces. Across the Mach cone the pressure is assumed to be continuous.

By either the first order Prandtl–Meyer expansion theory or the weak shock theory, the pressure inside each of the wedge-shaped regions is found to differ from the free stream pressure p_0 by $\pm\frac{\rho_0 U^2\epsilon}{\beta}\sec\psi\sin\alpha$, where ψ is defined by

$$\sin\psi = \frac{1}{\beta}\tan\lambda. \tag{3}$$

Thus if

$$p_1 = p_0 - \frac{\rho_0 U^2\epsilon}{\beta}\sec\psi\sin\alpha, \tag{4}$$

the pressure in those parts of the wedges above the wings $\theta = \alpha$, $\theta = \pi-\alpha$ is p_1 and $2p_0-p_1$ respectively. As in Part I, the wing divides the region of disturbance into two independent regions and it is only necessary to consider the upper region, the flow field below the wing being determined from the antisymmetry of the problem. The boundary condition on the surface of the wing is obtained from the condition of zero normal velocity. This implies

$$V_\theta = -U\epsilon\sin\alpha \tag{5}$$

on all the wing surfaces. It is sufficient to apply this boundary condition

on the planes $\theta = \alpha$, $\theta = \pi - \alpha$, although in yaw the wings are slightly disturbed from these positions. The error in so doing will be of the second order in ϵ.

If the field is mapped onto the polar coordinate plane (R, θ) by the transformation (2), the wing leading edges and the z-axis are represented by the three points E, F, and O (see Fig. 1) whose coordinates are respectively $(\operatorname{cosec}\psi, \alpha)$, $(\operatorname{cosec}\psi, \pi-\alpha)$, and $(0, 0)$. The perturbed region then

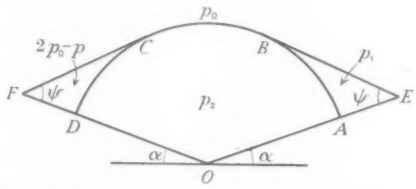

FIG. 1. The configuration in the (R, θ)-plane.

becomes the area enclosed by the wings OE and OF, the arc BC of the unit circle, and the tangents EB and FC to this circle. The pressure outside the whole area is p_0, whilst the pressure inside those parts of the area outside the unit circle, viz. BEA and CFD in Fig. 1, is p_1 and $2p_0-p_1$ respectively. If the pressure inside the unit circle is denoted by p_2, then $p_2 = 2p_0-p_1$ on CD, $p_2 = p_0$ on BC, and $p_2 = p_1$ on AB. If α is sufficiently large, the Mach planes EB and FC may intersect and be reflected at the wing surfaces. This was considered in more detail in Part I, where it was shown that the boundary conditions on the unit circle can be generalized to hold for all values of α. In terms of the non-dimensional pressure

$$p_3 = \frac{p_2-p_0}{p_1-p_0} \tag{6}$$

the antisymmetry of the boundary conditions gives

$$\lim_{\delta\to 0} \int_{-\delta+\gamma_1}^{\delta+\gamma_1} \frac{\partial p_3}{\partial \theta}\, d\theta = \frac{\sin\tau}{|\sin\tau|}, \qquad \lim_{\delta\to 0} \int_{-\delta+\gamma_2}^{\delta+\gamma_2} \frac{\partial p_3}{\partial \theta}\, d\theta = \frac{\sin\tau}{|\sin\tau|}, \tag{7}$$

on the unit circle, where γ_1 and γ_2 are such that

$$\left.\begin{aligned} \gamma_1 &\equiv \tfrac{1}{2}\pi+\alpha-\psi \mod(\pi-2\alpha) \\ \gamma_2 &\equiv \tfrac{1}{2}\pi-\alpha+\psi \mod(\pi-2\alpha) \end{aligned}\right\}, \tag{8}$$

and τ is defined by

$$\tau = \frac{\pi}{2}\left[\frac{\pi-2\psi}{\pi-2\alpha}\right]. \tag{9}$$

The boundary conditions on the lines $\theta = \alpha$, $\theta = \pi-\alpha$ are obtained by

replacing in equation (12) of Part I, the value of V_θ on the surface of the wings, given by (5). Thus

$$\frac{\partial p_3}{\partial \theta} = 0 \quad \text{on } \theta = \alpha,\ \pi-\alpha. \tag{10}$$

The region $OABCD$ of Fig. 1 is mapped on to the upper half of the ζ-plane by the transformations

$$z_2 = e^{-i\alpha\pi/(\pi-2\alpha)}(\rho e^{i\theta})^{\pi/(\pi-2\alpha)}, \tag{11}$$

$$\zeta = \xi+i\eta = -\frac{1}{2}\left(z_2+\frac{1}{z_2}\right). \tag{12}$$

As was shown in Part I, this transformation maps the points $OABCDO$ of the ρ, θ plane onto the points $-\infty$, -1, $-|\cos\tau|$, $+|\cos\tau|$, $+1$, and ∞ on the real axis of the ζ-plane.

We now define a complex function $W(\zeta)$ by

$$W(\zeta) = \frac{\partial p_3}{\partial \eta} + i\frac{\partial p_3}{\partial \xi} \tag{13}$$

and rewrite the boundary conditions in terms of W. Then on the real axis W is real for $|\xi| < 1$ and wholly imaginary for $|\xi| > 1$. Equations (7) suggest that W possesses simple poles at the points $\xi = \pm|\cos\tau|$, $\eta = 0$, whose residues are given by these equations. Moreover p_3 is bounded everywhere so that $W = O(\zeta^t)$ as $\zeta \to \infty$ where $t < -1$. A function which satisfies all these conditions in the plane is

$$W(\zeta) = \frac{\sin\tau}{\pi(1-\zeta^2)^{\frac{1}{2}}}\left[\frac{1}{\zeta+\cos\tau}+\frac{1}{\zeta-\cos\tau}\right], \tag{14}$$

where the branch of $(1-\zeta^2)^{\frac{1}{2}}$ is chosen to be that which is real and positive for $|\zeta| < 1$ on the real axis. On the surface of the wing $\theta = \alpha$,

$$\eta = \frac{\partial p_3}{\partial \eta} = 0$$

and equation (14) can be integrated to obtain the pressure p_3 at the surface. The value of p_3 on the line of symmetry is zero because of the antisymmetry of the boundary conditions. Hence

$$p_3 = \frac{2}{\pi}\arcsin\left\{\frac{\sin\tau}{(\xi^2-\cos^2\tau)^{\frac{1}{2}}}\right\}, \tag{15}$$

where the range of inverse sine is taken from $-\frac{1}{2}\pi$ to $+\frac{1}{2}\pi$. Equation (15) is valid for all α and ψ, including those values at which shock reflection occurs. Together with equations (4) and (6) it gives the pressure distribution on the surface of the wing.

When the angle of dihedral is small, the surface pressure distribution can be expanded as a power series in α. Taking the first term of this

expansion, we have the result previously obtained by Robinson and Hunter-Tod (**2**)

$$p_2 - p_0 = -\frac{2\rho_0 U^2 \epsilon\alpha}{\beta\pi\cos\psi} \arcsin\left\{\frac{\beta r\cos\psi}{(z^2 - r^2\tan^2\lambda)^{\frac{1}{2}}}\right\}. \tag{16}$$

Another special case occurs when the leading edges lie in the surface of the Mach cone. The pressure distribution is found from equations (4), (6), and (15) by taking the limit as $\tau \to 0$

$$p_2 - p_0 = -\frac{4\epsilon\rho_0 U^2 \sin\alpha}{\beta(\pi - 2\alpha)} \frac{\rho^{\pi/(\pi-2\alpha)}}{(1-\rho^{2\pi/(\pi-2\alpha)})}. \tag{17}$$

4. The leading edges inside the Mach cone

The situation in the physical plane has already been outlined in the previous section. All disturbances are confined to the interior of the Mach cone upon whose surface the internal pressure p_2 takes the value p_0. Unlike the case considered in § 3, the whole region inside the Mach cone is interconnected and the upper and lower surfaces of the wing must be considered together. The configuration of the wings is entirely symmetric about the plane $\theta = \frac{1}{2}\pi$, and from equation (5) the boundary conditions upon them are antisymmetrical. It follows that the dimensionless pressure

$$p_4 = \frac{p_2 - p_0}{\rho_0 U^2} \tag{18}$$

will also be antisymmetrical about the plane $\theta = \frac{1}{2}\pi$. Thus $p_4 = 0$ on the lines $\theta = \frac{1}{2}\pi$, $\theta = -\frac{1}{2}\pi$ and it is only necessary to consider one-half of the Mach cone, viz. that half given by $-\frac{1}{2}\pi \leqslant \theta \leqslant \frac{1}{2}\pi$ and containing the wing $\theta = \alpha$.

In the (ρ, θ) plane given by equation (2) the configuration is identical to that obtained in § 6 of Part I. The z-axis becomes the origin $(0, 0)$ and is designated E or B according to whether we consider the upper or lower surface of the wing at that point. The leading edge becomes the point A having coordinates (l, α) where

$$\frac{2l}{1+l^2} = \beta\cot\lambda \tag{19}$$

and the half Mach cone $(-\frac{1}{2}\pi \leqslant \theta \leqslant \frac{1}{2}\pi)$ is transformed into the unit semicircle $CBEDC$ (see Fig. 2). Considering the circuit $ABCDEA$, we denote the derivative along the circuit by $\partial/\partial s$ and the derivative along the inward normal to the circuit by $\partial/\partial n$, so that the boundary conditions for p_4 are

$$\left.\begin{aligned} \frac{\partial p_4}{\partial s} &= 0 \quad \text{on } BC,\ CD,\ DE \\ \frac{\partial p_4}{\partial n} &= 0 \quad \text{on } EA,\ AB \end{aligned}\right\}. \tag{20}$$

Consider the conformal transformation

$$\rho e^{i\theta} = i\left\{\frac{(\gamma^2-1)^{\frac{1}{2}}(\zeta^2-1)^{\frac{1}{2}}+\gamma\zeta+1}{\zeta+\gamma}\right\}^{-\{(\pi+2\alpha)/2\pi\}}\left\{\frac{(\delta^2-1)^{\frac{1}{2}}(\zeta^2-1)^{\frac{1}{2}}-\delta\zeta+1}{\zeta-\delta}\right\}^{(\pi-2\alpha)/2\pi}. \tag{21}$$

It was shown in Part I that this maps the interior of the configuration $ABCDEA$ onto the upper half of the $\zeta = \xi+i\eta$ plane, with the points

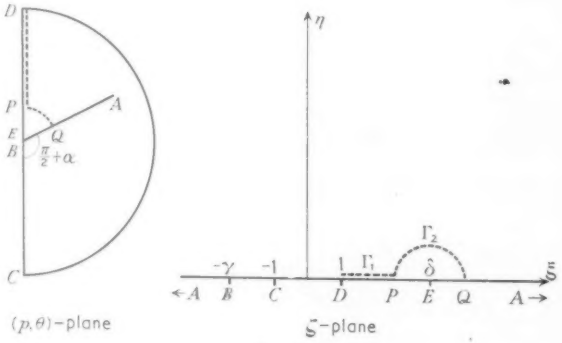

FIG. 2.

A, B, C, D, E, and A corresponding to $-\infty$, $-\gamma$, -1, 1, δ, and ∞ respectively (Fig. 2). In this transformation the branch of $(\zeta^2-1)^{\frac{1}{2}}$ is chosen to be that which is real and positive for ζ real and greater than 1, and γ and δ are positive constants defined by

$$\frac{\pi-2\alpha}{\pi+2\alpha} = \frac{(\gamma^2-1)^{\frac{1}{2}}}{(\delta^2-1)^{\frac{1}{2}}} \tag{22}$$

$$l = |(\gamma^2-1)^{\frac{1}{2}}+\gamma|^{-\{(\pi+2\alpha)/2\pi\}}|(\delta^2-1)^{\frac{1}{2}}-\delta|^{(\pi-2\alpha)/2\pi}. \tag{23}$$

In the ζ-plane we define a complex function $W(\zeta)$ such that

$$W(\zeta) = \frac{\partial p_4}{\partial \eta}+i\frac{\partial p_4}{\partial \xi}. \tag{24}$$

Rewriting conditions (20) in terms of W, it follows that on the real axis $W(\xi)$ is real for $\xi < -\gamma$ and $\xi > \delta$, and totally imaginary for $-\gamma < \xi < \delta$. Moreover, as in Part I, it can be shown that $W(\zeta)$ possesses no singularities on the real axis at E and B. At the wing leading edge, however, which corresponds in the ζ-plane to the point at infinity, a comparison with singularities incurred in analogous problems suggests that $W \sim A/\zeta+B$ as $\zeta \to \infty$. This assumption is reinforced by a more detailed study of the boundary conditions at the wing leading edge. On both upper and lower surfaces of the wing, equation (5) shows that $V_\theta = -U\epsilon \sin\alpha$, so that we

may use the theory of Part I (Appendix) to assert

$$\mathrm{re}\left\{\lim_{k\to\infty}\int_{\bar{k}}^{-k} W\,d\zeta\right\} = 0, \tag{25}$$

where the integral is taken around a large semicircle in the ζ-plane. A function which satisfies all these conditions and is integrable at all finite points of the upper half-plane is

$$W(\zeta) = \frac{Ai(2\zeta+\gamma-\delta)}{(\zeta-\delta)^{\frac{1}{2}}(\zeta+\gamma)^{\frac{1}{2}}}, \tag{26}$$

where A is a real constant and the branch of $(\zeta^2-\delta\zeta+\gamma\zeta-\delta\gamma)^{\frac{1}{2}}$ is chosen to be that which is real and positive for $\xi > \delta$, $\eta = 0$.

As $\partial p_4/\partial\eta$ is zero on the wing surface, equation (26) may be integrated to give the pressure on the upper wing surface,

$$p_4 = 2A(\xi-\delta)^{\frac{1}{2}}(\xi+\gamma)^{\frac{1}{2}}. \tag{27}$$

There is no constant of integration since the pressure p_4 is zero at $\zeta = \delta$. The constant A is evaluated from the boundary conditions on the line of symmetry. An examination of the components of the perturbation velocity near this line reveals that $V_\theta \to -U\epsilon$ as $r \to 0$ in the plane $\theta = \frac{1}{2}\pi$. Since V_θ is zero on the Mach cone, equation (12) of Part I may be integrated to give

$$\epsilon = \beta\int_0^1 \frac{1-\rho^2}{2\rho^2}\frac{\partial p_4}{\partial\theta}\,d\rho. \tag{28}$$

Upon transforming to the ζ-plane and substituting for $\frac{1}{\rho}\frac{\partial p_4}{\partial\theta}$ on the real axis we have

$$\frac{2\epsilon}{\beta} = -A\,{}^*\!\int_1^\delta \frac{1-\rho^2}{\rho}\frac{2\xi-\delta+\gamma}{|(\delta-\xi)^{\frac{1}{2}}(\gamma+\xi)^{\frac{1}{2}}|}\,d\xi \quad (\alpha \neq 0), \tag{29}$$

where the asterisk denotes the finite part of the integral as defined by Hadamard (**6**). This is made necessary by the divergence of the integral when $\alpha < 0$. A detailed justification of equation (29) for this case is given in Appendix II.

When the angle of dihedral is small, the pressure distribution on the wing can be obtained explicitly in terms of the flow parameters and the physical coordinates. To the first order equations (22) and (23) give $\gamma = \delta = (1+l^2)/2l$ so that the transformation (21) can be simplified on the wing surface to

$$\xi = \frac{1}{2}\frac{(1+l^2)(1-\rho^2)}{(l^2-\rho^2)^{\frac{1}{2}}(1-\rho^2l^2)^{\frac{1}{2}}}, \tag{30}$$

and equation (27) becomes

$$p_4 = \frac{A(1-l^2)}{l} \frac{r}{(z^2 \cot^2\lambda - r^2)^{\frac{1}{2}}}. \tag{31}$$

To evaluate the constant A from equation (29) we need only consider the behaviour of the integral in the neighbourhood of the endpoint $\xi = \delta$. At this point the integrand behaves as $K(\delta-\xi)^{-\{(\pi-\alpha)/\pi\}}$ for some constant K, so that to the first order

$$A = \frac{-4\epsilon\alpha l^2}{\beta\pi(1-l^4)}. \tag{32}$$

Substituting for A in equation (31), the actual pressure on the wing surface is found to be

$$p_2 = p_0 - \frac{2\epsilon\alpha\rho_0 U^2}{\pi} \frac{r}{(z^2 - r^2\tan^2\lambda)^{\frac{1}{2}}}, \tag{33}$$

a result which was previously found for this case by Robinson and Hunter-Tod (**2**).

When the leading edge approaches the Mach cone we may write $l = 1-t$ where t is small. The parameters γ and δ are then given approximately by

$$\gamma = 1 + \frac{1}{2}\left(\frac{\pi t}{\pi+2\alpha}\right)^2, \qquad \delta = 1 + \frac{1}{2}\left(\frac{\pi t}{\pi-2\alpha}\right)^2, \tag{34}$$

and the transformation (21) gives the relations

$$\xi = 1 + \frac{1}{2}\left(\frac{\pi t}{\pi-2\alpha}\right)^2 \left[\frac{1-\rho^{2\pi/(\pi-2\alpha)}}{1+\rho^{2\pi/(\pi-2\alpha)}}\right]^2 \quad \text{on } \theta = \tfrac{1}{2}\pi, \tag{35}$$

$$\xi = 1 + \frac{1}{2}\left(\frac{\pi t}{\pi-2\alpha}\right)^2 \left[\frac{1+\rho^{2\pi/(\pi-2\alpha)}}{1-\rho^{2\pi/(\pi-2\alpha)}}\right]^2 \quad \text{on } \theta = \alpha. \tag{36}$$

To the first order in t, equation (29) can be integrated by ordinary methods to give the constant $A = -(\epsilon \sin\alpha)/\pi\beta t$. Substituting this in the expression (27) for p_4 and taking the limit as $t \to 0$ the pressure distribution when the leading edge lies on the surface of the Mach cone is given by

$$p_2 = p_0 - \frac{4\epsilon\rho_0 U^2 \sin\alpha}{\beta(\pi-2\alpha)} \frac{\rho^{\pi/(\pi-2\alpha)}}{1-\rho^{2\pi/(\pi-2\alpha)}}. \tag{37}$$

This agrees with the result (17), obtained from the limit as the leading edge approaches the Mach cone from the outside. Thus all the aerodynamic derivatives in sideslip are continuous as the leading edges pass through the Mach cone.

5. The aerodynamic derivatives in sideslip

The derivatives are derived for a wing of delta planform. Thus if the maximum chord is c, the trailing edge is given by $z = c$, $\theta = \alpha$, $\pi-\alpha$, and the semi-span and area of the wing surface are $c\tan\lambda$ and $c^2\tan\lambda$ respectively.

Let (x, y, z) be a left-handed system of cartesian coordinates such that the z-axis coincides with the z-axis of the polar coordinate system already defined and the x-axis is given by $\theta = z = 0$. We resolve the force and couple acting on the wings into force components X, Y, and Z along the axes x, y, z respectively and moments L, M, and N about these axes. From a consideration of the antisymmetry condition it follows that

$$Y = Z = L = 0,$$

and we define the non-dimensional derivatives m_ϵ, n_ϵ, x_ϵ as follows:

$$\left.\begin{aligned} \text{Non-dimensional yawing derivative } m_\epsilon &= \frac{2M\tan^2\lambda}{\rho_0 U^2 \epsilon c^3} \\ \text{Non-dimensional rolling derivative } n_\epsilon &= \frac{2N\tan^2\lambda}{\rho_0 U^2 \epsilon c^3} \\ \text{Non-dimensional sideslip derivative } x_\epsilon &= \frac{2X\tan\lambda}{\rho_0 U^2 \epsilon c^2} \end{aligned}\right\}. \tag{38}$$

(The yawing derivative is referred to the origin, i.e. the vertex of the wing leading edges.)

When the leading edges lie outside the Mach cone, the pressure on the upper surface of the wing $\theta = \alpha$ may be considered in two parts: firstly, the pressure p_1 on the whole wing, secondly, the pressure $p_2 - p_1$ on that part of the wing inside the Mach cone. (This does not hold at values of α for which reflection of the Mach wedges occurs, i.e. $\alpha > \frac{1}{4}\pi + \frac{1}{2}\psi$: there will then be another term from outside the Mach cone.) The contribution to X from the upper surface is thus

$$2\sin\alpha\left\{\int_0^c \int_0^{z/\beta} (p_2 - p_1)\, dr dz + \int_0^c \int_0^{z\cot\lambda} p_1\, dr dz\right\}. \tag{39}$$

One integration may be completed by a substitution into the cone-field coordinate $R = \beta r/z$. Furthermore, p_2 and p_1 are given by equations (4) and (6) so that with similar results for M and N the derivatives are given by

$$m_\epsilon = \tfrac{2}{3}\beta x_\epsilon \sin\psi$$

$$= -\frac{4\sin^2\psi\sin^2\alpha}{3\cos\psi}\left[2(\operatorname{cosec}\psi - 1) + \int_0^1 p_3(\alpha, \psi, R)\, dR + \int_0^1 p_3(-\alpha, \psi, R)\, dR\right], \tag{40}$$

$$\beta n_\epsilon = \frac{4\sin^2\psi\sin\alpha}{3\cos\psi}\left[\cot^2\psi + \int_0^1 p_3(\alpha, \psi, R) R\, dR + \int_0^1 p_3(-\alpha, \psi, R) R\, dR\right], \tag{41}$$

where

$$\int_0^1 p_3\,dR = 1+\frac{4\sin\tau}{\pi-2\alpha}\int_0^1 \frac{\xi}{(1+\rho^2)(\xi^2-\cos^2\tau)}\,d\rho, \tag{42}$$

$$\int_0^1 p_3 R\,dR = \tfrac{1}{2}+\frac{4\sin\tau}{\pi-2\alpha}\int_0^1 \frac{\xi\rho}{(1+\rho^2)^2(\xi^2-\cos^2\tau)}\,d\rho, \tag{43}$$

and

$$\xi = -\tfrac{1}{2}(\rho^{\pi/(\pi-2\alpha)}+\rho^{-\pi/(\pi-2\alpha)}). \tag{44}$$

When the leading edges lie inside the Mach cone, the results are simpler to obtain, and integrating over a similar wing surface we have

$$m_\epsilon = \tfrac{2}{3}x_\epsilon\tan\lambda = \frac{4\sin\alpha\tan^2\lambda}{3\epsilon\beta}\left[\int_0^{\beta\cot\lambda} p_4(\alpha,l,R)\,dR - \int_0^{\beta\cot\lambda} p_4(-\alpha,l,R)\,dR\right], \tag{45}$$

$$n_\epsilon = \frac{-4\tan^2\lambda}{3\epsilon\beta^2}\left[\int_0^{\beta\cot\lambda} p_4(\alpha,l,R)R\,dR - \int_0^{\beta\cot\lambda} p_4(-\alpha,l,R)R\,dR\right], \tag{46}$$

where

$$\int_0^{\beta\cot\lambda} p_4\,dR = \frac{8(\pi+2\alpha)bA(1-b^2c^2)}{\pi(1-b^2)^{\frac{1}{2}}(1-c^2)^{\frac{1}{2}}}\int_c^1 \frac{\rho(1-\rho^2)\,da}{2(1+\rho^2)^2(1-a^2b^2)^{\frac{1}{2}}(a^2-c^2)^{\frac{1}{2}}}, \tag{47}$$

$$\int_0^{\beta\cot\lambda} p_4 R\,dR = \frac{8(\pi+2\alpha)bA(1-b^2c^2)}{\pi(1-b^2)^{\frac{1}{2}}(1-c^2)^{\frac{1}{2}}}\int_c^1 \frac{\rho^2(1-\rho^2)\,da}{(1+\rho^2)^3(1-a^2b^2)^{\frac{1}{2}}(a^2-c^2)^{\frac{1}{2}}}, \tag{48}$$

$$\rho = \left[\frac{1-ab}{1+ab}\right]^{(\pi+2\alpha)/2\pi}\left[\frac{a-c}{a+c}\right]^{(\pi-2\alpha)/2\pi}, \tag{49}$$

and b and c are constants such that $\gamma = \dfrac{1+b^2}{1-b^2}$, $\delta = \dfrac{1+c^2}{1-c^2}$.

In Figs. 3 and 4, values of βn_ϵ and βx_ϵ are given for dihedral angles of $10°$ and $30°$, at varying values of $(\tan\lambda)/\beta$. The yawing derivative can be easily obtained from the values of βx_ϵ.

6. Modified derivatives when the leading edges are outside the Mach cone

If the wing has a finite span, the pressure on the wing surface outside the Mach cone is no longer constant but depends on the shape of the wing at its tip. However, apart from a factor $\sin\alpha$, this pressure is independent of the dihedral angle. Thus the force derivatives on such a wing can be calculated from the values at zero dihedral by superimposing those forces which are due to the modifying effect of dihedral inside the Mach cone. For this purpose modified derivatives are defined which are based only on

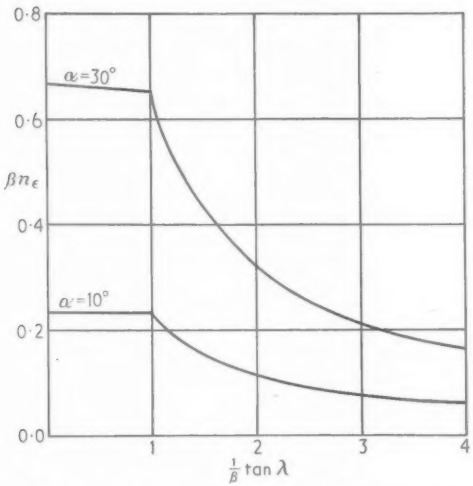

FIG. 3. The variation of the rolling derivative with sweep-back for dihedrals of 10° and 30°.

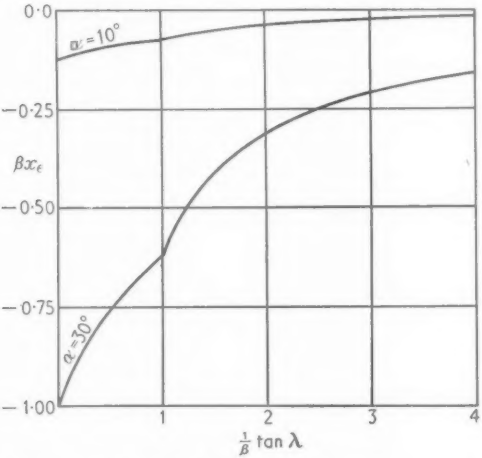

FIG. 4. The variation of the sideslip derivative with sweep-back for dihedrals of 10° and 30°.

the forces produced by the modified pressure (e.g. on the upper surface of the wing $\theta = \alpha$, the modified pressure inside the Mach cone is $p_2 - p_1$). If X', Y', Z' and L', M', N' are the force and moment components generated by the modified pressures, the modified derivatives of sideslip force and

yawing and rolling moments are defined as

$$x'_\epsilon = \frac{2X'\beta}{\rho_0 U^2 \epsilon c^2}, \qquad m'_\epsilon = \frac{2M'\beta^2}{\rho_0 U^2 \epsilon c^3}, \qquad n'_\epsilon = \frac{2N'\beta^2}{\rho_0 U^2 \epsilon c^3}, \tag{50}$$

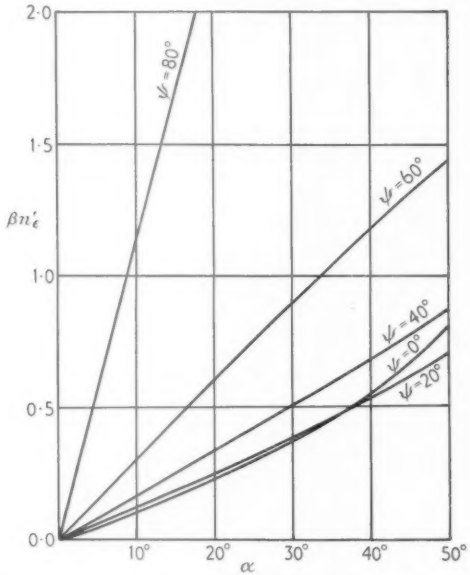

FIG. 5. The variation of the modified rolling derivative with dihedral.

respectively (from the antisymmetry condition $Y' = Z' = L' = 0$). Hence by an integration over the wing surface inside the Mach cone,

$$m'_\epsilon = \tfrac{2}{3}\beta x'_\epsilon = \tfrac{4}{3}\sec\psi \sin^2\alpha \left[2 - \int_0^1 p_3(\alpha, \psi, R)\, dR - \int_0^1 p_3(-\alpha, \psi, R)\, dR\right], \tag{51}$$

$$\beta n'_\epsilon = -\tfrac{4}{3}\sec\psi \sin\alpha \left[1 - \int_0^1 p_3(\alpha, \psi, R) R\, dR - \int_0^1 p_3(-\alpha, \psi, R) R\, dR\right], \tag{52}$$

where the integrals are given by equations (42) and (43). The variations of $\beta x'_\epsilon$, m'_ϵ, and $\beta n'_\epsilon$ with dihedral are given in Figs. 5 and 6 for $\psi = 0°$, 20°, 40°, 60°, 80°.

7. Conclusion

When the wing leading edges lie inside the Mach cone and

$$\beta \cot\lambda = 0{\cdot}645497,$$

solutions for the sideslip, rolling, and yawing derivatives have been given

by Nocilla (**5**). Expanding the derivatives as power series in α, he obtains values from the first two terms that agree very well for $\alpha < 30°$ with the results given here.

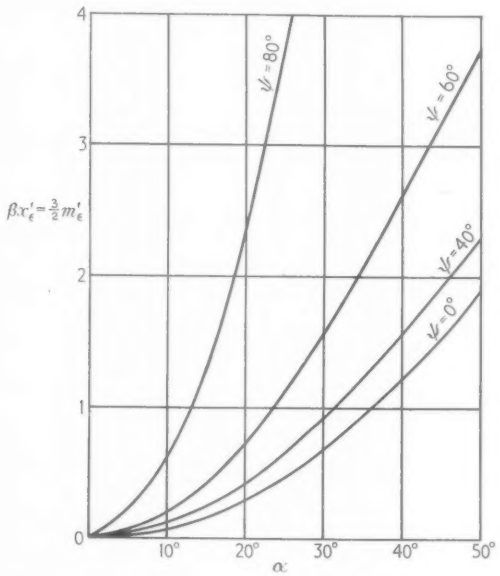

FIG. 6. The variation of the modified yawing and sideslip derivatives with dihedral.

At dihedral angles of less than 50°, the results suggest that for a given Mach number and sweepback, the rolling derivative is proportional to $\sin\alpha$ and the sideslip and yawing derivatives are proportional to $\sin^2\alpha$. Clearly, such a formula would enable the derivatives at any dihedral to be easily obtained as the results for small dihedral are already known explicitly (e.g. see **2**). The greatest deviation from this rule occurs when the leading edges lie inside and close to the surface of the Mach cone. At this point the true derivatives for a dihedral of 50° are approximately 10 per cent. less than the values given by the above rule. For dihedral angles less than 30° the error is less than 3 per cent.

In conclusion I would like to thank Dr. W. Chester for suggesting the subject of this paper and for his help in the preparation of it.

During the course of the work I was in receipt of a maintenance grant from the Department of Scientific and Industrial Research.

APPENDIX I

The pitching moment derivative

In Part I and the above paper all the derivatives except that due to the pitching moment have been determined for a delta wing. This last derivative is considered here.

Because of the antisymmetry conditions, no perturbations of the kind considered in the foregoing pages produce any contribution to the pitching moment. The only contribution to the moment comes from a displacement of the line of symmetry of the wing through an angle ϵ' in the plane $\theta = \frac{1}{2}\pi$; such a displacement was investigated in Part I. Denoting by L the pitching moment for a delta wing of maximum chord c, the aerodynamic pitching derivative l_ϵ (with respect to the vertex) is defined by

$$l_\epsilon = \frac{2L\tan^2\lambda}{\rho_0 U^2 \epsilon' c^3}. \tag{53}$$

An integration over the surface of the wing shows that for a delta wing

$$l_\epsilon = -\frac{2}{3\epsilon'} C_L \tan\lambda, \tag{54}$$

where C_L is the lift coefficient defined in Part I. Values of C_L are adequately given in Part I.

APPENDIX II

Consider the circuit DPQ in the (ρ,θ) plane, where QP is the arc $\rho = h, \alpha \leqslant \theta \leqslant \frac{1}{2}\pi$, and DP is the line $\theta = \frac{1}{2}\pi$, $1 \geqslant \rho \geqslant h$. If h is small the arc QP is represented in the ζ-plane by the circuit Γ_2 (see Fig. 2) where

$$\zeta = \delta + ke^{i\theta_1} + O(k^2) \tag{55}$$

and from the transformation (21), θ_1 and k are such that

$$\theta = \alpha + \frac{\pi - 2\alpha}{2\pi}\theta_1, \tag{56}$$

$$h = \left|\frac{\gamma+\delta}{(\gamma^2-1)^{\frac{1}{2}}(\delta^2-1)^{\frac{1}{2}}+\gamma\delta+1}\right|^{(\pi+2\alpha)/2\pi} \left|\frac{k}{2(\delta^2-1)}\right|^{(\pi-2\alpha)/2\pi}. \tag{57}$$

In the ζ-plane the line DP is represented by that part of the real axis for which $1 \leqslant \xi \leqslant \gamma - k$. This line is denoted by Γ_1, so that $\Gamma_1 + \Gamma_2$ refers to the whole circuit DPQ.

Now consider the following integral, whose path of integration in the ζ-plane is the circuit $\Gamma_1 + \Gamma_2$,

$$\int_{\Gamma_1+\Gamma_2} \frac{1-\rho^2}{\rho} W\, d\zeta. \tag{58}$$

Substituting from equation (24) and rewriting the integral in the (ρ,θ)-plane,

$$\int_{\Gamma_1+\Gamma_2} \frac{1-\rho^2}{\rho} W\, d\zeta = \int_{DPQ} \frac{1-\rho^2}{\rho}\left[\frac{1}{\rho}\frac{\partial p_1}{\partial\theta}\, d\rho - \rho\frac{\partial p_4}{\partial\rho}\, d\theta + i\frac{\partial p_4}{\partial\rho}\, d\rho + i\frac{\partial p_4}{\partial\theta}\, d\theta\right]. \tag{59}$$

On the circuit Γ_1, θ is constant and p_4 is zero, so that by substituting from equation (12) of Part I for $\frac{1}{\rho}\frac{\partial p_4}{\partial\theta}$,

$$\int_{\Gamma_1} \frac{1-\rho^2}{\rho} W\, d\zeta = \frac{2}{\beta U}[V_\theta]_{\Gamma_1}, \tag{60}$$

where $[\ ]_{\Gamma_1}$ here indicates the change in value upon completing the circuit Γ_1. In a like manner equation (59) can be simplified for the circuit Γ_2 by a substitution for $\partial p_4/\partial\rho$ by equation (11) of Part I:

$$\int_{\Gamma_2} \frac{1-\rho^2}{\rho} W\, d\zeta = \frac{2}{\beta U} \int_{PQ} V_r\, d\theta + \frac{i}{h}[p_4]_{\Gamma_2} + \frac{2}{\beta U}[V_\theta]_{\Gamma_2} + O(h^2). \tag{61}$$

But from the boundary conditions on the wing surface $V_r \sim +U\epsilon\cos\theta$ as $\rho \to 0$ so that equations (60) and (61) together give

$$\int_{\Gamma_1+\Gamma_2} \frac{1-\rho^2}{\rho} W\, d\zeta = \frac{2\epsilon\sin\alpha}{\beta} - \frac{2\epsilon}{\beta} + \frac{i}{h}[p_4]_{\Gamma_1+\Gamma_2} + \frac{2}{\beta U}[V_\theta]_{\Gamma_1+\Gamma_2} + O(h). \tag{62}$$

At the Mach cone boundary the perturbation velocity V_θ is zero and on the wing the condition of zero normal velocity gives $V_\theta = -U\epsilon\sin\alpha$. p_4 is zero on the Mach cone and its value on the wing surface is given by equation (27). W is given by equation (26), so that

$$A \int_{\Gamma_1+\Gamma_2} \frac{1-\rho^2}{\rho} \frac{i(2\zeta+\gamma-\delta)}{(\zeta-\delta)^{\frac{1}{2}}(\zeta+\gamma)^{\frac{1}{2}}}\, d\zeta = -\frac{2\epsilon}{\beta} + \frac{2Aik^{\frac{1}{2}}(\gamma+\delta)^{\frac{1}{2}}}{h} + O(h). \tag{63}$$

Taking the limit as $h \to 0$, it follows at once that

$$\frac{2\epsilon}{\beta} = -A \overset{*}{\int_1^\delta} \frac{1-\rho^2}{\rho} \frac{2\xi-\delta+\gamma}{|(\delta-\xi)^{\frac{1}{2}}(\gamma+\xi)^{\frac{1}{2}}|}\, d\xi \quad (\alpha \neq 0). \tag{64}$$

REFERENCES

1. J. B. L. Powell, 'The effect of dihedral on the lift and drag coefficients of airfoils in supersonic flow', *Quart. J. Mech. App. Math.* **9** (1956), 51.
2. A. Robinson and J. H. Hunter-Tod, 'The aerodynamic derivatives with respect to sideslip for a delta wing with small dihedral at zero incidence at supersonic speeds' (1947) A.R.C. R and M, No. 2410.
3. H. Multhopp, 'A unified theory of supersonic flow employing conical fields' (1951), R.A.E. report, Aero. No. 2415.
4. S. Nocilla, 'Su di un problema di aerodinamica relativo alle ali a delta', *Rend. Acc. Naz. Lincei*, **15** (1953), 177.
5. —— 'Sul problema dell' ala triangolare a diedro qualsiasi a relativo supersonica, con incidenza e deriva piccola del prim' ordine', *L'Aerotecnica*, **34** (1954), 3, 126.
6. J. Hadamard, *Lectures on Cauchy's Problem in Linear Partial Differential Equations* (Yale, 1923).

ON THE THEORY OF SOURCE-FLOW FROM AEROFOILS

By L. C. WOODS (*University of Sydney, Australia*)†

[Received 8 December 1955]

SUMMARY

An exact theoretical treatment of the influence of sources of fluid on and within two-dimensional aerofoils is developed. In the case of a source placed within an aerofoil the fluid is ejected through a duct, the shape of which is taken into account in the theory. The theory is given for incompressible flow but it could be extended to deal with linearized subsonic compressible flow. Formulae for the thrust, lift, and moment are derived from Blasius's theorem. The case of the 'directed' source receives attention, and the influence of the angle of ejection is determined.

List of symbols

q, θ	velocity vector in polar coordinates.
U	undisturbed velocity magnitude (at infinity).
f	$\equiv \log(U/q)+i\theta$.
w	$= \phi+i\psi$, the complex stream function.
$_0$	a subscript to denote values relating to a particular fictitious flow (not satisfying Joukowski's condition).
t, ζ, σ	analytic functions of w_0, defined by equations (1), (4), and (6).
η, γ	the real and imaginary parts of ζ.
c	aerofoil chord length.
α	incidence measured from the no-lift attitude.
a	the aerofoil lies in $-2a \leqslant \phi_0 \leqslant 2a$, $\psi_0 = 0$.
z	the real physical plane.
Q	the source strength.
C_Q	$\equiv Q/Uc$, the mass coefficient of the source.
t_0, P, δ, a_0	convenient functions of the source strength, defined by equations (2), (3), (5), and (12).
b_1, b_2	coefficients defined by equation (18).
ρ	density.
D, L, M	drag, lift, and moment forces.
C_D, C_L, C_M	drag, lift, and moment coefficients.
s	distance measured around the aerofoil surface.
l	distance of source from trailing edge.
1, 2	as subscripts to denote quantities relating to the real non-circulating flow and the real circulating flow respectively.
β	the trailing edge is at $\gamma = \pi-\beta$.
δ, λ	values of γ defining the positions of the stagnation points.

† Now at the N.S.W. University of Technology, Sydney.

1. Introduction

SOURCE and sinks on aerofoils have long been considered as possible means of controlling boundary layer separation and the circulation. The mathematical theory for the influence of *sinks* on the lift of aerofoils has been given in various forms by a number of authors (see, for example, Ehlers, 1), but to the author's knowledge existing accounts ignore the effect of duct

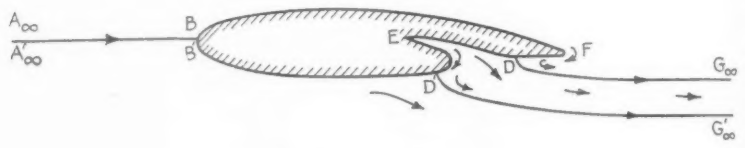

FIG. 1.

shape, and usually consider only the simple case of a sink right on the aerofoil surface.

In this paper we present an exact theory for *sources* within aerofoils, the fluid from which is conveyed by a duct of general shape and emitted into the main stream. The special cases of (*a*) a source right on the aerofoil surface, and (*b*) a parallel walled duct ejecting fluid at a given angle into the main stream, receive detailed attention.

The fluid is supposed to be inviscid and incompressible. Also the source fluid is assumed to be at the same total head as the main stream fluid, so that both the pressure and the velocity is continuous across the streamlines separating the source fluid from the main stream.

2. The basic conformal transformations

Consider the flow shown in Fig. 1. There are three stagnation points on the surface, namely those at B, D, and D', the positions of which are fixed as follows. First the Joukowski condition at the trailing edge F is satisfied by movement of D into coincidence with F, and then the positions of D' and B are uniquely determined by the strengths of the source and the circulation.

The first transformation we introduce can be regarded as a fictitious non-circulating flow about the aerofoil such that the points D and D' are at the same velocity potential. This flow plane is termed the w_0-plane, where $w_0 = \phi_0 + i\psi_0$, and is shown in Fig. 2. The aerofoil is assumed to lie in the interval $-2a \leqslant \phi_0 \leqslant 2a$ in this plane. The actual relation between $4a$ and the aerofoil chord length in the z-plane c will be determined later. The source output is Q units per second, so we can assign $\psi_0 = 0$ on $D'G'_\infty$ and

$\psi_0 = Q$ on DG_∞. The leading edge streamline is a line of discontinuity of the stream function ψ_0, but this causes no confusion in the following analysis.

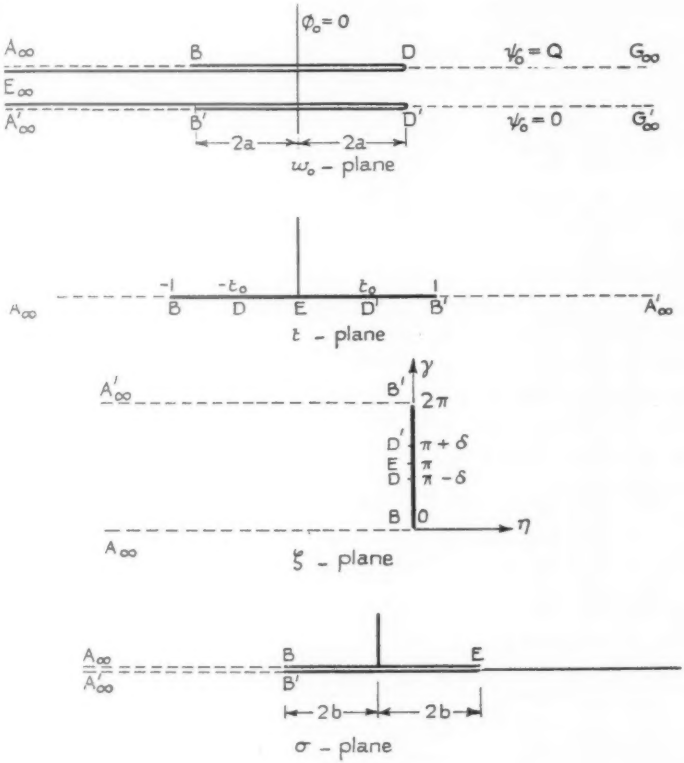

The basic conformal transformations

FIG. 2.

Also shown in Fig. 2 are three further planes derived by conformal transformations from the w_0-plane. These mappings are readily calculated by the Schwarz–Christoffel mapping theorem. First the w_0-plane is mapped into the upper half of the t-plane by

$$w_0 = 4aP(1-t^2) + \frac{Q}{\pi}\ln t - 2a, \tag{1}$$

$$\frac{Q}{8a\pi} = \frac{t_0^2}{1 - t_0^2 + t_0^2 \ln(t_0^2)}, \tag{2}$$

where $$P = \frac{1-(Q/4\pi a)\ln t_0}{1-t_0^2}, \tag{3}$$

and the points D', D map into $t = t_0$, $t = -t_0$, respectively.

The t-plane is mapped into the semi-infinite strip $-\infty \leqslant \eta \leqslant 0$, $0 \leqslant \gamma \leqslant 2\pi$ in the ζ $(= \eta + i\gamma)$ plane by

$$t = -\cosh \tfrac{1}{2}\zeta. \tag{4}$$

The points D', D map into $\gamma = \pi+\delta$, and $\gamma = \pi-\delta$, on $\eta = 0$, so that from (4)

$$t_0 = \sin \tfrac{1}{2}\delta. \tag{5}$$

Finally the σ-plane shown in Fig. 2 is derived from the t-plane by

$$\sigma = 2(1-2t^2). \tag{6}$$

Most of the detailed calculations will be made in the ζ-plane, but the σ-plane has been introduced for the purpose of applying Blasius's theorem to the problem. The symmetry of the mappings means that in this plane the characteristics of the real flow are continuous across $A_\infty B$, and hence closed contours enclosing the aerofoil surface will be closed contours enclosing the strip $-2 \leqslant \sigma \leqslant 2$ in the σ-plane.

The following equations, which are readily derived from (1) to (6), will be required later:

$$\frac{Q}{4a\pi P} = 2t_0^2 = 1-\cos\delta, \tag{7}$$

or if C_Q is the mass coefficient of the source defined by

$$C_Q = Q/cU, \tag{8}$$

where c is the chord length, then

$$C_Q = 2\pi\left(\frac{4aP}{cU}\right)\sin^2 \tfrac{1}{2}\delta. \tag{9}$$

Also $$e^{\zeta} = -\frac{1}{\sigma}\left\{1+\frac{1}{\sigma^2}+O(\sigma^{-4})\right\}, \tag{10}$$

and $$\frac{dw_0}{d\sigma} = aP\left\{1+\frac{a_0}{\sigma}+\frac{2a_0}{\sigma^2}+O(\sigma^{-3})\right\}, \tag{11}$$

where $$a_0 = \frac{Q}{2a\pi P} = 4\sin^2\tfrac{1}{2}\delta. \tag{12}$$

3. The general solution in the ζ-plane

Consider any circulating flow past the aerofoil. Let (q, θ) be the velocity vector in polar coordinates, and take $\lim_{z\to\infty}(q, \theta) = (U, \alpha)$, then if w is the complex stream function,

$$f = \ln\left(U\frac{dz}{dw}\right) = \ln\left(\frac{U}{q}\right)+i\theta, \tag{13}$$

where
$$\lim_{z\to\infty} f = i\alpha. \tag{14}$$

In the ζ-plane, although $\gamma = 0$ and $\gamma = 2\pi$ no longer correspond to the leading edge streamline, the flow conditions at a given value of η on these lines are identical. Now f is an analytic function of z, and since $z = z(\zeta)$, f is also an analytic function of ζ. The function satisfying these conditions is (see Woods, **2**)

$$f = \frac{1}{2\pi}\int_0^{2\pi} \theta(\gamma^*)\cot\tfrac{1}{2}(\gamma^*+i\zeta)\,d\gamma^*, \tag{15}$$

where $\theta(\gamma^*)$ is the value of θ on $\eta = 0$ at $\gamma = \gamma^*$. On the aerofoil surface (15) yields

$$\ln\left(\frac{U}{q}\right) = \frac{1}{2\pi}\int_0^{2\pi} \theta(\gamma^*)\cot\tfrac{1}{2}(\gamma^*-\gamma)\,d\gamma^*,$$

or
$$\ln\left(\frac{U}{q}\right) = -\frac{1}{\pi}\int_0^{2\pi} \ln|\sin\tfrac{1}{2}(\gamma^*-\gamma)|\,d\theta(\gamma^*), \tag{16}$$

on integrating by parts.

At large negative values of η equation (15) yields the expansion

$$f = b_0+b_1 e^{\zeta}+b_2 e^{2\zeta}+O(e^{3\zeta}), \tag{17}$$

where
$$\left.\begin{aligned} b_n &= \frac{i}{\pi}\int_0^{2\pi} \theta(\gamma^*)e^{-in\gamma^*}\,d\gamma^*, \quad n = 1, 2 \\ b_0 &= \frac{i}{2\pi}\int_0^{2\pi} \theta(\gamma^*)\,d\gamma^* \end{aligned}\right\}. \tag{18}$$

Now $z \to \infty$ implies $\sigma \to \infty$, and from (10), $\eta \to -\infty$; thus we deduce from (14), (17), and (18) that

$$\frac{1}{2\pi}\int_0^{2\pi} \theta(\gamma^*)\,d\gamma^* = \alpha. \tag{19}$$

Equations (10), (13), (17) to (19) now give the expansion

$$\frac{dw}{dz} = Ue^{-i\alpha}\left\{1+\frac{b_1}{\sigma}-(b_2-\tfrac{1}{2}b_1^2)\frac{1}{\sigma^2}+O(\sigma^{-3})\right\}. \tag{20}$$

As a particular value of the theory consider the flow characterized by w_0. We denote the velocity vector in this case by (q_0, θ_0) and set

$$\lim_{z\to\infty} (q_0, \theta_0) = (U, \alpha_0).$$

Then corresponding to the above equations we have

$$\ln\left(\frac{U}{q_0}\right) = -\frac{1}{\pi}\int_0^{2\pi} \ln|\sin\tfrac{1}{2}(\gamma^*-\gamma)|\, d\theta(\gamma^*), \tag{21}$$

$$\frac{dw_0}{dz} = Ue^{-i\alpha_0}\left\{1+\frac{b_{10}}{\sigma}-(b_{20}-\tfrac{1}{2}b_{10}^2)\frac{1}{\sigma^2}+O(\sigma^{-3})\right\}, \tag{22}$$

$$b_{n0} = \frac{i}{\pi}\int_0^{2\pi} \theta_0(\gamma^*)e^{-in\gamma^*}\, d\gamma^*, \tag{23}$$

and

$$\alpha_0 = \frac{1}{2\pi}\int_0^{2\pi} \theta_0(\gamma^*)\, d\gamma^*. \tag{24}$$

4. The closure conditions

Let C be any contour enclosing the aerofoil, then the aerofoil is closed if $\int_C dz = 0$. In the σ-plane this condition can be written

$$\int_C \left(\frac{dz}{dw_0}\right)\left(\frac{dw_0}{d\sigma}\right) d\sigma = 0.$$

Hence from (11) and (22)

$$\frac{aP}{U}e^{i\alpha_0}\int_C \left\{1-\frac{b_{10}}{\sigma}+O(\sigma^{-2})\right\}\left\{1+\frac{a_0}{\sigma}+O(\sigma^{-2})\right\} d\sigma = 0,$$

which requires that $a_0 = b_{10}$ from the residue theorem.

It now follows from (12) and (23) that

$$a_0 = 4\sin^2\tfrac{1}{2}\delta = \frac{1}{\pi}\int_0^{2\pi} \theta_0(\gamma^*)\sin\gamma^*\, d\gamma^*, \tag{25}$$

and

$$0 = \frac{1}{\pi}\int_0^{2\pi} \theta_0(\gamma^*)\cos\gamma^*\, d\gamma^*, \tag{26}$$

which are the required conditions.

5. The application of Blasius's theorem

In a general circulating flow the drag D, lift L, and nose-up moment (about the origin in the z-plane) M, are given by

$$e^{-i\alpha}(D-iL) = \tfrac{1}{2}i\rho\int_C \left(\frac{dw}{dz}\right)^2 dz, \tag{27}$$

and

$$M-iN = \tfrac{1}{2}\rho\int_C z\left(\frac{dw}{dz}\right)^2 dz, \tag{28}$$

the $e^{-i\alpha}$ term being introduced to allow for the fact that the undisturbed flow is at an angle α to the x-axis.

To find M we need the expansion for z in terms of σ. Now

$$\frac{dz}{d\sigma} = \left(\frac{dz}{dw_0}\right)\left(\frac{dw_0}{d\sigma}\right),$$

therefore
$$\frac{dz}{d\sigma} = \frac{aP}{U}e^{i\alpha_0}\left\{1+(b_{20}-\tfrac{1}{2}a_0^2+2a_0)\frac{1}{\sigma^2}+O(\sigma^{-3})\right\} \tag{29}$$

on using (11), (22) and $b_{10} = a_0$. Hence

$$z = \frac{aP}{U}e^{i\alpha_0}\sigma\left\{1-(b_{20}-\tfrac{1}{2}a_0^2+2a_0)\frac{1}{\sigma^2}+O(\sigma^{-3})\right\}, \tag{30}$$

where the constant of integration has been made zero. This is equivalent to fixing the origin of the z-plane at a certain point, termed the 'centre' of the profile.

To find this centre consider the surface integral

$$I = \int_0^{2\pi} z\, d\gamma.$$

We can write
$$I = i\oint z\frac{d\zeta}{d\sigma}\,d\sigma,$$

then from (10), (30) and the residue theorem we find that $I = 0$. Hence the centre of the profile is calculated from

$$\int_0^{2\pi} x\, d\gamma = 0, \qquad \int_0^{2\pi} y\, d\gamma = 0, \tag{31}$$

when x, y have been determined as functions of γ.

We can now evaluate (27) and (28) by the residue theorem. Equation (27) can be written

$$D-iL = \tfrac{1}{2}i\rho e^{i\alpha}\int_C \left(\frac{dw}{dz}\right)^2\left(\frac{dz}{d\sigma}\right)d\sigma,$$

and hence from (20), (29) and the residue theorem

$$D-iL = -2\pi a\rho PUe^{i(\alpha_0-\alpha)}b_1. \tag{32}$$

Similarly, from (20) and (28) to (30),

$$M-iN = -2\pi i\rho(aP)^2e^{2i(\alpha_0-\alpha)}(b_2-b_1^2). \tag{33}$$

A more explicit result for the drag can be obtained as follows. From (20) and (30),

$$\frac{dw}{dz} = Ue^{-i\alpha}\left\{1+\frac{b_1aP}{Uz}e^{i\alpha_0}+O(z^{-2})\right\},$$

so that
$$w = A+Ue^{-i\alpha}\left\{z+\frac{b_1aP}{U}e^{i\alpha_0}\ln(z)+O(z^{-1})\right\}.$$

Recalling that the real part of the coefficient of $\ln z$ in this expansion equals the strength of the source (or sink) at infinity divided by 2π, we deduce

$$Q = 2\pi a P \,\mathrm{re}\{e^{i(\alpha_0-\alpha)}b_1\}, \tag{34}$$

or, from (12),

$$a_0 = 4\sin^2\tfrac{1}{2}\delta = \mathrm{re}\{e^{i(\alpha_0-\alpha)}b_1\}. \tag{35}$$

But, from (32),

$$D = -2\pi a P \rho U \,\mathrm{re}\{e^{i(\alpha_0-\alpha)}b_1\},$$

and hence

$$D = -\rho U Q.$$

In terms of the drag and mass coefficients defined by $C_D = D/\frac{1}{2}\rho c U^2$, and equation (8), this reduces to the well-known result

$$C_D = -2C_Q. \tag{36}$$

Equations (32) and (35) enable us to rewrite the expression for the moment in a more convenient form. From (33)

$$M = 2\pi\rho(aP)^2 \,\mathrm{im}\{e^{2i(\alpha_0-\alpha)}b_2\} - 2\pi\rho(aP)^2 \,\mathrm{im}\{e^{i(\alpha_0-\alpha)}b_1\}^2;$$

but, from (32) and (35),

$$\mathrm{im}\{e^{i(\alpha_0-\alpha)}b_1\}^2 = 2\,\mathrm{im}\{e^{i(\alpha_0-\alpha)}b_1\}\mathrm{re}\{e^{i(\alpha_0-\alpha)}b_1\} = \frac{4L\sin^2\tfrac{1}{2}\delta}{\pi\rho a P U},$$

and hence

$$M = 2\pi\rho(aP)^2 \,\mathrm{im}\{e^{2i(\alpha_0-\alpha)}b_2\} - 2\left(\frac{4aP}{cU}\right)Lc\sin^2\tfrac{1}{2}\delta. \tag{37}$$

6. Real non-circulating flow past the aerofoil

We now consider the flow past the aerofoil which satisfies Joukowski's condition, and is such that no lift force acts on the aerofoil. Let θ_1 denote the value of θ on the aerofoil surface in this flow, and let $\lim_{z\to\infty} \theta = \alpha_1$, so that α_1 is the no-lift angle. Referring to Fig. 1 we notice that in this flow the rear stagnation point must move to coincidence with F, while the other stagnation points must move to new positions to maintain zero circulation and unchanging source strength. The difference $(\theta_1-\theta_0)$ is thus due only to the shift in the positions of these stagnation points.

Let the trailing edge be at $\gamma = \pi-\beta$, and let the stagnation points originally at D' ($\gamma = \pi+\delta$) and B' ($\gamma = 2\pi$) move to $\gamma = \pi+\delta_1$, and $\gamma = 2\pi-\lambda_1$, respectively, then

$$\theta_1-\theta_0 = \pi\begin{cases}(\pi-\beta < \gamma < \pi-\delta)\\ (\pi+\delta_1 < \gamma < \pi+\delta)\\ (2\pi-\lambda_1 < \gamma < 2\pi)\end{cases} \tag{38}$$

0 (elsewhere).

From (19) and (24),

$$\alpha_1-\alpha_0 = \frac{1}{2\pi}\int_0^{2\pi}(\theta_1-\theta_0)\,d\gamma,$$

hence

$$2(\alpha_1-\alpha_0) = \beta+\lambda_1-\delta_1, \tag{39}$$

from (38). In this equation α_0 and β can be regarded as known, α_0 following from (24), and β, which defines the position of the trailing edge, being determined as follows.

Let s be distance measured from B along the aerofoil surface, then

$$s = \int_0^{\phi_0} \frac{d\phi_0}{q_0}.$$

Therefore

$$sU = \int_0^{\gamma} \frac{U}{q_0}\left(\frac{d\phi_0}{dt}\right)\left(\frac{dt}{d\gamma}\right) d\gamma.$$

On the aerofoil surface (1) and (4) yield

$$\frac{d\phi_0}{dt} = -8aPt + \frac{Q}{\pi t}, \qquad t = -\cos\tfrac{1}{2}\gamma.$$

These relations and equation (12) enable us to deduce that

$$s = \frac{1}{2}\left(\frac{4aP}{cU}\right)\int_0^{\gamma} \frac{U}{q_0}(\cos\gamma + \cos\delta)\tan\tfrac{1}{2}\gamma\, d\gamma, \tag{40}$$

the value of U/q_0 in this being determined from (21). Suppose now that the source is placed at a distance l from the trailing edge, then it follows from (40) that

$$\frac{l}{c} = \frac{1}{2}\left(\frac{4aP}{cU}\right)\int_{\pi-\beta}^{\pi} \frac{U}{q_0}(\cos\gamma + \cos\delta)\tan\tfrac{1}{2}\gamma\, d\gamma. \tag{41}$$

It remains to calculate $(4aP/cU)$. Let the total length of the aerofoil perimeter be expressed as $2kc$, then k can be calculated from the known aerofoil shape; it will be approximately unity for thin aerofoils. Then from (40)

$$\left(\frac{cU}{4aP}\right) = \frac{1}{4k}\int_0^{2\pi} \frac{U}{q_0}(\cos\gamma + \cos\delta)\tan\tfrac{1}{2}\gamma\, d\gamma. \tag{42}$$

The parameter β can now be calculated from equations (41) and (42).

In addition to (39) there are two further relations between α_1, λ_1, and δ_1, which determine them uniquely. First we have equation (35), which expresses the invariance of the source strength. From (18), (25), (26), and (35) we find that for the flow considered in this section

$$2\pi(1-\cos\delta)(1-\cos(\alpha_0-\alpha_1))$$
$$= \cos(\alpha_0-\alpha_1)\int_0^{2\pi}(\theta_1-\theta_0)\sin\gamma\, d\gamma - \sin(\alpha_0-\alpha_1)\int_0^{2\pi}(\theta_1-\theta_0)\cos\gamma\, d\gamma,$$

which reduces to

$$2(1-\cos\delta) = \cos(\alpha_0-\alpha_1)+\cos(\alpha_0-\alpha_1+\lambda_1)-\cos(\delta_1-\alpha_0+\alpha_1)- \\ -\cos(\beta+\alpha_0-\alpha_1),$$

by (38). Equation (39) enables us to rewrite this in the concise form

$$\sin^2\tfrac{1}{2}\delta = \sin\tfrac{1}{2}\beta\sin\tfrac{1}{2}\delta_1\cos\tfrac{1}{2}\lambda_1. \tag{43}$$

Secondly the zero lift condition is found from (18), (25), (26), and (32) to require that

$$2\pi\sin(\alpha_0-\alpha_1)(1-\cos\delta)+\sin(\alpha_0-\alpha_1)\int_0^{2\pi}(\theta_1-\theta_0)\sin\gamma\,d\gamma + \\ +\cos(\alpha_0-\alpha_1)\int_0^{2\pi}(\theta_1-\theta_0)\cos\gamma\,d\gamma = 0,$$

which by (38) and (39) reduces to

$$\sin\tfrac{1}{2}(\lambda_1+\delta_1)\cos\tfrac{1}{2}\beta = \sin\tfrac{1}{2}\beta\cos\tfrac{1}{2}(\delta_1-\lambda_1). \tag{44}$$

Equations (39), (43), and (44) determine α_1, λ_1, and δ_1, so the flow is uniquely defined

7. The lifting aerofoil

Next we consider the case of a real circulating flow. The rear stagnation point remains fixed at the trailing edge, but the other stagnation points move with increasing incidence. Let θ_2 be the value of θ on the aerofoil surface in this circulating flow, and let $\lim_{z\to\infty}\theta = \alpha$, so that α is the angle of incidence. Suppose the stagnation points originally at $\gamma = \pi+\delta$, $\gamma = \pi-\delta$, and $\gamma = 2\pi$ are now at $\gamma = \pi+\delta_2$, $\gamma = \pi-\beta$ (Joukowski's condition), and $\gamma = 2\pi-\lambda_2$, respectively, then

$$\theta_2-\theta_0 = \pi\begin{cases}(\pi-\beta<\gamma<\pi-\delta)\\(\pi+\delta_2<\gamma<\pi+\delta)\\(2\pi-\lambda_2<\gamma<2\pi)\end{cases} \\ 0\ \text{(elsewhere)}. \tag{45}$$

The calculation now proceeds just as in section 6. Corresponding to (39), (43), and (44) we find

$$2(\alpha-\alpha_0) = \beta+\lambda_2-\delta_2, \tag{46}$$

$$\sin^2\tfrac{1}{2}\delta = \sin\tfrac{1}{2}\beta\sin\tfrac{1}{2}\delta_2\cos\tfrac{1}{2}\lambda_2, \tag{47}$$

and

$$L = 4\pi\rho aPU\{\sin\tfrac{1}{2}(\lambda_2+\delta_2)\cos\tfrac{1}{2}\beta-\sin\tfrac{1}{2}\beta\cos\tfrac{1}{2}(\delta_2-\lambda_2)\}.$$

By equations (46) and (47) we can eliminate λ_2 and δ_2 from the equation for L. Then replacing L by the lift coefficient $C_L = L/\frac{1}{2}\rho cU^2$, we find that

$$C_L = 2\pi\left(\frac{4aP}{cU}\right)\{\sin(\alpha-\alpha_0-\beta)+2\cot\tfrac{1}{2}\beta\sin^2\tfrac{1}{2}\delta\}, \tag{48}$$

or

$$C_L = 2\pi\left(\frac{4aP}{cU}\right)\sin(\alpha-\alpha_0-\beta)+2C_Q\cot\tfrac{1}{2}\beta, \tag{49}$$

by (9). The second term on the right-hand side of (49) does not necessarily represent all the effect of the source on the lift as both α_0 and β may also depend on C_Q.

From (18) and (37) it follows that the moment is given by

$$M = 2\rho(aP)^2\Big\{\sin 2(\alpha_0-\alpha)\int_0^{2\pi}(\theta_2-\theta_0)\sin 2\gamma\, d\gamma + \\ +\cos 2(\alpha_0-\alpha)\int_0^{2\pi}(\theta_2-\theta_0)\cos 2\gamma\, d\gamma + \\ +\sin 2(\alpha_0-\alpha)\int_0^{2\pi}\theta_0\sin 2\gamma\, d\gamma+\cos 2(\alpha_0-\alpha)\int_0^{2\pi}\theta_0\cos 2\gamma\, d\gamma\Big\}.$$

The integrals involving $(\theta_2-\theta_0)$ are evaluated from (45), then λ_2, δ_2, and L can be eliminated from the result by (46), (47), and (48). It is found that

$$C_M = \frac{\pi}{4}\left(\frac{4aP}{cU}\right)^2\Big\{\cos 2\delta\sin 2(\alpha-\alpha_0)+16\sin\tfrac{1}{2}\beta\cos(\alpha-\alpha_0-\tfrac{1}{2}\beta)\sin^2\tfrac{1}{2}\delta- \\ -16\cot\tfrac{1}{2}\beta\sin^4\tfrac{1}{2}\delta+\frac{1}{\pi}\sin 2(\alpha_0-\alpha)\int_0^{2\pi}\theta_0\sin 2\gamma\, d\gamma+ \\ +\frac{1}{\pi}\cos 2(\alpha_0-\alpha)\int_0^{2\pi}\theta_0\cos 2\gamma\, d\gamma\Big\}, \quad (50)$$

where C_M is the moment coefficient $M/\frac{1}{2}\rho c^2U^2$. This equation applies to the moment taken about the origin of the z-plane. Further reduction is possible only when the shape of the aerofoil and duct is known.

8. Sources on thin aerofoils

The theory so far developed is exact, regardless of the source strength and of the aerofoil thickness. To make further progress we need to know the shape of the aerofoil and duct. For simplicity we will confine our attention to the flat plate aerofoil, although the results obtained relating to the influence of the source on the aerofoil characteristics will be applicable to conventional aerofoil shapes with but little error. The effects of the source flow found below could be linearly superimposed on the thickness effects to give a reasonably close result for conventional aerofoil shapes.

As far as the duct is concerned only two simple cases will be considered here. These are (*a*) no duct at all, that is the case of a source placed directly on the aerofoil surface, and (*b*) a parallel walled duct of such a width that the stagnation points occur at the corners of the duct exit (see Fig. 3). If

the duct width at exit is too small, or too large, the flow will be required to turn the sharp exit corners, a physically unrealistic case that we wish to avoid.

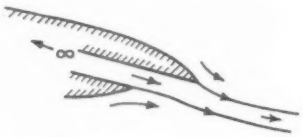

FIG. 3.

8.1. *Source on the aerofoil surface*

Fig. 4 shows the fictitious flow introduced in section 2. Assuming that the leading edge C is at $\gamma = 2\pi - \lambda$ we have the following table of values:

Point	B	F	D	E	D'	S	B'
γ	0	$\pi-\beta$	$\pi-\delta$	π	$\pi+\delta$	$2\pi-\lambda$	2π

Hence from Fig. 4 it is apparent that

$$\theta_0 = -\pi \begin{cases} (\pi-\beta < \gamma < \pi-\delta) \\ (\pi < \gamma < \pi+\delta) \\ (2\pi-\lambda < \gamma < 2\pi) \end{cases} \qquad (51)$$

0 (elsewhere).

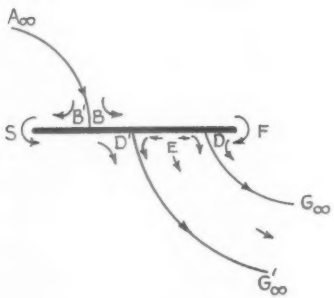

FIG. 4.

With these values of θ_0 equations (24), (25), and (26) yield $2\alpha_0+\lambda+\beta=0$, $\cos\beta = \cos\lambda$, and $\sin\beta = \sin\lambda$, respectively. Thus

$$\lambda = \beta, \qquad (52$$

and $$\alpha_0 = -\beta. \tag{53}$$

The next step is to find the relation between the perimeter distance s and γ from equations (16), (40), and (42). With the step function defined in (51) the Stieltjes integral in (16) degenerates to give

$$\ln\left(\frac{U}{q_0}\right) = \ln\left\{\frac{\sin\frac{1}{2}(\pi-\beta-\gamma)\sin\frac{1}{2}(\pi-\gamma)\sin\frac{1}{2}(2\pi-\lambda-\gamma)}{\sin\frac{1}{2}(\pi-\delta-\gamma)\sin\frac{1}{2}(\pi+\delta-\gamma)\sin\frac{1}{2}(2\pi-\gamma)}\right\},$$

and therefore $$\frac{q_0}{U} = \frac{2\cos\frac{1}{2}(\delta+\gamma)\cos\frac{1}{2}(\delta-\gamma)}{\sin(\beta+\gamma)}\tan\tfrac{1}{2}\gamma, \tag{54}$$

on making use of (52). With this value of q_0/U equation (40) gives

$$\frac{s}{c} = \frac{1}{2}\left(\frac{4aP}{cU}\right)\{\cos\beta-\cos(\gamma+\beta)\}, \tag{55}$$

s being measured from B. The chord length is $c = s(\pi-\beta)-s(2\pi-\lambda)$, that is, from (52) and (55),

$$c = \frac{4aP}{U}. \tag{56}$$

If S is the distance measured from the leading edge ($\gamma = -\beta$) then (55) and (56) give

$$S = \tfrac{1}{2}c(1-\cos\epsilon), \tag{57}$$

where $\epsilon = \gamma+\beta$ is the angular displacement measured from the leading edge. Finally, the source is at a distance $s(\pi-\beta)-s(\pi)$ from the trailing edge, that is, from (55) and (56),

$$l = \tfrac{1}{2}c(1-\cos\beta). \tag{58}$$

The lift coefficient now follows from (49), (53), and (56); it is

$$C_L = 2\pi\sin\alpha+2C_Q\cot\tfrac{1}{2}\beta, \tag{59}$$

which is identical with that for a sink on the upper surface at $\epsilon = \beta\,(\gamma = 0)$.

The moment coefficient is easily deduced from (9), (50), (51), (53), and (56). The result is

$$C_M = \tfrac{1}{4}\pi\sin 2\alpha+2C_Q\sin\tfrac{1}{2}\beta\cos(\alpha+\tfrac{1}{2}\beta)-\frac{C_Q^2}{\pi}\cot\tfrac{1}{2}\beta, \tag{60}$$

where from (31) and (55) this coefficient is for the moment about the mid-chord point.

The centre of pressure is at a distance $\bar{x} = cC_M/(C_L\cos\alpha+C_D\sin\alpha)$ upstream of the mid-chord point. From (36), (59), and (60) this distance is found to be

$$\bar{x} = c\left\{\frac{\frac{1}{4}\pi\sin 2\alpha+2C_Q\sin\frac{1}{2}\beta\cos(\alpha+\frac{1}{2}\beta)-(C_Q^2/\pi)\cot\frac{1}{2}\beta}{\pi\sin 2\alpha+2C_Q\operatorname{cosec}\frac{1}{2}\beta\cos(\alpha+\frac{1}{2}\beta)}\right\}. \tag{61}$$

For $C_Q = 0$ this gives the classical result $\bar{x} = \frac{1}{4}c$, while for $\alpha = 0$ we have

$$\bar{x} = c\left\{\sin^2\tfrac{1}{2}\beta - \frac{C_Q}{2\pi}\right\}. \tag{62}$$

We note here that if a source is placed on the aerofoil surface in such a way that the centre of pressure is at the mid-chord point, then the lift due to the source alone has the coefficient

$$C_L = 4(\tfrac{1}{2}\pi)\sqrt{\left\{\frac{2C_Q}{\pi}\left(1 - \frac{C_Q}{2\pi}\right)\right\}} \tag{63}$$

which follows from (9), (59), and (62).

8.2. *The 'directed' source at the trailing edge*

Fig. 5*a* shows the real non-circulating flow about an aerofoil with a straight walled duct discharging near the trailing edge; Fig. 5*b* shows the

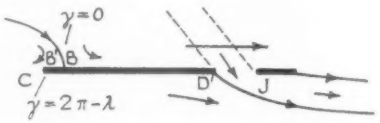

FIG. 5*a*.

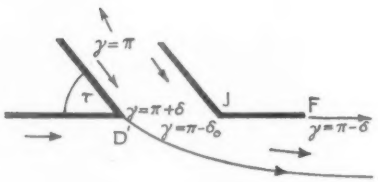

The directed source.

FIG. 5*b*.

details of the flow from the duct. This flow is also the 'fictitious' flow introduced in section 2—we have simply put $\beta = \delta$, but bearing the closure conditions in mind we have compensated for the loss of this parameter by introducing the parameter δ_0 defined in Fig. 5*b*. Later in the calculation we allow δ_0 to tend to δ making J and F coincide, and then we have the case of a directed source discharging right at the trailing edge.

The fact that the z-plane in Fig. 5*a* is doubly-covered is only a consequence of our using a thin aerofoil instead of one sufficiently thick to accommodate the duct. In practice the duct would be curved to lie within the aerofoil, but the principal characteristic of the duct as far as the external flow is

concerned will be the direction of flow at its exit, and provided the final section of the duct is straight and several times longer than it is wide it is unlikely that our model will introduce significant errors.

From Fig. 5 we find that

$$\theta_0 = \begin{cases} -\pi & (2\pi-\lambda < \gamma < 2\pi), \\ -\tau & (\pi-\delta_0 < \gamma < \pi+\delta), \end{cases} \tag{64}$$

so it follows from (24), (25), and (26) that

$$2\alpha_0 = -\frac{\tau}{\pi}(\delta_0+\delta)-\lambda, \tag{65}$$

$$1+\cos\lambda = \frac{\tau}{\pi}\cos\delta_0+\left(2-\frac{\tau}{\pi}\right)\cos\delta, \tag{66}$$

$$\sin\lambda = \frac{\tau}{\pi}(\sin\delta+\sin\delta_0). \tag{67}$$

Equations (66) and (67) show that δ_0 cannot in general be chosen arbitrarily.

However, if we restrict our attention to a theory correct only to first order in $\sqrt{(C_Q)}$ it follows from (9) that δ and hence δ_0 ($\delta_0 < \delta$) are small first order quantities, and equation (66) can be ignored. In this case (65) and (67) give

$$\alpha_0 = -\frac{\tau}{\pi}(\delta+\delta_0). \tag{68}$$

Now $(4aP/cU)$ will differ from unity only by a term of order δ, so to first order (48) and (68) give

$$C_L = 2\pi\alpha+2\tau(\delta+\delta_0), \tag{69}$$

on putting $\beta = \delta$. In the limit $\delta_0 \to \delta$, (9) and (69) then give

$$C_L = 2\pi\alpha+4\tau\sqrt{\left(\frac{2C_Q}{\pi}\right)}. \tag{70}$$

Similarly equation (50) reduces to

$$C_M = \tfrac{1}{2}\pi\alpha \tag{71}$$

whatever value is given to δ_0. For $\alpha = 0$ it follows from (70) and (71) that the centre of pressure is at the mid-chord point.

It is interesting to note that if a source is placed on the aerofoil surface so that the centre of pressure is also at the mid-chord point, the lift agrees to first order with that given in (70), provided we give τ its 'average' value of $\frac{1}{2}\pi$. This follows by a comparison of equations (63) and (70). This result is what we would expect on physical reasoning, and gives some confirmation of the approximations used in the derivation of (70) and (71).

9. Concluding remarks

The main results of some practical interest given in this paper are equations (70) and (71). It may seem that a much shorter method of deriving these results could be given by simply specifying the flow direction across the duct exit $D'J$ (see Fig. 5*b*). It could, for example, be taken to be constant and equal to τ over this exit. This procedure would obviate much of the algebra given in this paper, but unfortunately it is not a valid approximation for source flows. First it is apparent from Fig. 5*b* that the average value of θ on $D'J$, say θ_a, would be somewhat less than τ. The approximate theory (see below) actually yields

$$C_L = 4\theta_a\sqrt{(2C_Q)}, \tag{72}$$

and comparing this with (70) we see that $\theta_a = \tau/\sqrt{\pi}$. Secondly, it is difficult to give physical meaning to this artificial boundary condition. It could perhaps be regarded as being produced by a uniform downward motion of a solid surface placed across the duct exit.

Equation (72) can be derived as follows. From (69) we see that if $\theta = \theta_a$ over an interval $\pi-\delta < \gamma < \pi+\delta$, then the corresponding value of C_L is $4\theta_a\delta$, but here δ will not be related to C_Q by (9) as in this theory the source has no effect on the mapping of the z-plane on the ζ-plane. If we put $\delta = 0$ in (40) we find that for a thin aerofoil $s = \frac{1}{2}c(1-\cos\gamma)$, and hence if h is the width of the duct exit it is related to δ by $h/c = 1-\cos\delta = \frac{1}{2}\delta^2$, to first order. Assuming the velocity in the duct exit to be U, we have

$$C_Q = hU/cU = h/c,$$

and hence $C_L = 4\theta_a\delta = 4\theta_a\sqrt{(2C_Q)}$.

REFERENCES

1. F. Ehlers, 'On the influence of sinks on the lift and pressure distribution of airfoils with suction slots', MAP-VG 67–189T. A.R.C. 10,466—F.M. 1083 (1946).
2. L. C. Woods, 'The lift and moment acting on a thick aerofoil in unsteady motion', *Phil. Trans.* A, **247** (1954), 131.

ON THE CALCULATION OF HEAT AND MASS TRANSFER IN LAMINAR AND TURBULENT BOUNDARY LAYERS

I. THE LAMINAR CASE

By D. R. DAVIES *and* D. E. BOURNE (*University of Sheffield*)

[Received 1 December 1955; revise received 17 May 1956]

SUMMARY

This paper presents a new and convenient method of calculating the rate of heat transfer from a plane wall into a laminar incompressible boundary layer, for an arbitrary distribution of surface temperature and a main stream velocity distribution of the form $U_0 = cx^m$, where x is the downstream distance from the leading edge of the momentum boundary layer. It is assumed that the temperature difference between the surface and the main stream is small enough to ignore any buoyancy effects. A power law representation is first constructed of the calculated exact velocity profile for various values of m, with deviations from the exact profile, up to $U/U_0 = 0{\cdot}95$, of less than 4 per cent. for $0 \leqslant m \leqslant 1$ and 7 per cent. for $m = 4$. The ensuing temperature equation is transformed into a von Mises form and solved by the method of sources. When the surface temperature is independent of x and $0 \leqslant m \leqslant 4$, the numerical estimates of heat transfer rates are found to be within 3 per cent. of previously calculated values, based on the exact velocity profile, and the errors are considerably less than those involved in Lighthill's method, which is based on a linear approximation to the exact velocity profile. The method of sources leads to a particularly convenient form of solution when the surface temperature is given by a series in x, and the numerical results are in agreement with those of Chapman and Rubesin who used the exact velocity profile.

This source method of solving the von Mises form of the temperature equation is extended in a following paper to treat the problem of calculating heat and mass transfer in turbulent boundary layers.

1. Introduction

An approximate solution of the problem of forced convection in a developing laminar boundary layer, for a free stream velocity given by $U_0 = c_1 x^m$ and for an arbitrary temperature distribution on the surface of a semi-infinite flat plate, has been obtained recently by Lighthill (**1**). The Heaviside operational method was employed, and the analysis based on a linear approximation to the exact velocity profile in the region of flow very near the surface of the plate. In the particular case when the surface temperature of the plate is kept constant, a formal solution, based on the exact velocity profile, is easily obtained and is described by Lighthill (**1**); the associated numerical values of rate of heat transfer are tabulated (**1**, p. 367)

for various values of m, together with the numerical values calculated on the basis of the linear approximation to the velocity profile. For the Blasius case ($m = 0$) the numerical value given by this approximate solution is within 3 per cent. of the exact value, but the error increases as m increases, and at $m = 4$ the error due to the linear approximation is about 22 per cent.

The analysis given in this paper provides an alternative and convenient method of approach. It is based on power law approximations to the exact velocity profiles for various values of m: these may be constructed so that they deviate by not more than 4 per cent. for $0 \leqslant m \leqslant 1$, and 7 per cent. for $m = 4$, from the exact profiles (computed from the tables given by Hartree (**2**)) up to $U/U_0 = 0{\cdot}95$. The temperature equation, based on this type of approximation to the velocity profile for a given value of m, is first transformed into a von Mises form. The appropriate boundary conditions are specified by regarding the heated plate, assumed to be infinite in the lateral direction, as an assembly of continuous infinite line sources, each source being normal to the main stream. A solution of the temperature equation is then obtained for a single source, and the distribution of source strength (or local rate of heat transfer) is then determined, by solving an appropriate integral equation, so that the prescribed surface temperature is achieved. In the constant temperature case and when the values of m lie between 0 and 4, the numerical values of rate of heat transfer computed by this method are within 3 per cent. of the values computed on the basis of the exact velocity profile; the errors involved in the application of Lighthill's linear approximation are therefore considerably reduced.

We find that the source method is particularly useful in dealing with the general case when the temperature of the plate is an arbitrary function of the distance x from the leading edge of the plate. If, for example, the surface temperature of the plate is represented by a series in x, then the coefficients of the series describing the temperature distribution in the flow over the plate are obtained as simple quadratures, and are in exact agreement with the numerical results obtained by Chapman and Rubesin (**3**), when $m = 0$, by numerical integration of an ordinary differential equation for each term in the series.

2. Solution of the temperature equation in a laminar incompressible boundary layer over a flat plate for an arbitrary surface temperature distribution and $U_0 = c_1 x^m$

Let (U, V) denote the components of velocity, in a laminar incompressible boundary layer, relative to coordinate axes Ox, in the plane of the plate and parallel to the direction of the main stream velocity, and Oy normal to the plate surface. Denoting the temperature by T and the thermal

diffusivity by κ, the equation describing the distribution of temperature (cf. Howarth (**4**, p. 760)) is

$$U\frac{\partial T}{\partial x}+V\frac{\partial T}{\partial y}=\frac{\partial}{\partial y}\left(\kappa\frac{\partial T}{\partial y}\right). \tag{1}$$

We consider the case in which the main stream velocity is given by

$$U_0=c_1x^m, \tag{2}$$

x being measured from the leading edge of the momentum boundary layer. The distribution of U and V needed to integrate equation (1) may be calculated from the well-known solution (cf. Goldstein (**5**, p. 140)) of the momentum boundary layer equation. This solution is expressed in terms of the similarity variable ξ, given by

$$\xi=\tfrac{1}{2}[U_0/(\nu x)]^{\frac{1}{2}}y=\tfrac{1}{2}(c_1/\nu)^{\frac{1}{2}}x^{(m-1)/2}y, \tag{3}$$

where ν denotes the kinematic viscosity of air. The stream function ψ is given by

$$\psi=(\nu U_0x)^{\frac{1}{2}}f(\xi)=(\nu c_1)^{\frac{1}{2}}x^{(m+1)/2}f(\xi), \tag{4}$$

and consequently, using the relation $U=\partial\psi/\partial y$, the x component of velocity is given by

$$U=\tfrac{1}{2}U_0f'=\tfrac{1}{2}c_1x^mf'; \tag{5}$$

the derived function $f'(\xi)$ has been tabulated for various values of m by Hartree (**2**). We now suppose that numerical values of the coefficient b_1 and the index β can be determined to give a good power law representation of the exact velocity profile (5), in the form

$$U=c_1x^mb_1\xi^\beta, \tag{6}$$

the accuracy of the approximation being discussed in § 3. The form of the function f (and hence of ψ) *which is associated with the approximation* (6) is then given by (4) and (6), namely

$$f=2b_1(1+\beta)^{-1}\xi^{1+\beta}, \tag{7}$$

since $\psi=f=0$ at $\xi=0$; the velocity U at a given x value is then expressed in terms of the stream function ψ by the relation

$$U=b_1c_1x^m[(1+\beta)\psi\{2b_1(\nu c_1)^{\frac{1}{2}}x^{(m+1)/2}\}^{-1}]^{\beta/(1+\beta)}. \tag{8}$$

Using the von Mises method (**5**, p. 126) we now simplify the left-hand side of equation (1), replacing x and y as independent variables by x and ψ. The basic equation (1) is transformed into

$$\frac{\partial T}{\partial x}=\kappa\frac{\partial}{\partial\psi}\left(U\frac{\partial T}{\partial\psi}\right), \tag{9}$$

when κ is independent of temperature. Substituting (8) into (9), the temperature equation becomes

$$\frac{\partial T}{\partial x} = c_2 x^{[(2+\beta)m-\beta]/(2+2\beta)} \frac{\partial}{\partial \psi}\left(\psi' \frac{\partial T}{\partial \psi}\right), \tag{10}$$

where

$$c_2 = b_1 c_1 \kappa[(c_1/\nu)^{\frac{1}{2}}(1+\beta)(2b_1 c_1)^{-1}]^{\beta/(1+\beta)} \quad \text{and} \quad t = \beta/(1+\beta).$$

Writing $x^s = X$, where $s = (1+m)(2+\beta)(2+2\beta)^{-1}$, equation (10) simplifies to

$$\frac{\partial T}{\partial X} = c \frac{\partial}{\partial \psi}\left(\psi' \frac{\partial T}{\partial \psi}\right), \tag{11}$$

in which $c = c_2/s$.

We now suppose that a continuous infinite line source, normal to the x-axis, is stationed on the surface $\psi = 0$ at $x = x_0$ and emits Q units of heat per unit time, per unit length of source. We write

$$\eta = x^s - x_0^s = X - X_0. \tag{12}$$

With the source stationed at $\eta = 0$ the basic temperature equation (11) becomes

$$\frac{\partial T}{\partial \eta} = c \frac{\partial}{\partial \psi}\left(\psi' \frac{\partial T}{\partial \psi}\right). \tag{13}$$

We seek solutions of (13) in the form

$$T - T_0 = A \eta^{\lambda} g(u), \tag{14}$$

where $u = \psi \eta^{-\mu}$ and T_0 is a constant, which satisfy the conditions associated with a line source, namely

$$T \to \infty, \qquad \eta \to 0, \qquad \psi = 0, \tag{15}$$

$$T \to T_0, \qquad \eta > 0, \qquad \psi \to \infty, \tag{16}$$

and

$$T \to T_0, \qquad \eta \to 0, \qquad \psi > 0. \tag{17}$$

The condition that the downstream flux of heat from the source, per unit width of any section normal to the plate, is independent of η is expressed in the form

$$\rho c_p \int_{\psi=0}^{\psi=\infty} (T - T_0)\, d\psi = Q, \tag{18}$$

where ρ and c_p denote appropriate values of the density and specific heat of air. Substituting (14) into (18) shows that

$$\lambda + \mu = 0, \tag{19}$$

and

$$A = (Q/\rho c_p) \int_0^{\infty} g(u)\, du. \tag{20}$$

Substituting (14) and (19) into (13) then leads to the relations

$$\mu = 1/(2-t) = (1+\beta)/(2+\beta), \tag{21}$$

and

$$B\frac{d}{du}\left(u^t\frac{dg}{du}\right)+u\frac{dg}{du}+g = 0, \tag{22}$$

where

$$B = (2-t)c = 2b_1c_1\kappa(1+m)^{-1}[(c_1/\nu)^{\frac{1}{2}}(1+\beta)(2b_1c_1)^{-1}]^{\beta/(1+\beta)}. \tag{23}$$

A suitable exponential form of solution of (22) exists; we find

$$g(u) = \exp\{-u^{(2-t)}B^{-1}(2-t)^{-1}\}, \tag{24}$$

leading to the expression for temperature

$$T-T_0 = A\eta^{-1/(2-t)}\exp\{-u^{(2-t)}B^{-1}(2-t)^{-1}\}, \tag{25}$$

which satisfies conditions (15), (16), and (17). Substituting (24) into (20) shows that the quantities A and Q are related by the expression

$$A = Q[\rho c_p B^{1/(2-t)}(2-t)^{(t-\beta)/(2-t)}\Gamma\{(2-t)^{-1}\}]^{-1}. \tag{26}$$

Consider now an assembly of continuous sources (of infinite extent in a direction perpendicular to the x-axis), the strength Q of each source being a function of x, spread along the surface $\psi = 0$, $x \geqslant a_1$, say, and suppose this arrangement leads to a temperature $T_1(x)$ on $\psi = 0$, $x \geqslant a_1$. The temperature excess $T-T_0$ at a point P at a downstream distance $x > x_0$ on $\psi = 0$, due to a single source at $x = x_0$ is, by (25), equal to

$$A(x^s-x_0^s)^{-1/(2-t)}, \tag{27}$$

and consequently the temperature excess at P due to the whole assembly of sources is given by

$$\int_{x_0=a_1}^{x_0=x}(x^s-x_0^s)^{-1/(2-t)}A(x_0)\,dx_0 = T_1(x)-T_0. \tag{28}$$

When $T_1(x)$ is prescribed, this is an integral equation for $A(x_0)$ and hence, by (26), for $Q(x_0)$, the local rate of heat transfer. Writing

$$x^s = X, \qquad x_0^s = \phi, \qquad 1/(2-t) = \mu, \tag{29}$$

equation (28) is transformed into the Abel form (**6**, p. 229)

$$\int_{a_1^s}^{X}(X-\phi)^{-\mu}u(\phi)\,d\phi = T_1(X)-T_0, \tag{30}$$

where

$$u(\phi) = A(\phi)\phi^{(1-s)/s}s^{-1}. \tag{31}$$

The solution of (30) is known (**6**) to be

$$u(\phi) = \frac{\sin\mu\pi}{\pi}\frac{d}{d\phi}\int_{a_1^s}^{\phi}(\phi-X)^{\mu-1}[T_1(X)-T_0]\,dX, \tag{32}$$

provided $\mu < 1$; the form of equation (21) shows that this condition is satisfied. In § 3 we consider the form of solution in the special case given by $a_1 = 0$ and $T_1(X) =$ constant, and in § 4 the case

$$T_1 - T_0 = \sum_{n=0}^{\infty} a_n x^n.$$

3. Forced convection from a semi-infinite flat plate through a laminar incompressible boundary layer when the surface is kept at a uniform temperature and $U_0 = c_1 x^m$

In this problem a_1 is zero, T_0 is the constant free stream temperature, and T_1 is the constant temperature of the plate. The solution, expressed in terms of the $u(\phi)$ function, is given by equation (32) to be

$$u(\phi) = (T_1 - T_0)\pi^{-1} \sin \mu\pi \, \phi^{\mu-1}, \tag{33}$$

and hence, using (31),

$$A = (T_1 - T_0)s\pi^{-1} \sin \mu\pi \, x_0^{(m-1)/2}. \tag{34}$$

Equations (26) and (34) then give the local rate of heat transfer as

$$Q(x_0) = [U_0/(\nu x_0)]^{\frac{1}{2}} F, \tag{35}$$

where the coefficient

$$F = (T_1 - T_0)k\sigma^{1/(2+\beta)}\pi^{-1} b_1^{1/(2+\beta)} (1+m)^{1/(2+\beta)} (1+\beta)^{-1/(2+\beta)} \times$$
$$\times (1+\beta/2)^{(1+\beta)/(2+\beta)} \sin[(1+\beta)(2+\beta)^{-1}\pi] \Gamma[(1+\beta)(2+\beta)^{-1}];$$

k is the thermal conductivity and σ the Prandtl number. Using equations (25) and (34) the associated temperature distribution at a point (x, ψ) is expressed in the form

$$T - T_0 = (T_1 - T_0)s\pi^{-1} \sin \mu\pi \int_0^x (x^s - x_0^s)^{-1/(2-t)} x_0^{(m-1)/2} \times$$
$$\times \exp\{-\psi^{(2-t)} B^{-1} (2-t)^{-1} (x^s - x_0^s)^{-1}\} \, dx_0. \tag{36}$$

As in § 2 we write $x_0^s = \phi$, $x^s = X$, $1/(2-t) = \mu$, and in addition we write $\psi^{(2-t)} B^{-1} (2-t)^{-1} = \gamma$; equation (36) then reduces to

$$\theta = (T - T_0)/(T_1 - T_0) = \pi^{-1} \sin \mu\pi \int_0^X (X - \phi)^{-\mu} \phi^{\mu-1} \exp[-\gamma(X-\phi)^{-1}] \, d\phi. \tag{37}$$

It was noted by Calder (**7**, p. 170) in another context, that this integral is a degenerate case of the confluent hypergeometric function and it may be expressed, in terms of Pearson I functions (**8**), in the form

$$\theta = 1 - I(\gamma/X, -\mu). \tag{38}$$

Expressed in terms of the original quantities this may be written in the form

$$\theta = 1 - I\{2\nu(1+m)b_1(1+\beta)^{-1}(2+\beta)^{-1}\kappa^{-1}\xi^{2+\beta}, -(1+\beta)(2+\beta)^{-1}\}. \quad (39)$$

We see that $Q(x_0)$ is proportional to $(U_0/x)^{\frac{1}{2}}$, i.e. to $x^{(m-1)/2}$, as given by Howarth (**4**, p. 794). The total rate of heat transfer from a plate of length x_1 is then given by

$$\int_0^{x_1} Q(x_0)\, dx_0 = 2(1+m)^{-1}(c_1/\nu)^{\frac{1}{2}}x^{(1+m)/2}F. \quad (40)$$

Expressed in terms of the Nusselt number $Nu = \int_0^{x_1} Q(x_0)\, dx_0/k(T_1-T_0)$ and Reynolds number $R = x_1 U_0(x_1)/\nu = c_1 x_1^{1+m}/\nu$, this finally becomes

$$NuR^{-\frac{1}{2}} = \pi^{-1}\, 2^{1/(2+\beta)}(1+\beta)^{-1/(2+\beta)}(2+\beta)^{(1+\beta)/(2+\beta)} \sin[(1+\beta)(2+\beta)^{-1}\pi] \times$$
$$\times \Gamma[(1+\beta)(2+\beta)^{-1}]b_1^{1/(2+\beta)}(1+m)^{-(1+\beta)(2+\beta)^{-1}}\sigma^{1/(2+\beta)}. \quad (41)$$

This expression has been calculated numerically for $\sigma = 0{\cdot}72$ and $m = 0$, $\frac{1}{9}$, $\frac{1}{3}$, 1, 4 using values of b_1 and β which were obtained by fitting a power law to the appropriate exact velocity profile for each value of m. These profiles were computed from the tables given by Hartree (**2**). It was found possible to choose the values of b_1 and β (given in Table 1) so that the power laws deviated by only small amounts (about 4 per cent. at most for $m = 0$, $\frac{1}{9}$, $\frac{1}{3}$, 1 and 7 per cent. for $m = 4$) from the exact velocity profiles for values of ξ from zero up to the values corresponding to $U/U_0 = 0{\cdot}95$, i.e. over the significant part of the boundary layer. The results based on the power law approximations and Lighthill's (**1**) linear approximation are shown in Table 1 together with the values based on the exact velocity profiles. The error in the calculated values of heat transfer rates based on the linear approximation increases with the value of m, because the deviation of the actual profile from the tangent at the origin increases with the value of m. Using the power law approximation we see that the error is reduced very considerably. The choice of a good power law fit is, of course, to some extent arbitrary, but the definite result which Table 1 illustrates is that for $0 \leqslant m \leqslant 4$ power law representations can be constructed with a maximum deviation from the exact profile (up to $U/U_0 = 0{\cdot}95$) of 4 per cent. for $0 \leqslant m \leqslant 1$ and 7 per cent. for $m = 4$, and calculations based on these are within 3 per cent. of the heat transfer rates calculated on the basis of the exact velocity profiles.

In the case $m = 0$, the temperature distribution function (39) was calculated, for $\sigma = 0{\cdot}6$, $1{\cdot}1$, $15{\cdot}0$, using (i) the Lighthill linear approximation, and (ii) the power law approximation ($b_1 = 0{\cdot}61$, $\beta = 0{\cdot}88$). These are displayed in Table 2, together with the values calculated by numerical

TABLE 1

Calculated rate of heat transfer from a flat plate at constant temperature

m	0	$\frac{1}{9}$	$\frac{1}{3}$	1	4
b_1	0·61	0·81	0·99	1·35	1·78
β	0·88	0·86	0·80	0·76	0·66
Per cent. maximum deviation of power law profile from exact profile (up to $U/U_0 = 0{\cdot}95$)	3	3	4	3	7
$NuR^{-\frac{1}{2}}$ based on exact profile	0·585	0·596	0·576	0·495	0·325
$NuR^{-\frac{1}{2}}$ based on linear approximation to profile	0·601	0·648	0·653	0·587	0·398
$NuR^{-\frac{1}{2}}$ based on power law approximation to profile	0·569	0·610	0·587	0·512	0·331
Per cent. error due to linear approximation	+3	+9	+13	+18½	+22½
Per cent. error due to power law approximation	−3	+2	+2	+3	+2

integration of the formula, given by Howarth (**4**, p. 781), which is based on the exact Blasius velocity profile. The differences in the temperature distributions are seen to be very small.

TABLE 2

Calculated values of $(T-T_0)/(T_1-T_0) = \theta$, *the temperature distribution function, when* $m = 0$, *for* $\sigma = 0{\cdot}6$, $1{\cdot}1$, *and* $15{\cdot}0$: θ_A, θ_B, θ_C *refer to calculated values based on the exact velocity profile, the power law approximation* ($b_1 = 0{\cdot}61$, $\beta = 0{\cdot}88$), *and the linear approximation* ($b_1 = 0{\cdot}664$, $\beta = 1{\cdot}0$) *respectively*

σ	0·6			1·1			15·0		
ξ	θ_A	θ_B	θ_C	θ_A	θ_B	θ_C	θ_A	θ_B	θ_C
0·25	0·139	0·140	0·143	0·171	0·173	0·175	0·406	0·423	0·412
0·50	0·275	0·279	0·284	0·340	0·343	0·348	0·752	0·766	0·755
0·75	0·410	0·414	0·422	0·502	0·505	0·512	0·946	0·948	0·945
1·00	0·541	0·545	0·554	0·650	0·650	0·659	0·995	0·995	0·995
1·25	0·654	0·658	0·671	0·769	0·771	0·780			
1·50	0·751	0·757	0·773	0·862	0·864	0·873			
1·75	0·838	0·845	0·860	0·965	0·966	0·972			
2·0	0·891	0·898	0·912						

4. Forced convection from a semi-infinite flat plate through a laminar incompressible boundary layer when U_0 is independent of x and T_1-T_0 is given by $\sum_0^\infty a_n x^n$

The method of analysis given in this paper is found to be particularly convenient when the surface of the flat plate is kept at a temperature which is a function of distance x from the leading edge. The only available calculations based on the exact velocity profile are those by Chapman and Rubesin (**3**) for the case when T_1-T_0 is given as a series $\sum_{n=0}^{\infty} a_n x^n$ and $m = 0$.

It is interesting to compare our results with those based on the exact velocity profile in this case.

Writing

$$T_1 - T_0 = \sum_{n=0}^{\infty} a_n x^n \tag{42}$$

in equation (32) we obtain

$$u(\phi) = \sum_{n=0}^{\infty} \frac{a_n \sin \mu\pi}{\pi} \frac{d}{d\phi} \int_0^{\phi} \frac{X^{(n/s)}}{(\phi - X)^{1-\mu}} \, dX$$

$$= \pi^{-1} \sin \mu\pi \sum_{n=0}^{\infty} a_n (n/s + \mu) \phi^{(n/s+\mu-1)} B_n(\mu, n/s+1), \tag{43}$$

where B_n is a beta function (**6**, p. 253) and, following the analysis given in preceding sections, the local rate of heat transfer at a point x is given by

$$Q(x) = k[U_0/(\nu x)]^{\frac{1}{2}} \sum_{n=0}^{\infty} a_n x^n [2^{-(1+\beta)(2+\beta)^{-1}} \pi^{-1} (1+\beta)^{(1+\beta)(2+\beta)^{-1}} (2+\beta)^{-1/(2+\beta)} \times$$

$$\times \sin\{\pi(1+\beta)(2+\beta)^{-1}\} \Gamma\{(1+\beta)(2+\beta)^{-1}\} b_1^{1/(2+\beta)} \sigma^{1/(2+\beta)} (1+2n) \times$$

$$\times B_n\{(1+\beta)(2+\beta)^{-1}, 1+2n(1+\beta)(2+\beta)^{-1}\}], \tag{44}$$

where U_0 is the uniform free stream velocity, and the other quantities have been previously defined. Using the linear approximation to the velocity profile ($\beta = 1$, $b_1 = 0{\cdot}664$) this reduces, as expected, to the formula given by Lighthill (**1**, p. 369) using his operational method; for $\sigma = 0{\cdot}72$ this has been shown by Lighthill to yield results which are within 3 per cent. of those obtained by Chapman and Rubesin. A calculation of (44) based on the power law approximation ($\beta = 0{\cdot}88$, $b_1 = 0{\cdot}61$) reduces this error to less than 1 per cent.

The temperature distribution in the flow over the surface, following the analysis described in § 3, is then given by

$$T - T_0 = (2\pi)^{-1} \sin[(1+\beta)(2+\beta)^{-1}\pi] \sum_{n=0}^{\infty} a_n (1+2n) \times$$

$$\times B_n\{(1+\beta)(2+\beta)^{-1}, 1+2n(1+\beta)(2+\beta)^{-1}\} \int_0^x (x^s - x_0^s)^{-1/(2-t)} x_0^{(n-\frac{1}{2})} \times$$

$$\times \exp\{-\psi^{(2-t)}(2-t)^{-1} B^{-1} (x^s - x_0^s)^{-1}\} \, dx_0. \tag{45}$$

Writing $x_0^s = \phi$, $x^s = X$, and $\phi/X = u$, this reduces to the form, discussed by Chapman and Rubesin,

$$T - T_0 = \sum_{n=0}^{\infty} a_n x^n X_n(\xi), \tag{46}$$

where

$$X_n(\xi) = \pi^{-1}(1+\beta)(2+\beta)^{-1}\sin[(1+\beta)(2+\beta)^{-1}\pi](1+2n)\times$$
$$\times B_n\{(1+\beta)(2+\beta)^{-1},\ 1+2n(1+\beta)(2+\beta)^{-1}\}\int_0^1 (1-u)^{-\mu}u^{\mu(1+2n)-1}\times$$
$$\times\exp\{-2b_1\nu U_0^{-1}(1+\beta)^{-1}(2+\beta)^{-1}\kappa^{-1}(1-u)^{-1}\xi^{2+\beta}\}\,du. \quad (47)$$

The first term ($n = 0$) in the series reduces, as in § 3, to a Pearson I function, and we obtain

$$X_0(\xi) = 1-I\{2b_1\nu\kappa^{-1}(1+\beta)^{-1}(2+\beta)^{-1}\xi^{2+\beta},\ -(1+\beta)(2+\beta)^{-1}\}. \quad (48)$$

The $X_n(\xi)$ functions were obtained by Chapman and Rubesin by numerical integration of an ordinary differential equation in the cases $n = 0$, 1, 2, 3, 4, 5, 10. A considerable simplification of the calculation is thus obtained by using a power law approximation to the exact velocity profile. For $n = 0$ we find from Pearson's I Tables (**8**) that the expression (48) gives numerical results in exact agreement with those given by Chapman and Rubesin (**3**, Fig. 5). It has not been found possible to reduce the form of the integral in equation (47) for $n > 0$, but it has been evaluated numerically for a number of values of ξ for $n = 1$, 2, and 10, and the ensuing numerical values of $X_n(\xi)$ are found to be in agreement with those given by Chapman and Rubesin.

5. Conclusions

The method used here of calculating the rate of heat transfer from a flat plate into a laminar incompressible boundary layer, for an arbitrary distribution of surface temperature and a main stream velocity distribution of the form $U_0 = c_1 x^m$, is based on a power law approximation to the exact velocity profile for various values of m and leads to convenient formulae describing the rate of heat transfer and the temperature distribution. These power laws may be constructed so that they deviate by not more than 4 per cent. for $0 \leqslant m \leqslant 1$, and 7 per cent. for $m = 4$, from the exact velocity profiles up to $U/U_0 = 0{\cdot}95$. We find that in the case of uniform surface temperature, the errors involved in Lighthill's linear approximation, giving rate of heat transfer for $m = \frac{1}{9}$, $\frac{1}{3}$, 1, and 4, are considerably reduced by using the appropriate power law.

The case in which $m = 0$ and $T_1 - T_0 = \sum_{n=0}^{\infty} a_n x^n$ has been discussed by Chapman and Rubesin (**3**), and the tedious method adopted by these authors of computing the $X_n(\xi)$ functions in the solution

$$T - T_0 = \sum_{n=0}^{\infty} a_n x_n X_n(\xi)$$

is considerably simplified by our method of approach. In particular the $X_0(\xi)$ function is expressed in terms of a tabulated Pearson I function (8) and the $X_n(\xi)$ functions, for $n > 0$, are expressed as simple quadratures. Their numerical evaluation replaces the Chapman and Rubesin step-by-step numerical integration of an ordinary differential equation for each value of n. The numerical results are found to be in agreement with those of Chapman and Rubesin.

Acknowledgement

The research reported in this paper was supported by a research fellowship of the University of Sheffield to one of the authors (D. E. Bourne).

REFERENCES

1. M. J. Lighthill, *Proc. Roy. Soc.* A, **202** (1950), 359.
2. D. R. Hartree, *Proc. Camb. Phil. Soc.* **33** (1937), 223.
3. D. R. Chapman and M. W. Rubesin, *J. Aero. Sci.* **16** (1949), 547.
4. L. Howarth (ed.), *Modern Developments in Fluid Dynamics* (Oxford, 1953).
5. S. Goldstein (ed.), *Modern Developments in Fluid Dynamics* (Oxford, 1938).
6. E. T. Whittaker and G. N. Watson, *Modern Analysis* (Cambridge, 1946).
7. K. L. Calder, *Quart. J. Mech. Appl. Math.* **2** (1949), 153.
8. K. Pearson, *Tables of the Incomplete Gamma Function* (London, H.M.S.O., 1922).

ON THE CALCULATION OF HEAT AND MASS TRANSFER IN LAMINAR AND TURBULENT BOUNDARY LAYERS

II. THE TURBULENT CASE

By D. R. DAVIES *and* D. E. BOURNE (*University of Sheffield*)

[Received 1 December 1955; revise received 17 May 1956]

SUMMARY

The method of analysis described in Part I (**7**) is applied in this paper to obtain a solution of the problem of heat transfer from a flat plate through a fully turbulent boundary layer, when the surface of the plate is kept at a steady constant temperature; the temperature difference between the surface and the main stream is assumed to be small enough to ignore any buoyancy effects, and the main stream velocity is independent of downstream position. The equality of heat and momentum eddy diffusivities is assumed, and the analysis is based on power law representations of (i) the experimentally determined velocity profile, and (ii) the distribution of eddy viscosity, deduced from Townsend's experimental work concerning the structure of the turbulent boundary layer on a plane wall. The ensuing theoretical temperature distribution over the plate and the distribution of local heat flux along the surface of the plate are found to be in close agreement with the results of experiments by Elias.

On the basis of equality of momentum and vapour eddy diffusivities the method is extended to treat the problem of calculating the rate of evaporation from a saturated liquid surface into the developing turbulent boundary layer adjacent to a smooth wind-tunnel wall. The analysis takes into account the effects of the transition and laminar sub-layers over the evaporating surface, and the theoretical values of rate of evaporation are found to be in reasonable agreement with the results of evaporation experiments in a wind-tunnel.

1. Introduction

MEASUREMENTS have been made, e.g. by Pasquill (**1**) and Davies and Walters (**2**), of the rate of evaporation from saturated liquid surfaces into developing fully turbulent boundary layers, and theories of turbulent diffusion in boundary layers, see, for example, Sutton (**3**), have been discussed in relation to experiments of this type. However, these theories are strictly applicable when (i) the thickness of the momentum boundary layer is independent of downstream distance so that, if the downstream pressure gradient may be ignored, the Reynolds shearing stress is independent of position in the boundary layer, and (ii) the contribution to the

total downstream flux of vapour within the laminar sub-layer and transition layer near the surface may be ignored. In large-scale evaporation experiments in the open atmosphere the downstream flux in these sub-layers may be neglected, and it is also possible that condition (i) is a good approximation in the atmospheric case. However, in the developing turbulent boundary layer on a plane wind-tunnel wall this condition is not valid, as Townsend's recent observations (**4**) show, and we shall demonstrate in this paper that the downstream flux in the laminar sub-layer and transition layer can be quite considerable. A theoretical treatment is thus required which does not depend on the validity of conditions (i) and (ii).

The method of obtaining a solution of the diffusion equation in terms of a simple similarity variable, applied recently by Davies (**5**) to the problem of heat transfer from a flat plate at constant temperature, is not suitable when the leading edge of the vapour boundary layer is at some distance downstream from the origin of the momentum boundary layer—as it is in general in wind-tunnel evaporation experiments. We introduce an alternative method in which we regard the evaporating area, assumed to be infinite in the lateral direction, as an assembly of continuous infinite line sources, each being normal to the main stream velocity. The distribution of source strength (or local rate of evaporation) is determined so that the surface vapour concentration is zero upstream of the leading edge and a constant (the saturated value) downstream of this edge. The analysis is based on a power law representation of the eddy viscosity distribution, given by Townsend (**4**), and is applied firstly to the problem of turbulent flow over a flat plate kept at a constant temperature. It is found to lead to theoretical results for rate of heat transfer which are within about 3 per cent. of the results of experiments by Elias (**6**) and of the theoretical results obtained by Davies (**5**), using the similarity approach. The method of sources, described in Part I (**7**) and incorporating in addition an approximate treatment of the flux in the transition and laminar sub-layer, is then applied to the evaporation problem and we find that the theoretical results for rate of evaporation are in reasonable agreement with the results of experiments by Davies and Walters (**2**).

2. The temperature equation in a fully turbulent boundary layer over a semi-infinite flat plate

Let (U, V) denote components of *mean* velocity, in a fully turbulent boundary layer, relative to coordinate axes Ox, in the plane of the plate and parallel to the direction of the free stream, and Oy, normal to the plate surface. Denoting the *mean* temperature by T, the thermal diffusivity by

κ, and the eddy heat diffusivity by ϵ_H, the equation describing the distribution of temperature, given by Howarth (**8**, p. 821), is

$$U\frac{\partial T}{\partial x}+V\frac{\partial T}{\partial y}=\frac{\partial}{\partial y}\left(\kappa\frac{\partial T}{\partial y}+\epsilon_H\frac{\partial T}{\partial y}\right). \tag{1}$$

It has been shown by Davies (**5**) that a consistent diffusion model may be constructed by generalizing Townsend's results (**4**) and writing the momentum eddy viscosity in the form

$$\epsilon = KU_0x^ph(\xi), \tag{2}$$

where x is measured from the origin of the momentum boundary layer and the similarity variable ξ is given by

$$\xi = y/(kx^q); \tag{3}$$

the parameters k, K, q, and p are derived from the observed velocity profiles in the particular conditions to be considered, and $h(\xi)$ is obtained from Townsend's results as in previous work (**5**): U_0 is the main stream velocity. We now suppose that Townsend's values of $h(\xi)$ may be adequately represented by a power law form

$$h(\xi) = a\xi^\alpha, \tag{4}$$

a detailed discussion of the problem of evaluating a and α and the dependence of the theoretical transfer rates on the numerical values of these parameters being given in sections 3 and 4 of this paper: in this connexion we note also that it has not been found possible to carry out the analysis on the basis of a polynomial representation of the function $h(\xi)$. A mathematical treatment of the complex differential equation obtained by substituting equations (2) and (4) into (1) has not yet been achieved but, apart from the extremely thin region in the neighbourhood of the laminar sub-layer and transition layer, ϵ_H is numerically considerably larger than κ which we therefore ignore in the fully turbulent region of flow. An approximate correction, of the type used previously by Davies (**5**), to allow for the effect of the sub-layer is later incorporated in the analysis described in sections 3 and 4. In this paper we write our basic diffusion equation in the form

$$U\frac{\partial T}{\partial x}+V\frac{\partial T}{\partial y}=\frac{\partial}{\partial y}\left(\epsilon\frac{\partial T}{\partial y}\right), \tag{5}$$

using the result obtained by Davies (**5**) that $\epsilon_H = \epsilon$ in forced convection.

Following the Reynolds turbulence technique of taking mean values over a sufficiently long time-interval at a point, the continuity condition for an incompressible fluid applies to the *mean* flow, i.e.

$$\frac{\partial U}{\partial x}+\frac{\partial V}{\partial y}=0,$$

and hence we may write

$$V = -\frac{\partial \psi}{\partial x} \quad \text{and} \quad U = \frac{\partial \psi}{\partial y}, \tag{6}$$

where ψ is the stream function associated with the *mean* flow. Using the von Mises method (**9**, p. 126), as in Part I, we now simplify the left-hand side of equation (5), replacing x and y as independent variables by x and ψ. The basic equation (5) is transformed into the equation

$$\frac{\partial T}{\partial x} = KU_0 a x^p \frac{\partial}{\partial \psi}\left(\xi^\alpha U \frac{\partial T}{\partial \psi}\right). \tag{7}$$

We find that Townsend's mean velocity profile may be represented by a power law, $U/U_0 = 1{\cdot}72\xi^{0{\cdot}15}$, quite accurately (to about 1 per cent. of the actual velocity profile) over almost the whole thickness of the boundary layer, and very accurately in the crucial inner zone $\xi < 0{\cdot}01$. We write in general

$$U/U_0 = b\xi^\beta. \tag{8}$$

Following Davies (**5**) we then write

$$\psi = x^q f(\xi), \tag{9}$$

and, using equations (6) and (8), we find that

$$f(\xi) = kU_0 b(1+\beta)^{-1}\xi^{1+\beta}. \tag{10}$$

Substituting expressions for ξ and U in terms of ψ, obtained from (8), (9), and (10), into equation (7), and introducing a new variable defined by

$$x^s = X, \tag{11}$$

where $s = 1+p-q(\alpha+\beta)(1+\beta)^{-1}$, leads to the equation

$$\frac{\partial T}{\partial X} = c\frac{\partial}{\partial \psi}\left(\psi^t \frac{\partial T}{\partial \psi}\right), \tag{12}$$

where $t = (\alpha+\beta)(1+\beta)^{-1}$ and

$$c = KabU_0^2(1+\beta)^{(\alpha+\beta)(1+\beta)^{-1}}(kbU_0)^{-(\alpha+\beta)(1+\beta)^{-1}}s^{-1}.$$

The temperature equation (12) is identical in form with the basic equation of Part I (**7**, equation (11)), and the analysis of the source method described in Part I (from equations (11) to (32) of that paper) is therefore applicable in the physical context of this section. For a prescribed surface temperature, the distribution of source strength (or local rate of heat transfer) can then be computed from equation (32) of Part I. The particular case of constant surface temperature on a flat plate is considered in section 4, and in section 5 the analysis is extended to treat the problem of evaporation, when the leading edge of the evaporating area is positioned downstream from the leading edge of the momentum boundary layer. A correction is made in both cases for the presence of laminar and transition sub-layers.

3. Forced convection from a semi-infinite flat plate through a turbulent boundary layer when the plate is kept at a uniform temperature

In order to test the validity of our analysis based on a power law representation of the eddy viscosity distribution, we first apply the method of sources to the problem of heat transfer from a semi-infinite flat plate through a turbulent boundary layer, when the plate is kept at a constant temperature and there is no appreciable completely laminar layer near the leading edge. This case has been previously analysed by Davies (**5**) using the actual values of viscosity given by Townsend (**4**) over the whole thickness of the boundary layer. Comparison of the results obtained by the two methods serves as a check on the method of analysis described in this paper and provides support for its application to other cases.

We first solve the problem with the sub-layers neglected. The temperature of the plate is taken to be independent of x and is denoted by T_1' in this case; the main-stream temperature is denoted by T_0'. With $a_1 = 0$ and using the appropriate values for s, t, and c, evaluated in the preceding section, the solution of the integral equation (32) of Part I (**7**) may be written in the form

$$A = (T_1'-T_0')s\pi^{-1}(\sin\mu\pi)x_0^{-1+[(1+p)(1+\beta)-q(\alpha+\beta)](2+\beta-\alpha)^{-1}}, \tag{13}$$

where

$$\mu = 1/(2-t) = (1+\beta)/(2+\beta-\alpha). \tag{14}$$

The variable A is related to Q by equation (26) of Part I to give the local rate of heat transfer at a downstream distance x_0, and the parameter B involved in this equation takes the new form

$$B = KabU_0^2(2+\beta-\alpha)(1+\beta)^{(\alpha+\beta)(1+\beta)^{-1}}\times \\ \times(kbU_0)^{-(\alpha+\beta)(1+\beta)^{-1}}[(1+p)(1+\beta)-q(\alpha+\beta)]^{-1}. \tag{15}$$

Following the analysis discussed by Davies (**5**, p. 330) it may be shown that the representation of $h(\xi)$ by $a\xi^\alpha$ leaves the result $1+p = 2q$, obtained previously (**5**), unchanged in form and consequently (13) simplifies to

$$A = (T_1'-T_0')s\pi^{-1}x_0^{q-1}\sin\mu\pi. \tag{16}$$

The derivation of the temperature distribution function then follows as in section 3 of Part I, and this distribution may be written in the form

$$(T-T_0')/(T_1'-T_0') = 1-I(\gamma/X, -\mu), \tag{17}$$

where I is the Pearson I function (**10**) and $\gamma = \psi^{2-t}B^{-1}(2-t)^{-1}$: using equations (9), (10), (11), (14), and (15) the ratio γ/X in the turbulent case may be written in the form

$$\gamma/X = k^2qb\xi^{(2+\beta-\alpha)}[Ka(1+\beta)(2+\beta-\alpha)]^{-1} = u, \text{ say.}$$

We now introduce an *approximate* treatment to allow for the presence

of a laminar sub-layer and transition layer following the method, introduced by Davies (**5**), in which use was made of empirical mean velocity forms. These empirical formulae (cf. Howarth (**8**, p. 824), Goldstein (**9**, p. 334), and Preston (**11**)) are based on measurements over a wide range of Reynolds numbers and are expressed in the forms

$$U/U_\tau = U_\tau y/\nu = y_\tau \quad (y_\tau \leqslant 5) \tag{18}$$

in the laminar sub-layer,

$$U/U_\tau = -3{\cdot}05 + 5\log_e y_\tau \quad (5 \leqslant y_\tau \leqslant 30) \tag{19}$$

in the transition layer, and

$$U/U_\tau = 5{\cdot}5 + 2{\cdot}5\log_e y_\tau \quad (y_\tau \geqslant 30) \tag{20}$$

in the fully turbulent layer. U_τ is the 'friction velocity', which we determine as a function of x by fitting the empirical form (20) to the measured velocity profile $U(y)$ at various distances from the leading edge of the plate, and ν is the kinematic viscosity of air. Equations (18), (19), and (20) are known to give a good description of the mean velocity profile very near a wall. As indicated by Preston (**11**), there is some variation in the values of the coefficients given by various experimenters, but we find that this scatter ultimately leads to no significant variation in the predicted rates of transfer or temperature distributions.

TABLE 1

Calculated heights of laminar sub-layer, transition layer, and fully turbulent layer over a flat plate when $U_0 = 3{,}500$ *cm./sec.*

x (*cm.*):	10	20	30	40	50
Laminar sub-layer height (cm.) calculated from equation (18)	0·004	0·005	0·005	0·005	0·005
Transition layer height (cm.) calculated from equation (20)	0·02	0·03	0·03	0·03	0·03
Approximate transition layer height (cm.) calculated from equation (21)	0·01	0·02	0·03	0·03	0·03
Approximate height (cm.) of fully turbulent layer taken from Elias's experiments	0·3	0·5	0·7	0·8	1·0

To calculate the distribution of temperature, and hence of downstream heat flux, at a given downstream distance x_1, say, we first calculate, from the known values of $U_\tau(x)$, the height $y_* = 30\nu/U_\tau$ of the transition zone at this particular x value. The corresponding value of ξ, say $\xi_* = y_*/(kx_1^q)$, is then calculated and, following the method used by Davies (**5**), we take the values of $y_T(x)$ satisfying

$$\xi_* = y_T/(kx^q) \tag{21}$$

to be our approximation to the top of the transition zone for $x \leqslant x_1$. As

seen later in this section, this procedure yields a value of T_1' which is independent of x—this is necessary to ensure the validity of the analysis leading to equations (16) and (17). Taking $x_1 = 50$ cm. and $U_0 = 3{,}500$ cm./sec., Table 1 shows that these values of y_T approximate very closely to the values of $y_*(x)$ given by equation (20), for values of x between about 20 cm. and 50 cm.; for values of x less than about 20 cm. there is a small error, but the y_T values are certainly well above the top of the laminar sub-layer. The error involved in taking $y_T(x)$ to be the height of the transition layer is thus localized to values of x less than about 20 cm., and represents only a small percentage of the total thickness of the turbulent boundary layer; this is not likely to influence the theoretical values of temperature and flux at downstream distances of the order of $x = 50$ cm. In fact it has been shown by Davies (**5**) that the theoretical values of temperature based on this method, when applied to a plate of length $x_1 = 50$ cm., for example, are in very close agreement with the experimental results of Elias at $x = 30, 40, 50$ cm. (**5**, Fig. 2). It was also shown (**5**) that the calculated values of heat flux from a section of the plate are in agreement with the experimental values given by Elias.

The flow is now taken to be fully turbulent in the region $\xi \geqslant \xi_*$ and, if T_1^* denotes the temperature at the assumed lower limit of the fully turbulent layer, then

$$(T_1^*-T_0)/(T_1'-T_0) = 1-I(u_*, -\mu), \tag{22}$$

where $u_* = k^2qb\xi_*^{(2+\beta-\alpha)}[Ka(1+\beta)(2+\beta-\alpha)]^{-1}$. Using (17), we obtain finally

$$\begin{aligned}\theta_* &= (T-T_1^*)/(T_0-T_1^*)\\ &= 1-(T-T_0)/(T_1^*-T_0) = [I(u)-I(u_*)]/[1-I(u_*)],\end{aligned} \tag{23}$$

which is the result obtained by Davies (**5**, p. 330) by a different method.

We now assume that the mean shear stress and vertical heat flux in the laminar sub-layer and transition zone are independent of y. Denoting the mean shearing stress by τ_0 and the vertical heat flux by q_0 we have, following Howarth (**8**, p. 823),

$$q_0 = \rho c_p U_\tau T_\tau, \tag{24}$$

where T_τ is the 'friction temperature'. At $x = x_1$, on the surface $\xi = \xi_*$, an expression for q_0 may also be derived from equations (17) and (22). We obtain

$$\begin{aligned}q_0 &= -\rho c_p K U_0 a x_1^p \xi^\alpha \left(\frac{\partial T}{\partial y}\right)_{\xi=\xi_*}\\ &= -\rho c_p K U_0 k^{-1} x_1^{p-q}(T_0-T_1^*)N,\end{aligned} \tag{25}$$

where

$$N = \frac{a[k^2qba^{-1}K^{-1}(1+\beta)^{-1}]^{(1-\alpha)(2+\beta-\alpha)^{-1}}(2+\beta-\alpha)^{(1+\beta)(2+\beta-\alpha)^{-1}}}{\Gamma\{(1-\alpha)(2+\beta-\alpha)^{-1}\}[1-I(u_*)]e^{u_*}}. \tag{26}$$

An expression is given by Howarth (**8**, p. 831) for the temperature in the transition zone. This is applied here to evaluate T_1^* at the top of the transition zone, and is written in the form

$$(T_1'-T_1^*)/T_\tau' = 5\log_e(5\sigma+1)+5\sigma, \tag{27}$$

where T_1' is the actual (constant) temperature of the plate and σ is the Prandtl number ν/κ. By eliminating q_0 and T_τ' from equations (24), (25), and (27) we then obtain the result

$$(T_1'-T_1^*)/(T_0'-T_1^*) = -5U_0\,KNk^{-1}U_\tau^{-1}x_1^{p-q}\{\log_e(5\sigma+1)+\sigma\}, \tag{28}$$

giving T_1^*.

We now find by numerical evaluation of the friction velocity that, in the particular conditions of Elias's experiments (Davies (**5**) gives $p = 0{\cdot}78$ and $q = 0{\cdot}89$), U_τ is proportional to $x^{-0{\cdot}11}$, i.e. to x^{p-q}, and τ_0 (or ρU_τ^2) is proportional to $x^{-0{\cdot}22}$ which is in approximate agreement with the result given by Goldstein (**9**, p. 362). We note that the factor N, given by (26), is independent of x, if we take the values of y_T given by (21) as our approximation to the height of the transition layer, and consequently

$$(T_1'-T_1^*)/(T_0'-T_1^*)$$

is independent of x. The expression

$$\begin{aligned}\frac{T_1'-T_0}{T_1-T_0} &= \frac{(T_1'-T_0)}{(T_1^*-T_0)}\left[1-\frac{(T_1-T_1^*)}{(T_0-T_1^*)}\right]^{-1}\\ &= [1-I(u_*)]^{-1}[1+5U_0\,KNk^{-1}U_\tau^{-1}x_1^{p-q}\{\log_e(5\sigma+1)+\sigma\}]^{-1},\end{aligned} \tag{29}$$

for T_1', obtained from (22) and (28), is also independent of x: as mentioned earlier in this section this is a necessary condition for the validity of the analysis.

The temperature distribution function is now given by

$$\begin{aligned}\theta(\xi) = \frac{T-T_1}{T_0-T_1} &= \frac{\dfrac{(T-T_1^*)}{(T_0-T_1^*)}-\dfrac{(T_1-T_1^*)}{(T_0-T_1^*)}}{1-\dfrac{(T_1-T_1^*)}{(T_0-T_1^*)}}\\ &= \frac{\dfrac{I(u)-I(u_*)}{1-I(u_*)}+\dfrac{5KU_0N\{\log_e(5\sigma+1)+\sigma\}}{kU_\tau x_1^{q-p}}}{1+\dfrac{5KU_0N\{\log_e(5\sigma+1)+\sigma\}}{kU_\tau x_1^{q-p}}}.\end{aligned} \tag{30}$$

An expression for the total flux of heat, $Q_*(x_1)$, across the top of the transition zone into the fully turbulent zone, obtained by integrating (25) with respect to x, is

$$Q_*(x_1) = K\rho c_p\,U_0(T_1^*-T_0)N(kq)^{-1}x_1^q: \tag{31}$$

we note that expressions (30) and (31) are identical with the corresponding expressions obtained by Davies (**5**) if N^{-1} is replaced by the integral $\int_{\xi_*}^{\infty} F\,d\xi$ calculated by Davies.

An expression for the downstream flux of heat, at $x = x_1$, across the transition zone, per unit width of a plane section normal to the flat plate, can be obtained by using the empirical velocity and temperature forms (**8**, p. 831). This contribution to the total flux is given by the integral

$$\rho c_p \int_{5\nu/U_\tau}^{30\nu/U_\tau} U(T-T_0)\,dy$$
$$= \rho c_p (T_1-T_0) U_\tau \int_{5\nu/U_\tau}^{30\nu/U_\tau} [-3{\cdot}05+5\log_e(U_\tau y\nu^{-1})]\times$$
$$\times\left\{1-\frac{\log_e[1-\sigma+\sigma U_\tau y/(5\nu)]+\sigma}{\log_e(5\sigma+1)+\sigma+kU_\tau x_1^{q-p}(5NKU_0)^{-1}}\right\}dy. \quad (32)$$

Similarly, it can be shown that the downstream flux through the laminar sub-layer is given by the integral

$$\rho c_p \int_0^{5\nu/U_\tau} U(T-T_0)\,dy$$
$$= \rho c_p (T_1-T_0)\nu\left[25/2-\frac{125\sigma KU_0}{3kU_\tau x_1^{q-p}N^{-1}+15KU_0\{\log_e(5\sigma+1)+\sigma\}}\right]. \quad (33)$$

The sum of (31), (32), and (33) then gives the total downstream flux of heat across $x = x_1$.

An alternative and very convenient method of calculating the flux may be obtained by first integrating equation (16) with respect to x_0, noting that (16) neglects the presence of the sub-layers. We obtain, using also (29), the form

$$Q'(x_1)$$
$$= \rho c_p (T_1-T_0)[1-I(u_*)]^{-1}[1+5NKU_0 x_1^{p-q}(kU_\tau)^{-1}\{\log_e(5\sigma+1)+\sigma\}]^{-1}\times$$
$$\times\frac{1}{\pi}\left(\frac{U_0 b}{1+\beta}\right)^{\mu(1-\alpha)(1+\beta)^{-1}}\left[\frac{(2+\beta-\alpha)aKU_0}{q}\right]^{\mu} k^{-\mu(\alpha+\beta)(1+\beta)^{-1}}\Gamma(\mu)x_1^q\sin(\pi\mu), \quad (34)$$

where $\mu = (1+\beta)(2+\beta-\alpha)^{-1}$. On the same basis the flux across the region from $y_\tau = 0$ to $y_\tau = 30$ is given by

$$\rho c_p \int_0^{30\nu/U_\tau} U(T-T_0)\,dy$$
$$= \frac{(T_1-T_0)\rho c_p bU_0(kx_1)^{-\beta}}{[1-I(u_*)][1+5NKU_0 x_1^{p-q}(kU_\tau)^{-1}\{\log_e(5\sigma+1)+\sigma\}]}\int_0^{30\nu/U_\tau}[1-I(u)]y^\beta\,dy. \quad (35)$$

The result obtained by subtracting (35) from (34) then gives the flux into the fully turbulent zone, and the total downstream flux across $x = x_1$ is obtained by adding to this the flux in the sub-layer given by the sum of (32) and (33).

Numerical evaluation of these expressions for the flux and θ distributions depends on a determination of appropriate values of the parameters a and α. Fig. 1 illustrates that a power law may be fitted fairly well to the ϵ distri-

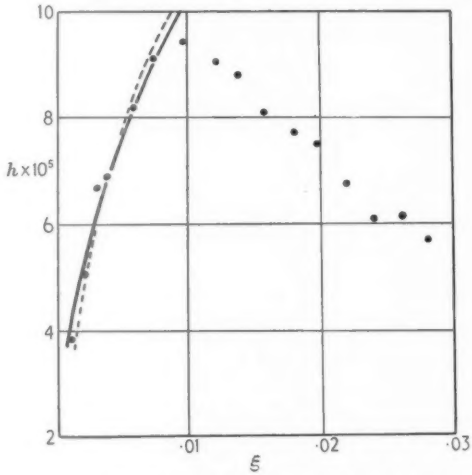

FIG. 1. Distribution of eddy viscosity given by Townsend. $h = \epsilon/(xU_0)$, where ϵ = eddy viscosity, x = distance from virtual origin of momentum boundary layer, U_0 = free stream mean velocity; $\xi = y/x$, where y = height above the surface; ——— power law $h = 0{\cdot}00065\xi^{0{\cdot}40}$. ------ power law $h = 0{\cdot}00088\xi^{0{\cdot}46}$.

bution given by Townsend for $\xi < 0{\cdot}01$, but for $\xi > 0{\cdot}01$ there is clearly a buffer region between the intense turbulence in the region immediately above the transition zone and the smaller degree of turbulence in the main stream, and it is not possible to represent by a power law the actual ϵ values over the whole thickness of the boundary layer. However, the arguments given by Fage and Falkner (**12**) and Lighthill (**13**) in the laminar case suggests that the crucial part of the boundary layer in the heat transfer problem is the inner zone, $\xi < 0{\cdot}01$. We find that the calculated distribution of θ, based on a power law representation of ϵ in this inner part of the boundary layer, is in agreement (apart from a small deviation of, at most, 2 per cent. for values of ξ greater than 0·025) with the values of θ calculated by Davies (**5**, Fig. 2), on the basis of the Townsend ϵ distribution taken

over the entire thickness of the boundary layer. This result shows that the outer layer, $\xi > 0{\cdot}01$, is only important in controlling the rate at which θ approaches its asymptotic value 1·0 in the free stream, and the error incurred in using a representation of the inner boundary layer over the whole thickness of the layer is small.

In order to obtain a reasonably good power law representation for $\xi < 0{\cdot}01$ we find that the numerical value of α must be chosen to lie between 0·40 and 0·46 and the associated value of a must lie between 0·00065 and 0·00088 respectively. However, we find that the differences in calculated values of rates of heat transfer discussed in this section, and of evaporation rates discussed in section 4, are not significant when based on

$$\text{(i)} \quad h = 0{\cdot}00065\xi^{0{\cdot}40} \quad \text{and} \quad \text{(ii)} \quad h = 0{\cdot}00088\xi^{0{\cdot}46}.$$

These are the extreme power laws (shown in Fig. 1) which lead to a reasonable fit for the inner boundary layer $\xi < 0{\cdot}01$. Using both power laws (i) and (ii) we now calculate the factor N, having determined appropriate values of q, b, and β from Elias's measurements (**6**), following the method discussed by Davies (**5**). The numerical value of the parameter k is chosen so that Elias's velocity profile fits the Townsend profile $U/U_0 = 1{\cdot}72\xi^{0{\cdot}15}$, where in Elias's flat plate experiments $\xi = y/(kx^{0{\cdot}89})$. Since the velocity profile forms then agree and the flows are over a plane smooth surface with no buoyancy effects, we then assume, as in (**5**), that the values of $h(\xi)$ given by Townsend apply in the conditions of Elias's experiments. We find that the numerical values of N^{-1}, based on power laws (i) and (ii) are within 4 and 3 per cent. respectively of the equivalent factor $\int_{\xi_*}^{\infty} F\, d\xi$ which was evaluated by Davies (**5**) on the basis of the actual ϵ values over the whole thickness of the boundary layer. Consequently, taking $\sigma = 0{\cdot}72$ for air, the numerical values of the flux expression (31) for $Q_*(x_1)$, using (i) and (ii) respectively, are within 4 and 3 per cent. of the value calculated previously by Davies (**5**). The numerical values of $Q(x_1)/(T_1 - T_0)$, where Q is the total flux, calculated from equations (32) to (35), using power law forms (i) and (ii), are 0·58 watts per °C. and 0·575 watts per °C. respectively for a length of 50 cm. of plate and a free stream velocity of 35 m./sec. These results are both within about $3\frac{1}{2}$ per cent. of the experimental value of 0·56 watts per °C. given by Elias (**6**).

This calculation can also be used to illustrate the importance of the presence of the laminar sub-layer and transition zones in calculating the θ distribution, although it has been calculated by Davies (**5**) that, at the higher speeds involved in Elias's experiments, only 5 per cent. of the total downstream heat flux takes place in the sub-layers. We find, for example, that

the value of θ given by equation (30) at the top of the transition layer is as high as 0·56; we note that this value is also indicated approximately by Elias, although there is considerable scatter of his experimental points in this region. Moreover, we find that, if a solution is computed which leaves out the laminar sub-layer and transition zone in equation (30), the calculated θ values are about 25, 7, and 2 per cent. less than the experimental θ values at $\xi = 0{\cdot}01$, 0·02, and 0·03 respectively, thus emphasizing the considerable error involved in this case if we leave out the sub-layers.

The analysis described in this section therefore indicates that the method of approach based on a power law representation of the eddy viscosity in the inner part ($\xi < 0{\cdot}01$) of the fully turbulent boundary layer, together with the approximate treatment given of the laminar sub-layer and transition zone, gives numerical results for θ and Q in close agreement with those derived by a previous method, which was based on the actual values of ϵ over the whole boundary layer thickness. These results are also in close agreement with the experimental values given by Elias. This suggests that we may extend the treatment to the problem of evaporation into a *developing* boundary layer from an area source whose leading edge is at a distance downstream from the leading edge of the momentum boundary layer; a solution in terms of the similarity variable ξ is not attainable in this case.

4. The problem of evaporation into a developing fully turbulent boundary layer

The rates of evaporation calculated in this section are based on the conditions recorded in the experiments of Davies and Walters (**2**) at Sheffield. In these experiments the rates of evaporation from various rectangular saturated surfaces (of aniline) were measured in order to determine the dependence of evaporation on the dimensions of the area at a given wind speed. In conformity with previous notation we replace $\rho c_p T$ by χ, the mean concentration of vapour, in the analysis of section 2. If we measure x from the origin of the momentum boundary layer and suppose the area source is positioned with its leading edge along $x = a_1$, the conditions of the problem can be expressed in the form

$$\chi = \chi_0 \text{ (the up-stream value)}, \qquad x < a_1, \qquad y \geqslant 0, \tag{36}$$

$$\chi \to \chi_1 \text{ (the saturation value)}, \qquad x \geqslant a_1, \qquad y = 0, \tag{37}$$

and

$$\chi \to \chi_0, \qquad x \geqslant a_1, \qquad \text{and} \qquad y \to \infty. \tag{38}$$

We now assume that vapour and momentum diffusivities are equal; the appropriate solution of the integral equation (32) of Part I (**7**) then

becomes

$$u(\phi) = (\chi_1'-\chi_0)\pi^{-1}(\sin\mu\pi)\frac{d}{d\phi}\int_{a_1^s}^{\phi}(\phi-X)^{\mu-1}\,dX$$

$$= (\chi_1'-\chi_0)\pi^{-1}\sin\mu\pi(\phi-a_1^s)^{\mu-1}, \tag{39}$$

where χ_1' is taken to be the constant value of χ on the area when the sub-layers are at first neglected in the analysis. The expression for A becomes

$$A = s\pi^{-1}\sin\mu\pi(\chi_1'-\chi_0)(x_0^s-a_1^s)^{(\mu-1)}x_0^{(s-1)}, \tag{40}$$

and consequently the equation for θ, given by (37) in Part I, is replaced by

$$(\chi-\chi_0)/(\chi_1'-\chi_0)$$

$$= \pi^{-1}\sin\mu\pi\int_0^{(X-A_1)}(X-A_1-\phi)^{-\mu}\phi^{\mu-1}\exp\{-\gamma(X-A_1-\phi)^{-1}\}\,d\phi, \tag{41}$$

where $A_1 = a_1^s$. As in Part I the integral can be expressed in the form of a Pearson I function and we obtain

$$(\chi-\chi_0)/(\chi_1'-\chi_0) = 1-I\{\gamma X^{-1}[1-(a_1/x)^s]^{-1}, -\mu\}, \tag{42}$$

where $\mu = (1+\beta)(2+\beta-\alpha)^{-1}$.

Now in the wind-tunnel evaporation work of Davies and Walters (**2**) the numerical values of p and q were not calculated; it was only possible to measure the mean velocity profile in the neighbourhood of the evaporation plate and no measurements could be made of the mean shearing stress distribution. However, the experimental investigations carried out by Townsend and by Davies and Walters were both over a smooth wind-tunnel wall, and we assume that the result $p = q = 1$, shown to be suitable in Townsend's work, also applies to that of Davies and Walters. The variable $\gamma X^{-1}[1-(a_1/x)^s]^{-1}$ in expression (42) may then be written in the form

$$\frac{k^2b[y(kx)^{-1}]^{(2+\beta-\alpha)}}{Ka(1+\beta)(2+\beta-\alpha)[1-(a_1/x)^s]} = v, \text{ say.}$$

The approximate treatment of the transition and laminar sub-layers is now introduced. If we denote by χ_* the mean concentration at the top of the transition layer, calculated from (20), at $x = x_1$, the downstream distance at which we wish to evaluate the χ distribution and flux, then

$$(\chi_*-\chi_0)/(\chi_1'-\chi_0) = 1-I(v_*, -\mu), \tag{43}$$

where v_* corresponds to the top of the transition zone, at $x = x_1$. The function corresponding to θ_* may then be obtained following the method of section 3.

We assume that heat flux and mean shearing stress in the sub-layers are independent of y. Following the method described in section 3, we equate

the expressions for vapour flux at the upper and lower limits of the sub-layers at $x = x_1$, and obtain

$$(\chi_1 - \chi_1^*)/(\chi_0 - \chi_1^*) = -5KU_0(kU_\tau)^{-1}[\log_e(5\sigma_1+1)+\sigma_1]\{x_1^s(x_1^s - a_1^s)^{-1}\}^{(1-\alpha)(2+\beta-\alpha)^{-1}}M, \quad (44)$$

where

$$M = \frac{a[k^2ba^{-1}K^{-1}(1+\beta)^{-1}]^{(1-\alpha)(2+\beta-\alpha)^{-1}}(2+\beta-\alpha)^{(1+\beta)(2+\beta-\alpha)^{-1}}}{\Gamma\{(1-\alpha)(2+\beta-\alpha)^{-1}\}[1-I(v_*)]e^{v_*}}, \quad (45)$$

and $\sigma_1 = \nu/D$, D being the molecular diffusivity into air of the vapour concerned, replacing ν/κ the Prandtl number. The χ distribution may then be obtained as in section 3. We note at this stage that the value of y_* and v_* are first obtained from equation (20) and the measured velocity profile, at a point over the downstream edge of the evaporation plate, and for other values of x, $v_*(x)$ must be chosen numerically so that the expression

$$(\chi_1' - \chi_0)/(\chi_1 - \chi_0) = [1-I(v_*)]^{-1}[1-(\chi_1 - \chi_1^*)/(\chi_0 - \chi_1^*)]^{-1} \quad (46)$$

is independent of x, this being a necessary condition for the validity of the analysis. Taking $a_1 = 20$ cm., $x_1 = 50$ cm., and $U_0 = 676$ cm./sec. (the relevant values in the evaporation tests), Table 2 shows that the ensuing approximation to the top of the transition zone is in close agreement (apart from a small error near the leading edge of the evaporation area) with the position of the top of the transition layer, calculated from equation (20).

TABLE 2

Calculated height of the laminar sub-layer, the transition layer, and the fully turbulent layer over an evaporation plate, 30 cm. in length, positioned with its leading edge 20 cm. downstream from the origin of the momentum boundary layer: $U_0 = 676$ cm./sec.

Downstream distance from leading edge of plate (cm.):	0	10	20	30
Laminar sub-layer height (cm.), calculated from (18) .	0·02	0·02	0·02	0·02
Transition layer height (cm.) calculated from (20) .	0·12	0·13	0·13	0·14
Approximate transition layer height calculated from (46)	0·10	0·12	0·13	0·14
Approximate height (cm.) of the fully turbulent zone deduced from the experimental results of Davies and Walters	0·8	1·2	1·6	2·0

A convenient expression for the rate of evaporation from an area of length l may now be obtained in two ways. We first choose a value of k so that the measured mean velocity profile is in agreement with Townsend's velocity profile which may be represented by the power law

$$U/U_0 = 1{\cdot}72\xi^{0{\cdot}15}.$$

The expression for the downstream flux of vapour in the fully turbulent

zone at a given station $x = x_1 = a_1 + l$ may then be written in the form

$$Q_*(x_1) = \int_{30\nu/U_\tau}^{\infty} U(\chi - \chi_0)\, dy = 1{\cdot}72 U_0(\chi_1 - \chi_0)(kx_1)^{-0{\cdot}15} \int_{30\nu/U_\tau}^{\infty} (1-\theta) y^{0{\cdot}15}\, dy, \tag{47}$$

where θ is the vapour concentration distribution corresponding to equation (30). The flux in the transition and laminar sub-layers is given by the sum of expressions (32) and (33) with $\rho c_p T$ replaced by χ, N by M, and with $p = q = 1$.

An alternative expression may be obtained, as in section 3, by integrating expression (40), assuming the sub-layers are absent, and using equation (26) of Part I. The total flux from an area of length l, when its leading edge is at $x = a_1$, is then given by

$$Q'(l) = d[(a_1 + l)^s - a_1^s]^{1/s}, \tag{48}$$

where

$$d = (\chi_1 - \chi_0)\pi^{-1}[1 - I(v_*)]^{-1} \times$$
$$\times [1 + 5MKU_0(kU_\tau)^{-1}\{\log_e(5\sigma_1 + 1) + \sigma_1\}(1 - a_1^s/x_1^s)^{(\alpha-1)(2+\beta-\alpha)^{-1}}]^{-1} \times$$
$$\times \left(\frac{U_0 b}{1+\beta}\right)^{\mu(1-\alpha)(1+\beta)^{-1}} [aKU_0(2+\beta-\alpha)]^{\mu} k^{-\mu(\alpha+\beta)(1+\beta)^{-1}} \Gamma(\mu)\sin(\mu\pi).$$

On the same basis an expression for the flux in the region from $y_\tau = 0$ to $y_\tau = 30$ is given by (35) with χ and M replacing $\rho c_p T$ and N, and $p = q = 1$. Following the method of section 3, corrections for the presence of the sub-layers are then applied and the total flux across $x = x_1$ may be calculated.

In order to evaluate these flux-expressions numerically appropriate values of a_1, k, K, etc., are first deduced from the results of experimental work by Davies and Walters (**2**). Since the velocity profile was measured at one value of x only, the exact position of the virtual origin of the momentum boundary layer is not known, and consequently an exact determination of a_1 is not attainable. However, an approximate value may be deduced, and we find that the calculated values of rate of evaporation E are not very sensitive to our numerical choice of a_1—at least in the conditions investigated. The experimental results obtained by Davies and Walters (**2**) show that the dependence of E on length l may be represented as a power law proportional to $l^{0{\cdot}76}$ for plates of lengths between 8 and 30 cm., and we now *choose* the value of the parameter a_1 so that a power law l^β may be fitted to the values of the expression $Q' = d[(a_1+l)^s - a_1^s]^{1/s}$, given by (48), for values of l between 8 and 30 cm. We find that for $a_1 < 10$ cm., $\beta > 0{\cdot}80$ and for $a_1 > 45$ cm., $\beta < 0{\cdot}70$ and for 17 cm. $< a_1 <$ 23 cm.,

β is approximately 0·76. We first take $a_1 = 20$ cm. and later check the sensitivity of the calculated evaporation values on this choice, by taking $a_1 = 15$ cm. and $a_1 = 45$ cm. This application of the Q' expression is justified by the result that its computed value is found to be within 2 per cent. of the value calculated later in this section for the total rate of evaporation.

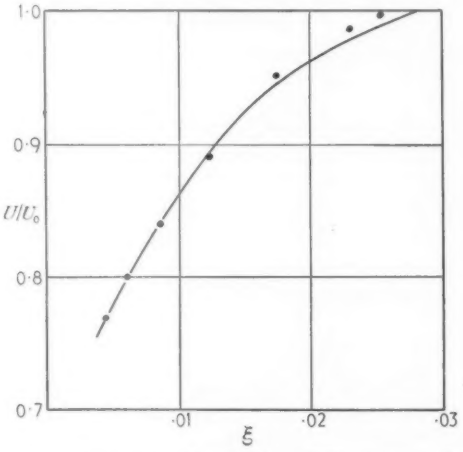

FIG. 2. Mean flow distribution U/U_0, measured by Davies and Walters at $U_0 = 676$ cm./sec. $\xi = y/(1{\cdot}3x)$, where $x = 85$ cm. and is measured from the estimated position of the leading edge of the momentum boundary layer; ——— $U/U_0 = 1{\cdot}72\xi^{0{\cdot}15}$.

The parameter k is now determined by considering the wind velocity profile measured at a point over the downstream edge of the flat surface of the faired holder used by Davies and Walters (**2**); these velocity measurements are shown in Fig. 2. The downstream distance of this velocity profile from the leading edge of the evaporation area was 65 cm. so that its distance from the virtual origin of the momentum boundary layer is found (by adding the a_1 value) to be about 85 cm. Values of the similarity variable ξ at this downstream distance are then given by $y/(85k)$, and by choosing $k = 1{\cdot}3$ we find that, except for the values very near the top of the turbulent boundary layer, the measured mean velocities are reasonably close to Townsend's profile: the departures near the top of the boundary layer are probably due to a different degree of turbulence in the free streams of the two experiments. It is suggested that the value of k is greater than 1·0 (the value found by Townsend) due to some thickening of the turbulent layer induced by the slight curvature near the leading edge of the faired

holder used in the experiments. Since the measured thickness of the turbulent boundary layer at this downstream position was about 3 cm., the approximate value of ξ corresponding to the top of the boundary layer is now seen to be given by $3/(1{\cdot}3\times 85) = 0{\cdot}028$ which is roughly the value of ξ measured by Townsend (**4**) in this region, and, since the conditions of flow were similar, this approximate agreement provides further support for the numerical value of a_1 assumed in this calculation. We also note that, since the measured distance L from the tunnel entrance to the position of the leading edge of the evaporating plate was 190 cm. and a_1 is taken to be 20 cm., the boundary layer on the tunnel wall becomes fully turbulent at a Reynolds number given by $(L-a_1)U_0/\nu = 170\times 676/0{\cdot}15 = 7{\cdot}6\times 10^5$ which is within the range of possible Reynolds numbers given by Goldstein (**9**, p. 326). The velocity profile now coincides with the profile given by Townsend and we assume, following the arguments given by Davies (**5**), that K is 1·3 and the values of $h(\xi)$ given by Townsend are applicable. We work, as in section 3, with two power law representations between which lie these values of $h(\xi)$; we take

$$\text{(i)}\quad h = 0{\cdot}00065\xi^{0{\cdot}40} \quad \text{and} \quad \text{(ii)}\quad h = 0{\cdot}00088\xi^{0{\cdot}46}.$$

Appropriate numerical values of several other parameters required in the calculation of rate of evaporation are now easily obtained. In the conditions of the evaporation experiments by Davies and Walters (**2**), χ_0 is zero and χ_1 is calculated from a knowledge of the molecular weight of the liquid concerned, the temperature of the air stream, and a correction applied to obtain the surface temperature of the plate (this differs slightly from the air stream temperature due to the latent heat effect of the evaporating liquid). The value of D, the vapour diffusivity of aniline at the temperature (17° C.) of the plate, is also required and is given by Mack (**14**) to be 0·069, and ν is 0·15 cm. sec. units for air; this leads to a value for σ_1 $(= \nu/D)$ of 2·17.

The expression (47), giving the flux of vapour and the associated sub-layer correction factors were first computed by numerical integration for $a_1 = 20$ cm., $l = 30$ cm. (the maximum length tested), $U_0 = 676$ cm./sec. (the measured free stream velocity), using firstly the power law $h = 0{\cdot}00065\xi^{0{\cdot}40}$. The total calculated flux by this method is found to be 0·0470 g./min. for a width of 10·1 cm. (or 4 in.), the contributions from the fully turbulent zone, the transition zone, and the laminar sub-layer being 0·0326 g./min., 0·0134 g./min., and 0·0010 g./min., respectively. This is in reasonable agreement with the experimental value for the total flux, given by Davies and Walters (**2**), of 0·0420 g./min. Calculations of evaporation from areas of width 4 in. are considered, as the dependence of evaporation on length of area was evaluated experimentally in detail by Davies and Walters (**2**) for this

particular width only. We assume in this paper that 4 in. is sufficiently large in the conditions of the experiment, and over the length range considered, to permit us to neglect any effect which the enhanced rate of evaporation in the neighbourhood of the longitudinal edges may have on the index β. In support of this assumption we note that measurements were also made by Davies and Walters to determine the dependence of E on width w of area, for lengths of area $l = 5$ in., 13 in., and 15 in., and from lines of regression obtained in each case for E against w, we find that for $w = 1{\cdot}5$ in., 2 in., 3 in., and 4 in. the associated β values are 0·71, 0·745, 0·755, and 0·76, which suggests that $\beta = 0{\cdot}76$ is close to the value of the index appropriate to evaporation from an area of very large width.

The second method of calculation using expression (48), with the appropriate correction factors, and the same power law $h = 0{\cdot}00065\xi^{0{\cdot}40}$ gives a calculated value of 0·0464 g./min., which is again in reasonable agreement with the experimental value and also in close agreement with the calculated results of the first method. This second method of calculation has the advantage of not requiring a numerical integration, and, due to our choice of a_1, the dependence of theoretical values of E on length of area is in agreement with the results of experiment.

Using the power law representation $h = 0{\cdot}00088\xi^{0{\cdot}46}$ and expression (48), for convenience, with the associated corrections, we now find that the total rate of evaporation in the same conditions, i.e. $a_1 = 20$ cm., $l = 30$ cm., and $U_0 = 676$ cm./sec., is 0·0444 g./min., compared with the result 0·0464 g./min. obtained on the basis of the power law representation $h = 0{\cdot}00065\xi^{0{\cdot}40}$. We note that these are theoretical values associated with extreme power laws enclosing the actual ϵ distribution given by Townsend; both are within reasonable agreement of the experimental value of 0·0420 g./min., and similar results are obtained for other values of l. Finally, in order to test the sensitivity of the dependence of the theoretical results on the value of a_1 we find by the second method of calculation (i.e. using expression (48)) at $l = 30$ cm. and $U_0 = 676$ cm./sec. that $E = 0{\cdot}0460$ g./min. and 0·0491 g./min. for $a_1 = 15$ cm. and 45 cm. respectively, the former being within 1 per cent. and the latter within 6 per cent. of the result computed for $a_1 = 20$ cm.

The results obtained in this section therefore suggest that, although an exact calculation was not attainable due to the absence of an experimentally determined a_1 value, no large error has been introduced into the calculation by (*a*) the approximate estimation of the parameter a_1, and (*b*) the existence of a small range of possible a and α values, giving power law representations of the eddy viscosity distribution. The results show that the two-dimensional diffusion model described in this section gives results in reasonable

agreement with experiment in the conditions discussed. However, the problem of accounting for lateral diffusion and finite width of area in these conditions of a developing momentum boundary layer remains to be solved.

5. Forced convection into a fully turbulent boundary layer which is preceded by an appreciable laminar boundary layer

Since the method of sources is found to lead to a relatively simple approximate method of approach to the heat transfer problem in both laminar and fully turbulent boundary layers, it is of interest to consider its possible application to the important problem of flow over a flat surface for Reynolds numbers at which there is a significant laminar zone of flow near the leading edge followed by a transition zone with a final fully turbulent region of flow. We have not been able to treat equation (1) and consequently we have not obtained a solution for the transition zone. However, it is possible that an *approximate* treatment could be constructed by ignoring the transition zone and assuming the existence of a laminar zone up to the virtual origin of the fully turbulent layer at $x = x_1$, say, calculated from the observed profiles at various points in a fully turbulent zone. If T_1 is the constant temperature of the whole plate and (as in section 3) T_1' the surface temperature of the turbulent layer when the sub-layers are assumed absent, then the temperature excess at a point P on $y = 0$ for $x \geqslant x_1$ due to the known distribution of sources in the laminar zone up to x_1 is

$$(T_1-T_0)\pi^{-1}(\sin\mu_1\pi)\int_0^{X_1}(X-\theta)^{-\mu_1}\theta^{\mu_1-1}\,d\theta = f(X), \tag{49}$$

where

$$X = x^{s_1}, \qquad X_1 = x_1^{s_1}, \qquad s_1 = (2+\beta)(2+2\beta)^{-1}, \qquad \mu_1 = (1+\beta)(2+\beta)^{-1},$$

and $f(X)$ is obtained by a numerical integration of (49). The temperature excess at P due to an unknown distribution of sources along $x \geqslant x_1$ is given (see Part I, section 2), by

$$s_2^{-1}\int_0^{X'}A(\phi)\phi^{(1-s_2)/s_2}(X'-\phi)^{-\mu_2}\,d\phi, \tag{50}$$

where

$$X' = (x-x_1)^{s_2}, \quad \mu_2 = (1+\beta)(2+\beta-\alpha)^{-1}, \text{ and } s_2 = q(2+\beta-\alpha)(1+\beta)^{-1},$$

and the integral equation to give the unknown function

$$A(\phi) = s_2\phi^{(s_2-1)/s_2}u(\phi)$$

is

$$f(X') + \int_0^{X'}(X'-\phi)^{-\mu_2}u(\phi)\,d\phi = T_1'-T_0. \tag{51}$$

Its solution is

$$u(\phi) = \pi^{-1} \sin \mu_2 \pi \frac{d}{d\phi} \int_0^{\phi} (\phi - X')^{\mu_2 - 1} [T_1' - T_0 - f(X')]\, dX'. \qquad (52)$$

As in section 3 two further equations could be obtained by using an approximate treatment of the sub-layers, such that T_1' is a constant and expressed in terms of T_1.

The numerical work involved, however, would be extremely heavy and, as the scatter in the experimental measurements by Elias does not allow a reasonably accurate determination of x_1, this has not been attempted in this paper.

6. Conclusions

A solution of the problem of forced convection from a flat plate through a fully turbulent boundary layer has been obtained by transforming the temperature equation into a von Mises form and using the method of sources to determine the distribution of rate of heat transfer on the plate and the associated temperature distribution over the plate. The treatment is based on (i) an application to flow over a flat plate of a power law representation of the eddy viscosity distribution, which was obtained by Townsend from his measurements of mean Reynolds shearing stress and mean velocity profiles over the plane wall of a wind-tunnel, (ii) the equivalence of momentum and heat eddy diffusivities, and (iii) an approximate treatment of the flow in the transition and laminar sub-layers. The agreement of the calculated results with those obtained previously by another method and by experiment then supports the application of the source method to discuss the problem of diffusion of vapour from a saturated surface into a developing boundary layer. The discussion of this problem includes the case when the leading edge of the vapour boundary layer is downstream of the leading edge of the momentum boundary layer, and incorporates an approximate treatment of the downstream flux of vapour in the sub-layers. The calculated values of evaporation rates are found to be in reasonable agreement with measured values in a wind-tunnel.

Acknowledgement

One of the authors (D. E. Bourne) wishes to acknowledge the receipt of a research fellowship of the University of Sheffield.

REFERENCES

1. F. Pasquill, *Proc. Roy. Soc.* A, **182** (1943), 75.
2. D. R. Davies and T. S. Walters, *Proc. Phys. Soc.* B, **65** (1952), 640.
3. O. G. Sutton, *Micrometeorology* (McGraw-Hill, 1953).
4. A. A. Townsend, *Proc. Camb. Phil. Soc.* **47** (1951), 375.

5. D. R. Davies, *Quart. J. Mech. Appl. Math.* **8** (1955), 326.
6. F. Elias, *Z. angew. Math. Mech.* **10** (1930), 1.
7. D. R. Davies and D. E. Bourne, *Quart. J. Mech. Appl. Math.*, above, p. 457.
8. L. Howarth (ed.), *Modern Developments in Fluid Dynamics* (Oxford, 1953).
9. S. Goldstein (ed.), *Modern Developments in Fluid Dynamics* (Oxford, 1938).
10. K. Pearson, *Tables of the Incomplete Gamma Function* (London, H.M.S.O., 1922).
11. J. H. Preston, *Rep. Aero. Res. Council, Lond.* (1955), No. 17443.
12. A. Fage and V. M. Falkner, *Rep. Memor. Res. Comm. Lond.* (1931), No. 1408.
13. M. J. Lighthill, *Proc. Roy. Soc.* A, **202** (1950), 359.
14. E. Mack, *J. Amer. Chem. Soc.* **47** (1925), 2468.

BOUNDARY-VALUE PROBLEMS OF SIMPLY-SUPPORTED ELASTIC PLATES

By T. BUCHWALD *and* R. TIFFEN (*Birkbeck College, London*)

[Received 8 December 1955]

SUMMARY

This paper is concerned with problems of thin elastic plates with simply-supported boundaries. Solutions are obtained for plates in the form of half-planes and strips, including cases of isolated interior loading. A uniqueness theorem is established to cover both cases.

1. Fundamental equations

THROUGHOUT this paper the mid-planes of the plates are chosen as the plane $Z = 0$ of a rectangular cartesian frame $O(x, y, Z)$, and the notation used is that of A. C. Stevenson (**1**). The displacement w of the mid-plane in the direction $\hat{\mathbf{k}} = \overrightarrow{OZ}$ satisfies the equation

$$\nabla_1^4 w = F(x, y), \tag{1.1}$$

where $F(x, y)$ is zero if the faces of the plates are stress-free. Corresponding to a right-handed orthogonal triad $\hat{\mathbf{n}}, \hat{\mathbf{s}}, \hat{\mathbf{k}}$ the mean stresses $n\breve{Z}$, $s\breve{Z}$ and the mean stress couples $\tilde{n}s$, $\tilde{s}n$, $\tilde{s}s$ $(= -\tilde{n}n)$ are given by the equations

$$\breve{nZ}+i\breve{sZ} = -2Pe^{-i\theta}\frac{\partial}{\partial\bar{z}}\nabla_1^2 w, \tag{1.2}$$

$$\tilde{ns}-\tilde{sn} = -P(1+\eta)\nabla_1^2 w, \tag{1.3}$$

$$\tilde{ns}+\tilde{sn}+2i\tilde{ss} = -4P(1-\eta)e^{-2i\theta}\frac{\partial^2 w}{\partial\bar{z}^2}, \tag{1.4}$$

where $z = x+iy$, $\hat{\mathbf{n}} = (\cos\theta, \sin\theta, 0)$, $\cos\theta = \hat{\mathbf{i}}.\hat{\mathbf{n}}$, η is Poisson's ratio, and P is a constant depending on the thickness T of the plate. The general solution to (1.1) may be written, in the case $F(x, y) = 0$, as

$$w = \bar{z}\Omega(z)+z\overline{\Omega}(\bar{z})+\omega(z)+\bar{\omega}(\bar{z}), \tag{1.5}$$

where $\Omega(z)$, $\omega(z)$ are functions of z which are regular in the region R occupied by the plate. From (1.3)–(1.5)

$$\tilde{ns}/P = -2(1+\eta)\{\Omega'(z)+\overline{\Omega}'(\bar{z})\}-(1-\eta)[e^{-2i\theta}\{z\overline{\Omega}''(\bar{z})+\bar{\omega}''(\bar{z})\}+ \\ +e^{2i\theta}\{\bar{z}\Omega''(z)+\omega''(z)\}]. \tag{1.6}$$

This paper is concerned with plates in the form of half-planes and infinite

strips, so that over the boundaries, chosen as $y = 0$, $y = a$ the angle $\theta = \pm\frac{1}{2}\pi$ and $\tilde{n}s = -\tilde{y}x$. From (1.6),

$$\tilde{y}x/P = 2(1+\eta)\{\Omega'(z)+\overline{\Omega}'(\bar{z})\}-(1-\eta)\{z\overline{\Omega}''(\bar{z})+\bar{z}\Omega''(z)+\omega''(z)+\bar{\omega}''(\bar{z})\}. \tag{1.7}$$

From (1.5), (1.7),

$$\frac{\tilde{y}x}{4P}+\frac{(1-\eta)}{4}\frac{\partial^2 w}{\partial x^2} = \frac{\tilde{y}x}{4P}+\frac{(1-\eta)}{4}\left(\frac{\partial}{\partial z}+\frac{\partial}{\partial \bar{z}}\right)^2 w = \Omega'(z)+\overline{\Omega}'(\bar{z}) = \frac{\partial^2 w}{\partial z \partial \bar{z}}. \tag{1.8}$$

2. Boundary conditions. Uniqueness of solutions

Problems of clamped elastic plates have been considered by many writers. In particular, Muskhelishvili (**2**) has given an extensive bibliography. Fewer attempts have been made to satisfy the conditions at free or simply-supported boundaries, e.g. Timoshenko (**3**). The problems considered here involve specified values of w and $\tilde{n}s$ along the boundaries. For half-planes and strips this requires the specification

$$w = f(x), \qquad \tilde{y}x = g(x) \tag{2.1}$$

along $y = 0$, with corresponding equations along $y = a$ in the case of the strips. If these boundaries are simply supported or hinged, then

$$f(x) = g(x) = 0, \text{ etc.}$$

From (1.8) it is clear that the boundary conditions (2.1) are equivalent to specification of

$$w = f(x), \qquad \frac{\partial^2 w}{\partial z \partial \bar{z}} = h(x). \tag{2.2}$$

To establish uniqueness of solutions let w_1, w_2, with corresponding pairs of potentials Ω_1, ω_1; Ω_2, ω_2 be distinct solutions to (1.1), having the same singularities in the closed region R defined by the plate and satisfying the same boundary conditions (2.2), etc. Also, let

$$\Omega_0 = \Omega_1-\Omega_2 \quad \text{and} \quad \omega_0 = \omega_1-\omega_2.$$

Then $\chi = w_1-w_2$ satisfies $\nabla_1^4 \chi = 0$ in R and on the boundaries

$$\chi = \nabla_1^2 \chi = 0.$$

Since R extends to infinity it is essential to postulate orders of magnitude at infinity. It will be assumed that the demands made at infinity do not involve terms of the orders

$$\Omega = o(1), \qquad \omega = O(1), \qquad \Omega', \omega' = o(z^{-1}), \qquad \Omega'' = o(z^{-2}), \tag{2.3}$$

where accents denote derivatives, but that all larger terms are specified. Comparison with the corresponding theorems for clamped plates (**4**) indicates that more information at infinity is required here in order to specify

a unique problem. From (2.3) it follows that, at infinity,

$$\chi = o(z), \qquad \frac{\partial \chi}{\partial z} = o(1), \qquad \frac{\partial^2 \chi}{\partial z \partial \bar{z}} = o(z^{-1}), \qquad \frac{\partial^3 \chi}{\partial z \partial \bar{z}^2} = o(z^{-2}). \quad (2.4)$$

Let C denote the real axis from $x = -L$ to $x = L$ and a semicircle of radius L above the real axis or the segments from $x = -L$ to $x = L$ of the lines $y = 0$ and $y = a$, together with straight joins of corresponding extremities. In both cases the integral I defined by

$$I = \int_C \left[\frac{\partial \chi}{\partial z} \frac{\partial^2 \chi}{\partial z \partial \bar{z}} \, dz + \chi \frac{\partial^3 \chi}{\partial z \partial \bar{z}^2} \, d\bar{z} \right] \quad (2.5)$$

tends to zero as L tends to infinity, since χ, $\nabla_1^2 \chi$ are zero on the straight sections, the integrands are $o(z^{-1})$ at infinity, and the lengths of C are $O(z)$ at most. Assuming continuity of Ω_0, Ω_0', Ω_0'', ω_0, ω_0' in R, (2.5) may be converted to the surface integral

$$I = 2i \int_R \left[\frac{\partial^2 \chi}{\partial z \partial \bar{z}} \right]^2 dS. \quad (2.6)$$

Thus $\nabla_1^2 \chi$ vanishes throughout R and, remembering the conditions at infinity, it is easily seen that $\Omega_0 = 0$. The problem has now been reduced to one in which $\chi = \omega_0(z) + \bar{\omega}_0(\bar{z})$, i.e. $\nabla_1^2 \chi \equiv 0$ throughout R, $\chi = O(1)$ and $\partial \chi / \partial z = o(z^{-1})$ at infinity, and χ vanishes on the straight boundaries. The integral

$$J = \int_C [\omega_0(z) + \bar{\omega}_0(\bar{z})] \omega_0'(z) \, dz \quad (2.7)$$

vanishes when L tends to infinity, and is equal to the surface integral

$$J = 2i \int_R [\omega_0'(z) \bar{\omega}_0'(\bar{z})] \, dS. \quad (2.8)$$

Thus $\omega_0'(z) = 0$ throughout R and from the conditions at infinity and along the real axis $\omega_0 = ik$, where k is a real constant, and hence $w_1 = w_2$.

3. The simply-supported half-plane

From (2.2), (1.5) it is evident that if w and $\tilde{y}\tilde{x}$ are specified along the real axis, then the complex potentials must satisfy the conditions

$$2 \operatorname{re}\{x\Omega(x) + \omega(x)\} = f(x), \qquad 2 \operatorname{re} \Omega'(x) = h(x). \quad (3.1)$$

These equations are satisfied by

$$\Omega'(z) = \frac{i}{2\pi} \int_{-\infty}^{\infty} \frac{h(t)\, dt}{z - t}, \qquad z\Omega(z) + \omega(z) = \frac{i}{2\pi} \int_{-\infty}^{\infty} \frac{f(t)\, dt}{z - t} \quad (3.2)$$

which are analytic in $y > 0$ provided that $f(t)$, $h(t)$ are sufficiently small at infinity (5).

4. Isolated loads in a simply-supported half-plane

The potentials

$$\Omega_0 = A(z-z_0)\log\{(z-z_0)/(z-\bar{z}_0)\}, \qquad \omega_0(z) = -\bar{z}_0\,\Omega_0(z),$$
$$A = -W/16\pi TP, \tag{4.1}$$

correspond to an isolated load W at $z = z_0 = \alpha+i\beta$ ($\beta > 0$) but are otherwise free from singularities in the upper half-plane. From (1.5), (1.8) the corresponding displacements are

$$w_0 = A(z-z_0)(\bar{z}-\bar{z}_0)\log\{[(z-z_0)(\bar{z}-\bar{z}_0)]/[(z-\bar{z}_0)(\bar{z}-z_0)]\}, \tag{4.2}$$

and

$$G(x,y) = \frac{\tilde{y}\tilde{x}_0}{4P}+\frac{(1-\eta)}{4}\frac{\partial^2 w_0}{\partial x^2} = A\left\{\log\frac{(z-z_0)(\bar{z}-\bar{z}_0)}{(z-\bar{z}_0)(\bar{z}-z_0)}+\frac{z_0-\bar{z}_0}{z-\bar{z}_0}+\frac{\bar{z}_0-z_0}{\bar{z}-z_0}\right\}. \tag{4.3}$$

When $y = 0$,

$$(w_0)_{y=0} = 0, \qquad G(x,0) = 4A\beta^2/\{(x-z_0)(x-\bar{z}_0)\}. \tag{4.4}$$

Thus the boundary $y = 0$ will be simply supported if potentials Ω_1, ω_1, obtained from (3.2) with $f(x) = 0$ and $h(x) = -G(x,0)$ are added. From (3.1), (3.2)

$$\Omega_1'(z) = \frac{i}{\pi}\int_{-\infty}^{\infty}\frac{2A\beta^2\,dt}{(t-z_0)(t-\bar{z}_0)(t-z)} = \frac{-2iA\beta}{z-\bar{z}_0} \tag{4.5}$$

and hence

$$\Omega_1(z) = -2iA\beta\log(z-\bar{z}_0), \qquad \omega_1(z) = -z\Omega_1(z). \tag{4.6}$$

Combining (4.1) and (4.6), potentials giving the isolated load and simple support along the real axis are

$$\Omega(z) = A(z-z_0)\log\{(z-z_0)/(z-\bar{z}_0)\}-A(z_0-\bar{z}_0)\log(z-\bar{z}_0), \tag{4.7}$$

$$\omega(z) = -A\bar{z}_0(z-z_0)\log\{(z-z_0)/(z-\bar{z}_0)\}+Az(z_0-\bar{z}_0)\log(z-\bar{z}_0). \tag{4.8}$$

At infinity the above solution is of the form

$$\left.\begin{aligned}\Omega(z) &= -A(z_0-\bar{z}_0)\log z+A(\bar{z}_0-z_0)+o(1)\\ \omega(z) &= A(z_0-\bar{z}_0)z\log z+O(1)\end{aligned}\right\}. \tag{4.9}$$

For the uniqueness theorem to apply in this case it must be supposed that the terms mentioned explicitly above at infinity have been specified along with the load W at z_0 and the boundary conditions along the real axis. The reason for this is that equilibrium is impossible without stresses or couples at infinity to balance the moment of W at z_0 about the real axis. The above terms are supplying the equilibrating forces. To this extent the above solution is non-physical. A physically satisfactory solution may be obtained by combining loads W_i at z_i ($i = 1,\ldots, n$) such that

$$\sum_i W_i(z_i-\bar{z}_i) = 0. \tag{4.10}$$

The solution in this case is

$$\Omega(z) = \sum_i A_i(z-z_i)\log\{(z-z_i)/(z-\bar{z}_i)\} - \sum_i A_i(z_i-\bar{z}_i)\log(z-\bar{z}_i), \quad (4.11)$$

$$\omega(z) = -\sum_i A_i\bar{z}_i(z-z_i)\log\{(z-z_i)/(z-\bar{z}_i)\} + z\sum_i A_i(z_i-\bar{z}_i)\log(z-\bar{z}_i). \quad (4.12)$$

At infinity $\Omega(z) = o(1), \qquad \omega(z) = O(1)$ (4.13)

and the solution is unique.

5. Alternative treatment of the half-plane

The above simple method of solving half-plane problems is not the most convenient for extension to consideration of infinite strips. An alternative method is therefore given. From (1.5), (1.7) it follows that

$$w = \bar{z}\Omega(z) + z\overline{\Omega}(\bar{z}) + \omega(z) + \bar{\omega}(\bar{z}), \quad (5.1)$$

$$\frac{(1+\eta)}{2}\frac{\partial^2 w}{\partial x^2} - \frac{\tilde{y}x}{2P} = v = \bar{z}\Omega''(z) + z\overline{\Omega}''(\bar{z}) + \omega''(z) + \bar{\omega}''(\bar{z}). \quad (5.2)$$

Problems involving specified values of w and $\tilde{y}x$ along lines parallel to the real axis may be solved by obtaining the corresponding values of v and w. Consider potentials Ω_1, ω_1 related by the equation

$$\omega_1(z) = -z\Omega_1(z). \quad (5.3)$$

If v_1, w_1 are the corresponding functions given by (5.1), (5.2), then

$$(v_1)_{y=0} = -4\,\mathrm{re}\,\Omega_1'(x), \qquad (w_1)_{y=0} = 0. \quad (5.4)$$

Similarly, if potentials Ω_2, ω_2 are related by the equation

$$\omega_2(z) = -z\,\Omega_2(z) + 2\int \Omega_2(z)\,dz, \quad (5.5)$$

then the corresponding functions v_2, w_2 satisfy the equations

$$(v_2)_{y=0} = 0, \qquad (w_2)_{y=0} = 4\,\mathrm{re}\int \Omega_2(x)\,dx. \quad (5.6)$$

As in the previous method the problem has been reduced to the determination of functions which are analytic in the upper half-plane and have specified real parts along the real axis. The boundary conditions

$$v_{y=0} = p(x), \qquad w_{y=0} = q(x) \quad (5.7)$$

may be obtained by potentials satisfying (5.3), (5.5) provided that

$$-4\Omega_1'(z) = \frac{1}{\pi}\int_0^\infty e^{izu}\,du \int_{-\infty}^{\infty} p(t)e^{-iut}\,dt = \frac{i}{\pi}\int_{-\infty}^{\infty}\frac{p(t)\,dt}{z-t}, \quad (5.8)$$

$$4\int \Omega_2(z)\,dz = \frac{1}{\pi}\int_0^\infty e^{izu}\,du \int_{-\infty}^{\infty} q(t)e^{-iut}\,dt = \frac{i}{\pi}\int_{-\infty}^{\infty}\frac{q(t)\,dt}{z-t}, \quad (5.9)$$

if $p(t)$, $q(t)$ may be expressed as Fourier integrals.

6. The infinite strip

Extension of the above theory to include a second boundary requires potentials which do not disturb the conditions obtained along the real axis. From (5.3), (5.4) it can be seen that the potentials Ω_3, ω_3, with corresponding functions v_3, w_3, where

$$\omega_3(z) = -z\Omega_2(z), \qquad \Omega_3(z) = \frac{i}{\pi}\int_0^\infty \{(\gamma_1+i\gamma_2)e^{izu}+(\gamma_1-i\gamma_2)e^{-izu}\}\,du \tag{6.1}$$

give $(v_3)_{y=0} = (w_3)_{y=0} = 0$ for all real functions γ_1, γ_2 of the real variable u (6). A similar statement holds for the functions Ω_4, ω_4, v_4, w_4, where

$$\left.\begin{aligned} \omega_4(z) &= -z\Omega_4(z)+2\int \Omega_4(z)\,dz \\ \int \Omega_4(z)\,dz &= \frac{1}{\pi}\int_0^\infty \{(\delta_1+i\delta_2)e^{izu}-(\delta_1-i\delta_2)e^{-izu}\}\,du \end{aligned}\right\}. \tag{6.2}$$

Thus, after obtaining specified conditions along the real axis by either of the methods given in §§ 3 and 5, the above pairs of potentials may be added and the functions γ_1, γ_2, δ_1, δ_2 determined to give specified conditions along a second boundary. This section is concerned with specified values of v, w along the line $y = a$. From (6.1), (6.2)

$$\left.\begin{aligned} (v_3+v_4)_{y=a} &= \frac{8}{\pi}\int_0^\infty \{[-a\mathbf{c}u^2(\gamma_1+u\delta_1)-\gamma_1 u\mathbf{s}]\cos xu+ \\ &\qquad +[a\mathbf{c}u^2(\gamma_2+u\delta_2)+\gamma_2 u\mathbf{s}]\sin xu\}\,du \\ (w_3+w_4)_{y=a} &= \frac{8}{\pi}\int_0^\infty \{[a\mathbf{c}(\gamma_1+u\delta_1)-\delta_1\mathbf{s}]\cos xu+ \\ &\qquad +[-a\mathbf{c}(\gamma_2+u\delta_2)+\delta_2\mathbf{s}]\sin xu\}\,du \end{aligned}\right\}, \tag{6.3}$$

where $\mathbf{c} = \cosh au$ and $\mathbf{s} = \sinh au$. It will be assumed that the conditions along $y = a$ can be expressed in the form

$$\left.\begin{aligned} v_{y=a} &= \frac{8}{\pi}\int_0^\infty (\tau_1\cos xu+\tau_2\sin xu)\,du \\ w_{y=a} &= \frac{8}{\pi}\int_0^\infty (\sigma_1\cos xu+\sigma_2\sin xu)\,du \end{aligned}\right\}. \tag{6.4}$$

The above functions are chosen to eliminate the unwanted terms obtained along $y = a$ when getting the required conditions along the real axis as

well as establishing specified conditions along the second boundary. Comparison of (6.3) and (6.4) gives the equations

$$\left.\begin{aligned} -ac u^2(\gamma_1+u\delta_1)-\gamma_1 us &= \tau_1 \\ ac u^2(\gamma_2+u\delta_2)+\gamma_2 us &= \tau_2 \\ ac(\gamma_1+u\delta_1)-\delta_1 s &= \sigma_1 \\ -ac(\gamma_2+u\delta_2)+\delta_2 s &= \sigma_2 \end{aligned}\right\}. \tag{6.5}$$

Hence

$$\left.\begin{aligned} \gamma_1 us^2 &= \tau_1(ac u-s)+ac u^3\sigma_1 \\ \delta_1 us^2 &= -ac\tau_1-(ac u+s)u\sigma_1 \\ \gamma_2 us^2 &= -\tau_2(ac u-s)-ac u^3\sigma_2 \\ \delta_2 us^2 &= ac\tau_2+(ac u+s)u\sigma_2 \end{aligned}\right\}. \tag{6.6}$$

From (6.6) it is evident that the differentiations employed in deriving (6.3) require restrictions on τ_1, τ_2, σ_1, σ_2 at infinity. It will be sufficient if, at infinity, τ_1, $\tau_2 = o(u^{-3})$ and σ_1, $\sigma_2 = o(u^{-5})$. Further, if τ_1, τ_2, σ_1, σ_2 are bounded at $u = 0$, then γ_1, γ_2 are also bounded, but δ_1, δ_2 are $O(u^{-3})$ and modifications are necessary before the solution is valid. However, the formal pair of potentials

$$\left.\begin{aligned} \omega_5(z) &= -z\,\Omega_5(z)+2\int \Omega_5(z)\,dz \\ \int \Omega_5(z)\,dz &= \frac{1}{\pi}\int_0^\infty \{(\delta_1+i\delta_2)(1+izu-z^2u^2/2)- \\ &\qquad -(\delta_1-i\delta_2)(1-izu-z^2u^2/2)\}\,du \end{aligned}\right\} \tag{6.7}$$

give $v_5 = w_5 = 0$ everywhere and may be subtracted from (6.2) to give satisfactory integrals without changing the boundary conditions or making changes in the conditions at infinity. Indicating the modified potentials by a star, (6.2) becomes

$$\left.\begin{aligned} \omega_4^*(z) &= -z\Omega_4^*(z)+2\int \Omega_4^*(z)\,dz \\ \int \Omega_4^*(z)\,dz &= \frac{1}{\pi}\int_0^\infty \{(\delta_1+i\delta_2)(e^{izu}-1-izu+z^2u^2/2)- \\ &\qquad -(\delta_1-i\delta_2)(e^{-izu}-1+izu+z^2u^2/2)\}\,du \end{aligned}\right\}. \tag{6.8}$$

The solution to the strip with specified w and $\tilde{y}x$ along $y = 0$, $y = a$ is therefore given by the potentials (6.1) and (6.8), τ_1, τ_2, σ_1, σ_2 being determined from the boundary conditions (6.4) and γ_1, γ_2, δ_1, δ_2 obtained from (6.6).

7. Extension to cases in which boundary functions are not expressible as Fourier integrals

In many cases of interest the boundary functions are not expressible as Fourier integrals. In this section a method is given for dealing with an infinite strip under the same conditions as above except that

$$w_{y=a} = r(x), \quad \text{where } \int_{-\infty}^{\infty} r'(x)\,dx \text{ exists} \tag{7.1}$$

but $r(x)$ is not expressible as a Fourier integral. This case arises in the next section when dealing with an isolated load in the interior of an infinite strip with simply-supported boundaries. It is well known (7) that $r(x)$ may be expressed in the form

$$r(x)-r(0) = \int_0^x r'(t)\,dt = \frac{1}{\pi}\int_0^{\infty}\frac{du}{u}\int_{-\infty}^{\infty} r'(t)\{\sin u(x-t)+\sin ut\}\,dt. \tag{7.2}$$

Thus
$$r(x) = r(0)+\frac{8}{\pi}\int_0^{\infty}\{\rho_1(\cos xu-1)+\rho_2\sin xu\}\frac{du}{u}, \tag{7.3}$$

where ρ_1, ρ_2 are effectively the sine and cosine transforms of $r'(x)$ respectively and are assumed to be finite but non-zero at $u = 0$. Writing $\rho_1 = \sigma_1 u$ and $\rho_2 = \sigma_2 u$, equation (7.3) becomes

$$r(x) = r(0)-\frac{8}{\pi}\int_0^{\infty}\sigma_1\,du+\frac{8}{\pi}\int_0^{\infty}\{\sigma_1\cos xu+\sigma_2\sin xu\}\,du, \tag{7.4}$$

where σ_1, σ_2 are $O(u^{-1})$ at $u = 0$. It is clear that, owing to the form of (7.4), direct comparison between boundary conditions as in (6.3), (6.4) is not possible. Consider the formal pair of potentials Ω_6, ω_6, where

$$\left.\begin{aligned}\omega_6(z) &= -z\,\Omega_6(z)\\ \Omega_6(z) &= ir(0)/(4a)-(2i/\pi)\int_0^{\infty}\{\mathbf{c}\gamma_1+(a\mathbf{c}u-\mathbf{s})\delta_1/a\}\,du\end{aligned}\right\}. \tag{7.5}$$

Clearly,

$$v_6 = 0, \qquad w_6 = 4y\left\{r(0)/(4a)-(2/\pi)\int_0^{\infty}[\mathbf{c}\gamma_1+(a\mathbf{c}u-\mathbf{s})\delta_1/a]\,du\right\}. \tag{7.6}$$

Thus the boundary conditions along $y = 0$ are unchanged by these potentials but

$$(w_6)_{y=a} = r(0)-(8/\pi)\int_0^{\infty}\{a\mathbf{c}\gamma_1+(a\mathbf{c}u-\mathbf{s})\delta_1\}\,du \tag{7.7}$$

$$= r(0)-(8/\pi)\int_0^{\infty}\sigma_1\,du \tag{7.8}$$

from (6.5). Thus these formal potentials give the first two terms in the expression for $w_{y=a}$ in (7.4) and the deduction of equations (6.5) is again possible. From (6.6) it is evident that δ_1, δ_2 are $O(u^{-3})$ at $u = 0$, as before, but γ_1, γ_2 are now $O(u^{-1})$ at $u = 0$ and further modification to ensure convergence at this point seems at first sight necessary. However, addition of Ω_3, ω_3 in (6.1) and Ω_6, ω_6 in (7.5) yields

$$\left.\begin{aligned} \omega_3^* &= \omega_3+\omega_6 = -z\,\Omega_3^* \\ \Omega_3^* &= \Omega_3+\Omega_6 \\ &= ir(0)/(4a)+(i/\pi)\int_0^\infty \{[(\gamma_1+i\gamma_2)(e^{izu}-\mathbf{c})+ \\ &\qquad +(\gamma_1-i\gamma_2)(e^{-izu}-\mathbf{c})]-2(a\mathbf{c}u-\mathbf{s})\delta_1/a\}\,du \end{aligned}\right\}, \quad (7.9)$$

and it can be seen that no further modification is necessary, since the only divergent term in the formal potentials Ω_6, ω_6 cancels the divergence at $u = 0$ in the potentials Ω_3, ω_3. The complete solution in this case is given by Ω_1, ω_1, Ω_2, ω_2 in (5.3), (5.5), (5.8), (5.9) which yield the required conditions along $y = 0$, and Ω_3^*, ω_3^*, Ω_4^*, ω_4^* from (6.8), (7.9) which give specified conditions along $y = a$.

8. Isolated load in the interior of a simply-supported infinite strip

The potentials given in (4.7), (4.8) correspond to an isolated load at $z = z_0 = \alpha+i\beta$ ($\beta > 0$) and give $w = \tilde{ns} = 0$, and therefore $v = 0$, along the real axis. Along $y = a$ they give

$$v_{y=a} = \frac{4A(a+\beta)^2}{(x-\alpha)^2+(a+\beta)^2}-\frac{4A(a-\beta)^2}{(x-\alpha)^2+(a-\beta)^2}, \quad (8.1)$$

$$w_{y=a} = A\{(x-\alpha)^2+(\alpha-\beta)^2\}\log\frac{(x-\alpha)^2+(a-\beta)^2}{(x-\alpha)^2+(a+\beta)^2}- \\ -4A\beta a\log\{(x-\alpha)^2+(a+\beta)^2\}. \quad (8.2)$$

Thus, bearing in mind that the above boundary conditions have to be eliminated, the functions τ_1, τ_2 defined in (6.4) are given by

$$\tau_1 e^{au}/(\pi A\cos\alpha u) = \tau_2 e^{au}/(\pi A\sin\alpha u) = -\beta\cosh\beta u+a\sinh\beta u. \quad (8.3)$$

The function $w_{y=a}$ is not expressible as a Fourier integral but

$$r'(x) = -\frac{d}{dx}\{w_{y=a}\} = 2A(x-\alpha)\log\left[\frac{(x-\alpha)^2+(a+\beta)^2}{(x-\alpha)^2+(a-\beta)^2}\right] \quad (8.4)$$

can be so expressed. Using the method given in the preceding section, the functions σ_1, σ_2 defined in (7.4) are, in the present case, given by

$$\sigma_1 u^3 e^{au}/(\pi A\cos au) = \sigma_2 u^3 e^{au}/(\pi A\sin au) = \beta u\cosh\beta u-(1+au)\sinh\beta u. \quad (8.5)$$

Also

$$r(0) = A\{\alpha^2+(a-\beta)^2\}\log\left(\frac{\alpha^2+(a+\beta)^2}{\alpha^2+(a-\beta)^2}\right)+4Aa\beta\log\{\alpha^2+(a+\beta)^2\}. \quad (8.6)$$

Since σ_1, σ_2 are $O(u^{-1})$ and τ_1, τ_2 are $O(1)$ at $u = 0$, and σ_1, σ_2, τ_1, τ_2 are $O(e^{u(\beta-a)})$ at $u = \infty$, the solution given by Ω_3^*, ω_3^*, Ω_4^*, ω_4^* is valid.

Conclusion

Comparison of the above with corresponding investigations on clamped elastic plates (**4**) shows the influence of boundary conditions on problems involving the biharmonic equation. For example, the conditions required at infinity in the case of the half-plane differ in the two cases, although these are sometimes dismissed by merely demanding 'infinitesimal stresses at infinity'. The same approach has been employed here as in the paper quoted on clamped elastic plates, but it does not appear possible to apply directly the methods employed by Muskhelishvili (**2**) and Green (**8**) to consideration of simply-supported boundaries.

REFERENCES

1. A. C. Stevenson, *Phil. Mag.* (7) **33** (1942), 639.
2. N. I. Muskhelishvili, *Some Basic Problems of the Mathematical Theory of Elasticity*, 3rd edition (Moscow, 1949), English edition (Groningen-Holland, 1953).
3. S. Timoshenko, *Theory of Plates and Shells* (1940), pp. 89–95.
4. R. Tiffen, *Quart. J. Mech. App. Math.* **8** (1955), 237.
5. —— ibid. **5** (1952), 344.
6. —— ibid. **6** (1953), 344.
7. E. C. Titchmarsh, *Introduction to the Theory of Fourier Integrals*, 2nd edition (Oxford, 1948), pp. 41–42.
8. A. E. Green and W. Zerna, *Theoretical Elasticity* (Oxford, 1954).

THE REFLECTION OF TRANSVERSE WAVES IN BEAMS

By R. P. N. JONES
(*Department of Applied Mechanics, University of Sheffield*)

[Received 6 August 1955]

SUMMARY

Timoshenko's theory of transverse vibrations of beams predicts the existence of two possible types of wave motion of given frequency. The first type is progressive for all frequencies, whilst for the second type there is a critical frequency above which the waves are progressive and below which they are stationary. The reflections of an incident wave at a beam end are determined, and it is shown that at a simply supported end there is a single reflected wave, whilst at a free or clamped end reflected waves of both types are produced. On the basis of this theory a brief discussion is given of the propagation and reflection of a flexural pulse.

1. Introduction

BEFORE discussing Timoshenko's theory it is useful to consider the reflection of waves according to the elementary equation for flexural vibrations of beams of density ρ, and mass m per unit length, viz.

$$EI\frac{\partial^4 y}{\partial x^4}+m\frac{\partial^2 y}{\partial t^2}=0. \tag{1}$$

In this equation put

$$y=ku, \qquad x=ks, \qquad t=\frac{k\tau}{c_0}, \tag{2}$$

where k is the radius of gyration of the beam section about the neutral axis, and $c_0=\sqrt{(E/\rho)}$. Equation (1) now becomes

$$\frac{\partial^4 u}{\partial s^4}+\frac{\partial^2 u}{\partial \tau^2}=0, \tag{3}$$

which has solutions in the form

$$u=\exp[i(\omega\tau-ps)], \tag{4}$$

where ω is assumed real and positive, and p may have any of the values $\pm\sqrt{\omega}$, $\pm i\sqrt{\omega}$. In these solutions, which represent transverse waves of circular frequency $c_0\omega/k$, the real values of p give progressive waves having phase-velocities $c=\pm c_0\sqrt{\omega}$, whilst the imaginary values give stationary waves. Because of their exponential shape the latter waves cannot exist as free waves in an infinite beam.

Consider a semi-infinite beam extending from $s = -\infty$ to $s = 0$, and let

$$u = \exp[i(\omega\tau - s\sqrt{\omega})] \tag{5}$$

be an incident wave at the end $s = 0$. Three types of end condition may be considered, namely,

(*a*) Simply supported: $u = 0, \quad \dfrac{\partial^2 u}{\partial s^2} = 0.$

(*b*) Free: $\dfrac{\partial^2 u}{\partial s^2} = 0, \quad \dfrac{\partial^3 u}{\partial s^3} = 0.$

(*c*) Clamped: $u = 0, \quad \dfrac{\partial u}{\partial s} = 0.$

The end conditions (*a*) are satisfied by taking a reflected wave in the form

$$u' = -\exp[i(\omega\tau + s\sqrt{\omega})]. \tag{6}$$

In this case the incident wave is reflected with equal amplitude but in opposite phase, and the amplitude of the shear force at the end is twice that of the incident wave.

With end conditions (*b*) and (*c*) it is necessary to introduce both a reflected progressive wave and a stationary wave, given respectively by the equations

$$u' = -i\exp[i(\omega\tau + s\sqrt{\omega})], \tag{7}$$

$$u'' = \pm(1-i)\exp[i\omega\tau + s\sqrt{\omega}], \tag{8}$$

in which the positive and negative signs refer to conditions (*b*) and (*c*) respectively. For these end conditions the incident wave is again reflected with equal amplitude, but with a phase change of $\frac{1}{2}\pi$. In the case of the clamped end the total amplitudes of both bending moment and shear force at the end are $2\sqrt{2}$ times those of the incident wave. Again, because of their exponential form, the stationary waves will be comparatively insignificant except near the end of the beam.

Green (**1**) has given a method of solution of flexural vibration problems in terms of the progressive and stationary waves considered above.

2. Timoshenko's equations

The elementary bending theory gives an approximation which is satisfactory only for low-frequency waves in which $\omega \ll 1$. A more accurate solution may be obtained by including Timoshenko's (**2**), (**3**) corrections for shear deflexion and rotary inertia, which lead to the following equations of motion

$$\frac{1}{\gamma}\frac{\partial^2 u_s}{\partial s^2} - \frac{\partial^2}{\partial \tau^2}(u_b + u_s) = 0, \tag{9}$$

$$\frac{\partial^3 u_b}{\partial s^3} - \frac{\partial^3 u_b}{\partial s \partial \tau^2} + \frac{1}{\gamma}\frac{\partial u_s}{\partial s} = 0. \tag{10}$$

Using the notation of a previous paper (**4**), ku_b and ku_s are the deflexion components due to bending and shear deformation respectively, and γ is a constant given by

$$\gamma = \frac{EI}{Ck^2}, \tag{11}$$

where C is the effective shear rigidity of the beam section. The calculations in this paper are based on a value $\gamma = 4$.

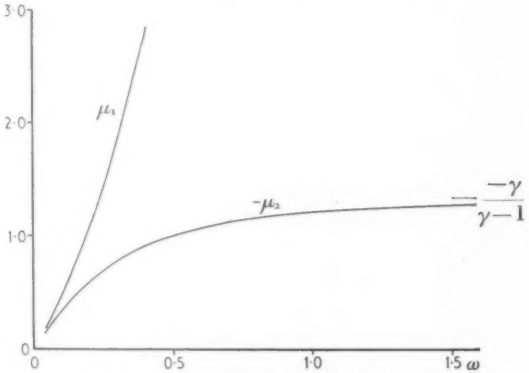

FIG. 1. Variation of μ_1 and μ_2 with ω.

The deflexion components are related to the bending moment M and shear force F by the equations

$$M = -\frac{EI}{k}\frac{\partial^2 u_b}{\partial s^2}, \tag{12}$$

$$F = C\frac{\partial u_s}{\partial s}. \tag{13}$$

It is interesting to note that if the 'coupling' terms $\frac{\partial^2 u_b}{\partial \tau^2}$ in (9) and $\frac{1}{\gamma}\frac{\partial u_s}{\partial s}$ in (10) are omitted, the two equations would each have the form of a simple wave equation, and would yield respectively a wave of pure shear deformation with a velocity of propagation $c_0\gamma^{-\frac{1}{2}}$, and a wave of pure bending deformation with a velocity c_0.

With the coupling terms present, solutions of (9) and (10) may be obtained in the form

$$\left.\begin{aligned} u_b &= \exp[i(\omega\tau - ps)] \\ u_s &= \mu\exp[i(\omega\tau - ps)] \end{aligned}\right\}, \tag{14}$$

where

$$\mu = \gamma(p^2 - \omega^2) \tag{15}$$

and p may have any of the values $\pm p_1$, $\pm p_2$, where p_1 and p_2 ($p_1 > p_2$) are the positive roots of the equation

$$(\gamma\omega^2 - p^2)(\omega^2 - p^2) - \omega^2 = 0. \tag{16}$$

There are thus two types of wave motion possible, each having a dispersive propagation and consisting of a mixture of bending and shear deformation. The first type, corresponding to $p = \pm p_1$, is a progressive wave since p_1 is real for all values of ω. The associated value of μ_1 is plotted in Fig. 1 for the particular case when $\gamma = 4$, and it is seen that the wave consists mainly of bending deformation at low frequencies, and shear deformation at high frequencies.

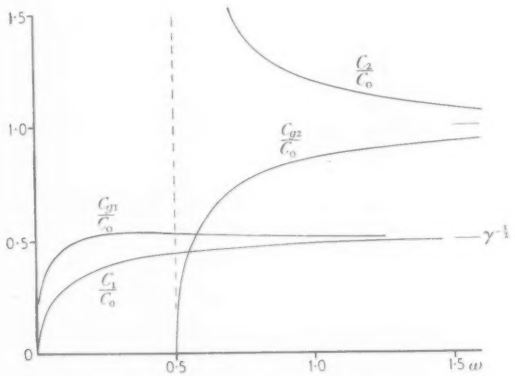

FIG. 2. Phase and group velocities.

For the second type of wave the value of p_2 is real or imaginary according as

$$\gamma\omega^2 \gtrless 1. \tag{17}$$

This type of wave is therefore either progressive or stationary according as the circular frequency is greater or less than a critical value $c_0/k\sqrt{\gamma}$. Again, the wave consists mainly of bending deformation at low frequencies, but at high frequencies μ_2 approaches a limiting value $-\gamma/(\gamma-1)$, and both bending and shear deformation are present. At low frequencies the two wave types approximate to the progressive and stationary waves predicted by the elementary theory.

When p is real, equations (14) represent a wave having a phase-velocity c and group-velocity c_g given by the equations

$$\frac{c}{c_0} = \frac{\omega}{p}, \tag{18}$$

$$\frac{c_g}{c_0} = \frac{d\omega}{dp}. \tag{19}$$

The phase and group velocities of the two types of wave are shown in Fig. 2.

3. Wave reflections

In order to determine the reflections of waves of the form (14) at the end $s = 0$ of a semi-infinite beam, it is necessary to express the end conditions in terms of the components u_b and u_s. By application of equations (12) and (13) the conditions may be obtained in the following forms

$$\left.\begin{aligned} &(a)\ \text{Simply supported:} && u_b+u_s = 0, && \frac{\partial^2 u_b}{\partial s^2} = 0 \\ &(b)\ \text{Free:} && \frac{\partial^2 u_b}{\partial s^2} = 0, && \frac{\partial u_s}{\partial s} = 0 \\ &(c)\ \text{Clamped:} && u_b+u_s = 0, && \frac{\partial u_b}{\partial s} = 0 \end{aligned}\right\}. \tag{20}$$

The last condition is obtained by noting from (12) that $\partial u_b/\partial s$ is continuous. However, the clamped condition does not impose restriction on $\partial u_s/\partial s$, since (13) permits discontinuity in this quantity.

At a simply supported end it may be shown that an incident wave of either type is reflected with the same amplitude but with a phase change of π, as in the elementary theory. At a free or clamped end, however, a single incident wave gives rise to two reflected waves, one of each type. By putting $p = p_1$ in (14) we obtain an incident wave of type 1, and if $\gamma\omega^2 > 1$ the reflected waves may be written in the form

$$\left.\begin{aligned} u'_b &= \alpha_{11}\exp[i(\omega\tau+p_1 s)]+\alpha_{21}\exp[i(\omega\tau+p_2 s)] \\ u'_s &= \mu_1\alpha_{11}\exp[i(\omega\tau+p_1 s)]+\mu_2\alpha_{21}\exp[i(\omega\tau+p_2 s)] \end{aligned}\right\}. \tag{21}$$

Similarly, for an incident wave of type 2 the reflected waves may be written

$$\left.\begin{aligned} u'_b &= \alpha_{12}\exp[i(\omega\tau+p_1 s)]+\alpha_{22}\exp[i(\omega\tau+p_2 s)] \\ u'_s &= \mu_1\alpha_{12}\exp[i(\omega\tau+p_1 s)]+\mu_2\alpha_{22}\exp[i(\omega\tau+p_2 s)] \end{aligned}\right\}. \tag{22}$$

The reflection coefficients α_{11}, α_{21}, α_{12}, α_{22} may be determined from the appropriate end conditions. Thus for a clamped end with an incident wave of type 1, conditions (20) (c) lead to the following equations:

$$1+\mu_1+\alpha_{11}(1+\mu_1)+\alpha_{21}(1+\mu_2) = 0, \tag{23}$$

$$-p_1+\alpha_{11}p_1+\alpha_{21}p_2 = 0, \tag{24}$$

giving

$$\alpha_{11} = \frac{p_1(1+\mu_2)+p_2(1+\mu_1)}{p_1(1+\mu_2)-p_2(1+\mu_1)}, \tag{25}$$

$$\alpha_{21} = \frac{2p_1(1+\mu_1)}{p_2(1+\mu_1)-p_1(1+\mu_2)}. \tag{26}$$

Similarly, it is found that

$$\alpha_{22} = -\alpha_{11}, \tag{27}$$

$$\alpha_{12} = \frac{2p_2(1+\mu_2)}{p_1(1+\mu_2)-p_2(1+\mu_1)}. \tag{28}$$

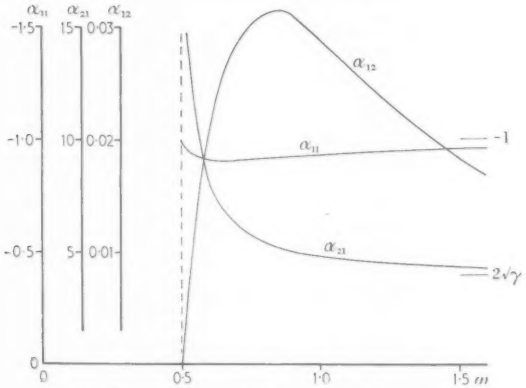

FIG. 3. Reflection coefficients for a clamped end.

Similar results may also be obtained for a free end in the following forms:

$$\alpha_{11} = -\alpha_{22} = \frac{\mu_2 p_1 + \mu_1 p_2}{\mu_1 p_2 - \mu_2 p_1}, \tag{29}$$

$$\alpha_{21} = \frac{p_1}{p_2}\frac{2\mu_1 p_1}{\mu_2 p_1 - \mu_1 p_2}, \tag{30}$$

$$\alpha_{12} = \frac{p_2}{p_1}\frac{2\mu_2 p_2}{\mu_1 p_2 - \mu_2 p_1}. \tag{31}$$

The numerical values of these coefficients are shown in Figs. 3 and 4.

When $\gamma\omega^2 < 1$, the waves of type 2 degenerate into stationary waves, and only reflections due to an incident wave of type 1 need be considered. At a free or clamped end there is now a reflected progressive wave and a stationary wave, and their forms may be determined by substituting $ip_2 = q$ (where q is real and positive) in (21) and in the appropriate equations for α_{11} and α_{21}. It is seen that these coefficients are now complex, and also that $|\alpha_{11}| = 1$. The incident wave is therefore reflected with equal amplitude but with a change of phase.

When an incident wave of either type is reflected at a simply supported end, it may be shown that the total amplitude of the shear force at the end is twice that of the incident wave. At a clamped end the ratios of the

total bending moment and shear force to those of the incident wave may be written ϕ_{m1} and ϕ_{f1} respectively for an incident wave of type 1, and

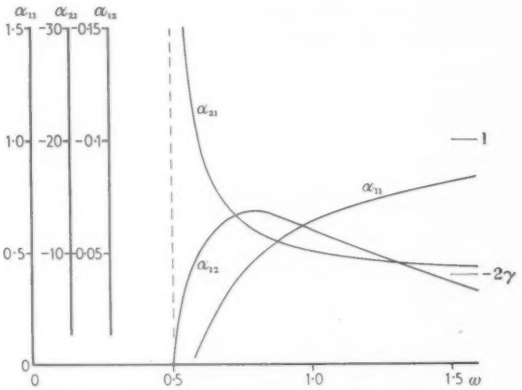

FIG. 4. Reflection coefficients for a free end.

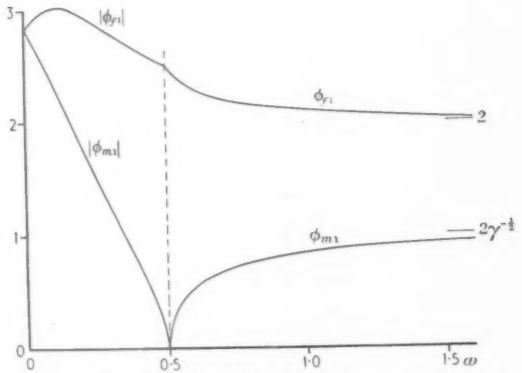

FIG. 5. Magnification of bending moment and shear force at a clamped end.

ϕ_{m2}, ϕ_{f2} for an incident wave of type 2. These ratios are given by the following equations

$$\phi_{m1} = \phi_{f2} = 1+\alpha_{11}+\alpha_{21}\left(\frac{p_2}{p_1}\right)^2, \tag{32}$$

$$\phi_{f1} = \phi_{m2} = 1-\alpha_{11}-\alpha_{21}\frac{\mu_2 p_2}{\mu_1 p_1}. \tag{33}$$

The numerical values of the ratios are plotted in Fig. 5.

4. The propagation and reflection of a pulse

The propagation of a flexural pulse according to Timoshenko's theory has been discussed by Davies and others (**4–7**).

If the beam is given a transient disturbance (such as a transverse impact) at some point, the subsequent distribution along the beam of wave components of various frequencies will be determined by their group velocities, provided a sufficient interval has elapsed for the dispersion to become well established. It may be shown (**4**) that three wave-fronts are propagated in each direction from the point of disturbance, and these wave-fronts are associated with stationary values of the group velocity, i.e.

$$\frac{\partial c_g}{\partial \omega} = 0. \tag{34}$$

The fastest wave-front (A) has a velocity c_0 and contains high-frequency components of type 2. The second wave-front (B) has a velocity somewhat greater than $c_0\gamma^{-\frac{1}{2}}$, and contains components of type 1 having a frequency given by $\omega = 0{\cdot}354$ when $\gamma = 4$. This wave-front differs from the other two in that it only exists in an asymptotic sense, and is not apparent except at large values of τ after the disturbance. The third wave-front (C) has a velocity $c_0\gamma^{-\frac{1}{2}}$ and contains high-frequency components of type 1. This wave-front is inverted, so that the disturbance associated with it lies ahead of the 'front' and not behind it. The first and third wave-fronts are of particular interest in problems of transverse impact, since the maximum stresses are likely to occur at these points.

The ultimate response at any point is composed of low-frequency waves having a small group velocity, and this response may be determined with sufficient accuracy by the elementary beam theory.

By considering the reflections of the individual wave components, it is possible to determine the nature of the reflected pulse due to the arrival of a flexural pulse at a beam end. When the end is simply supported it is easily seen that the reflected pulse is of the same form as the incident pulse, but of opposite sign. At a free or clamped end, however, the end conditions introduce an additional coupling effect between the two types of wave motion, and the reflected pulse is more complicated than the incident pulse. In particular it may be shown that the reflected pulse contains five wave-fronts.

The first wave-front (A) of the incident pulse will bring high-frequency components of type 2, and the reflections set up at a free or clamped end will contain high-frequency components of both types. The first part of the reflected pulse will therefore contain two wave-fronts, of types (A) and (C), travelling at velocities c_0 and $c_0\gamma^{-\frac{1}{2}}$ respectively. The first waves of type 1

arriving at the end will be those of frequency given by $\omega = 0{\cdot}354$ (for $\gamma = 4$), and the reflections of these waves will produce a corresponding wave-front, of type (B), in the reflected pulse. Since progressive waves of type 2 do not exist at this frequency, the reflected pulse can contain only one wave-front of type (B). Finally, the arrival of the third wave-front (C) will bring high-frequency components of type 1, and, as in the case of the first wave-front, will result in a further two wave-fronts, of types (A) and (C), in the reflected pulse.

5. Conclusion

It should be noted that Timoshenko's theory, on which the analysis and discussion in this paper is based, is only an approximation, although more accurate and physically more satisfactory than the elementary beam theory. Fundamentally the approximation lies in the one-dimensional character of the equations of motion (9) and (10), which give two types of wave motion, corresponding to the two roots of the frequency equation (16). In an exact two-dimensional solution of the problem (**3**), using the equations of elasticity, a transcendental frequency equation is obtained, giving an infinite number of possible types of wave motion.

It has been shown (**8**), (**9**) that the lowest phase velocity according to the exact solution agrees well, at all frequencies, with the velocity of waves of type 1 in Timoshenko's theory, but there is no close correspondence between the velocity of waves of type 2 and any of the higher velocities predicted by the exact solution. It seems likely that Timoshenko's theory will be satisfactory in problems where only the lowest velocity wave motion is important, but in other cases the accuracy of the theory requires further investigation.

REFERENCES

1. G. Green, *Phil. Mag.* **39** (1948), 539.
2. S. P. Timoshenko, ibid. **41** (1921), 744.
3. —— ibid. **43** (1922), 125.
4. R. P. N. Jones, *Quart. J. Mech. and App. Math.* **8** (1955), 373.
5. R. M. Davies, *Phil. Trans. Roy. Soc.* A, **240** (1948), 375.
6. R. A. Anderson, *J. App. Mech.* **21** (1954), 388.
7. H. Kolsky, *Stress Waves in Solids* (Oxford, 1953), 68.
8. J. Prescott, *Phil. Mag.* **33** (1942), 703.
9. L. Cremer, *Z. angew. Math. Mech.* **23** (1943), 291.
10. J. L. B. Cooper, *Phil. Mag.* **38** (1947), 1.

THE CLOSED-FORM SUMMATION OF SOME COMMON FOURIER SERIES†

By CHI-CHANG CHAO‡ (*New York, N.Y.*)

[Received 1 December 1955; revise received 27 March 1956]

SUMMARY

A method is presented for the summation in closed form of Fourier series whose coefficients are ratios of polynomials of certain types frequently encountered in practice. The result is obtained as the solution of a linear differential equation with constant coefficients, which can be solved by elementary methods.

1. Introduction

THE solutions of many problems in applied mechanics are most readily obtained in the form of Fourier series, and it is often not recognized that some of these may be summed in closed form, thus simplifying the results.

Consider, for example, the problem of the simply supported vibrating beam shown in Fig. 1 whose steady solution is (**1**):

$$y = \frac{4gw_0 L^4}{A\gamma\pi} \sin \omega t \sum_{i=1,3\ldots}^{\infty} \left\{ \frac{\sin(i\pi x/L)}{(i^4\pi^4 a^2 - \omega^2 L^4)i} \right\}, \tag{1}$$

which is a Fourier series whose coefficients are ratios of certain polynomials. A series of such nature is easily summed in closed form by the method described below. In this particular case the result is (see example at the end of the note)

$$y = \frac{gw_0}{2A\gamma\omega^2}\left[-2 + \operatorname{csc} \sqrt{\frac{\omega}{a}} L \sin \sqrt{\frac{\omega}{a}}(L-x) + \operatorname{csch} \sqrt{\frac{\omega}{a}} L \sinh \sqrt{\frac{\omega}{a}}(L-x) + \right.$$
$$\left. + \operatorname{csc} \sqrt{\frac{\omega}{a}} L \sin \sqrt{\frac{\omega}{a}} x + \operatorname{csch} \sqrt{\frac{\omega}{a}} L \sinh \sqrt{\frac{\omega}{a}} x \right] \sin \omega t. \tag{1a}$$

It may be of interest to note that the summation of Fourier series in closed form has attracted considerable attention in a number of recent papers (**2**, **3**). Some simple series of the type considered in the present note may be treated by the methods of the papers listed in (**2**); the present method is advantageous in these cases since it employs only elementary

† The results presented here were obtained in the course of research sponsored by the Office of Naval Research, Contract Nonr-266(20). The author also wishes to express his appreciation to Professor B. A. Boley for his invaluable advice.

‡ Research Assistant, Institute of Flight Structures, Columbia University, N.Y.

techniques. The method of (3) is applicable to a wider class of series than the one described below, but is more cumbersome in the present case since it requires quite complicated integrations.

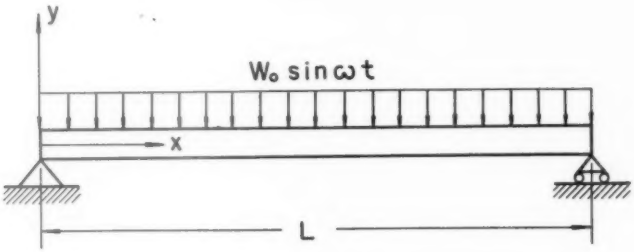

FIG. 1.

2. Summation of sine series

If a Fourier sine series is of the form†

$$f(x) = \sum_{i=1}^{\infty} \frac{iP(i^2)}{Q(i^2)} \sin\left(\frac{i\pi x}{L}\right), \tag{2}$$

where P and Q are polynomials, its summation can be easily performed as follows. Rewrite $f(x)$ as

$$f(x) = \frac{2}{L} \sum_{i=1}^{\infty} \frac{\sum_{k=0}^{m-1} b_k \alpha_i^{2(m-k)-1} + (-1)^i \sum_{k=0}^{m-1} c_k \alpha_i^{2(m-k)-1}}{\sum_{k=0}^{m} a_k \alpha_i^{2(m-k)}} \sin \alpha_i x \tag{2a}$$

$$= \frac{2}{L} \sum_{i=1}^{\infty} I_i \sin \alpha_i x,$$

where

$$\alpha_i = i\pi/L \tag{2b}$$

and the coefficients a_k, b_k, and c_k are known in any particular case. Without loss of generality one may take

$$a_0 = 1. \tag{2c}$$

Note that the denominator of (2) is a polynomial of degree $2m$, while each summation of the numerator is a polynomial of degree $(2m-1)$ at most; thus convergence is assured.

† The summation procedure described in this paper is valid for the sine series of form (2) and the cosine series of form (8) only. Thus, for example, those series derivable from $\log \cot \theta$ are not manageable by this method.

From (2), $$I_i = \int_0^L f(x)\sin\alpha_i x\,dx. \tag{3}$$

With the aid of two integrations by parts, one obtains

$$I_i = -(1/\alpha_i)[f(x)\cos\alpha_i x]_0^L + (1/\alpha_i)^2[f'(x)\sin\alpha_i x]_0^L - \\ -(1/\alpha_i)^2\int_0^L f''(x)\sin\alpha_i x\,dx, \tag{3a}$$

where primes indicate differentiation with respect to x. Introduce now a function $f_1(x)$ such that

$$f''(x) = a_1 f(x) - f_1(x). \tag{4}$$

Substitution into (2a) gives, after two additional integrations by parts and some rearranging of terms

$$(\alpha_i^2 + a_1)I_i = -\alpha_i[f(x)\cos\alpha_i x]_0^L - (1/\alpha_i)[f_1(x)\cos\alpha_i x]_0^L - \\ -(1/\alpha_i)^2\int_0^L f_1''(x)\sin\alpha_i x\,dx. \tag{4a}$$

Terms containing $(\sin\alpha_i x)$ to be evaluated at $x = 0$, L vanish and have therefore been omitted. Introduce now a function $f_2(x)$ such that

$$f_1''(x) = a_2 f(x) - f_2(x). \tag{5}$$

Repetition of the above operations gives, in general,

$$f_{j-1}''(x) = a_j f(x) - f_j(x) \quad (j = 1, 2, \ldots, m). \tag{5a}$$

The final result is

$$I_i = \frac{-\left[\sum_{k=0}^{m-1} f_k(x)\alpha_i^{2(m-k)-1}\cos\alpha_i x\right]_0^L + \int_0^L f_m(x)\sin\alpha_i x\,dx}{\sum_{k=0}^{m} a_k\,\alpha_i^{2(m-k)}}. \tag{6}$$

The denominator of this expression is identical with that of (2); the numerators will also be the same provided that

$$f_m(x) = 0 \tag{6a}$$

and $$f_k(0) = b_k, \qquad f_k(L) = -c_k. \tag{6b}$$

Equation (5a) is the typical equation of a set of m linear simultaneous ordinary differential equations of second order with the functions

$$f, f_1, f_2, \ldots, f_{m-1}$$

as dependent variables. Elimination of all functions f_j from (5a) yields the following single equation of order $2m$ for $f(x)$, namely

$$\sum_{k=0}^{m} (-1)^{m-k} a_k D^{2(m-k)} f(x) = 0, \tag{7}$$

where the operator $D = d/dx$. This equation may be solved under the boundary condition imposed by the $2m$ equation (6 b).

The form of (7) is virtually identical with the denominator of the Fourier series coefficient ((2 a) or (6)), in fact (7) may be immediately written by replacing $\alpha_i^{2(m-k)}$ by $(-1)^{m-k}D^{2(m-k)}f(x)$ in the denominator of these equations.

Thus, for a given Fourier series of form (2), the closed form summation of the series is obtained by the solution of an ordinary differential equation whose form (equation (7)) is immediately determined by the denominator of the Fourier series coefficients and with boundary conditions (equations (5 a) and (6 b)) determined from the numerator.

3. Summation of cosine series

A Fourier cosine series of the form

$$f(x) = \sum_{i=1}^{\infty} \frac{P(i^2)}{Q(i^2)} \cos\left(\frac{i\pi x}{L}\right) + \text{constant}, \tag{8}$$

where P and Q are again polynomials, may be similarly summed. Rewrite $f(x)$ as:

$$f(x) = \frac{K_0}{L} + \frac{2}{L} \sum_{i=1}^{\infty} \frac{\sum_{k=0}^{m-1} b_k \alpha_i^{2(m-k-1)} + (-1)^i \sum_{k=0}^{m-1} c_k \alpha_i^{2(m-k-1)}}{\sum_{k=0}^{m} a_k \alpha_i^{2(m-k)}} \cos \alpha_i x$$

$$= \frac{K_0}{L} + \frac{2}{L} \sum_{i=1}^{\infty} K_i \cos \alpha_i x, \tag{8 a}$$

in a notation similar to that of (2). Proceeding in a manner similar to that employed for the sine series, the equation analogous to (6) becomes, in this case,

$$K_i = \frac{\left[\sum_{k=0}^{m-1} f_k'(x) \alpha_i^{2(m-k-1)} \cos \alpha_i x\right]_0^L - \int_0^L f_m(x) \cos \alpha_i x \, dx}{\sum_{k=0}^{m} a_k \alpha_i^{2(m-k)} \quad (i \neq 0)}. \tag{9}$$

where the f_k functions are still defined by (5 a) and $a_0 = 1$. The denominator in this expression is again identical with that of (8); the numerator will also be the same provided that

$$f_m(x) = C = \text{constant} \tag{9 a}$$

and

$$f_k'(0) = -b_k, \qquad f_k'(L) = c_k. \tag{9 b}$$

The differential equation for the function f, analogous to (7), is

$$\sum_{k=0}^{m} (-1)^{m-k} a_k D^{2(m-k)} f(x) = C. \tag{10}$$

The constants of integration appearing in the solution of (10) are found with the aid of conditions (9 b). The constant C is evaluated from the condition

$$\int_0^L f(x)\,dx = K_0. \tag{11}$$

4. Example

As an example, consider the series

$$f(x) = \frac{2}{L}\sum_{i=1}^{\infty} \frac{\alpha_i[\theta_1-(-1)^i\theta_2]}{\alpha_i^6-\beta^4\alpha_i^2}\sin\alpha_i x, \tag{12}$$

which would be identical with equation (1) except a common multiplier if

$$\theta_1 = \theta_2 = \tfrac{1}{2} \quad \text{and} \quad \beta^2 = \frac{\omega}{a}.$$

Then, in the notation of (2 a),

$$m = 3, \qquad a_0 = 1, \qquad a_1 = 0, \qquad a_2 = \beta^4, \qquad a_3 = 0,$$
$$b_0 = b_1 = c_0 = c_1 = 0, \qquad c_2 = -\theta_2, \qquad b_2 = \theta_1. \tag{12 a}$$

The differential equation (7) is

$$f^{(\mathrm{vi})}+\beta^4 f'' = 0$$

and the boundary conditions are

$$f(0) = f(L) = f''(0) = f''(L) = 0,$$
$$f^{\mathrm{iv}}(L) = \theta_2, \qquad f^{\mathrm{iv}}(0) = \theta_1.$$

The final results are then

$$f(x) = \frac{1}{2\beta^4}\Big\{\theta_1\Big[\frac{2x}{L}-2+\operatorname{csc}\beta L\sin\beta(L-x)+\operatorname{csch}\beta L\sinh\beta(L-x)\Big]+$$
$$+\theta_2\Big[-\frac{2x}{L}+\operatorname{csc}\beta L\sin\beta x+\operatorname{csch}\beta L\sinh\beta x\Big]\Big\}. \tag{12 b}$$

With this result (1 a) is immediately obtained by setting $\theta_1 = \theta_2 = \frac{1}{2}$.

REFERENCES

1. S. Timoshenko, *Vibration Problems in Engineering* (3rd ed., New York, 1955), p. 350.
2. L. A. Pipes, *J. App. Phys.* **21** (1950), 292.
   I. F. Morrison, ibid. **21** (1950), 939.
   M. R. Spiegel, ibid. **23** (1952), 906.
   J. A. McFadden, ibid. **24** (1953), 364.
3. A. D. Wheeton, ibid. **25** (1954), 113.

found
n the

(11)

(12)

ier if

12a)

12b)

955),

THE QUARTERLY JOURNAL OF MECHANICS AND APPLIED MATHEMATICS

VOLUME IX PART 4 DECEMBER 1956

CONTENTS

R. R. LONG: Sources and Sinks at the Axis of a Rotating Liquid 385

G. N. LANCE and E. C. DELAND: The Shape of the Nappe of a Thin Waterfall 394

D. E. EDMUNDS: The Moving Aerofoil in the Neighbourhood of a Plane Boundary 400

J. B. L. POWELL: The Effect of Dihedral on the Aerodynamic Derivatives with respect to Sideslip for Airfoils in Supersonic Flow 425

L. C. WOODS: On the Theory of Source-flow from Aerofoils . 441

D. R. DAVIES and D. E. BOURNE: On the Calculation of Heat and Mass Transfer in Laminar and Turbulent Boundary Layers. I. The Laminar Case 457

D. R. DAVIES and D. E. BOURNE: On the Calculation of Heat and Mass Transfer in Laminar and Turbulent Boundary Layers. II. The Turbulent Case 468

T. BUCHWALD and R. TIFFEN: Boundary-value Problems of Simply-supported Elastic Plates 489

R. P. N. JONES: The Reflection of Transverse Waves in Beams . 499

CHI-CHANG CHAO: The Closed-form Summation of some common Fourier Series 508

The Editorial Board gratefully acknowledge the support given by: Bristol Aeroplane Company; Courtaulds Scientific and Educational Trust Fund; English Electric Company General Electric Company; Imperial Chemical Industries; Unilever.

CS

1956

385

394

400

425
441

57

68

89
99

08

ne
y